The role of iNKT cells and adenosine A_{2A} receptor activation

in the pathogenesis of pulmonary dysfunction in sickle cell disease

Kori L. Wallace
Lockport, New York

B.S. Biology and Society
Arizona State University
2002

A Dissertation presented to the Graduate Faculty
of the University of Virginia in Candidacy for the Degree of
Doctor of Philosophy

Department of Microbiology
University of Virginia
August 2009

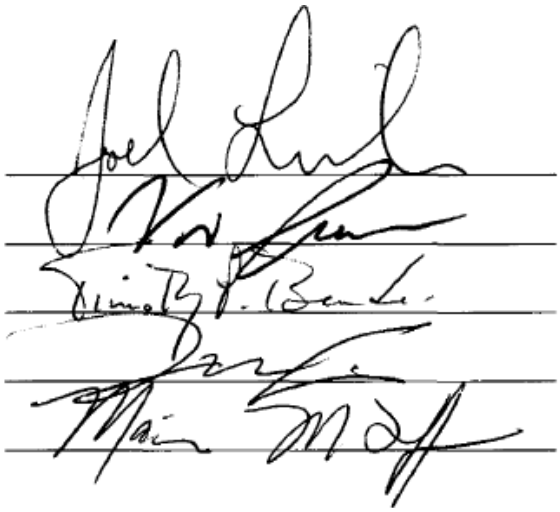

Abstract

In sickle cell disease (SCD), misshapen erythrocytes evoke repeated transient bouts of microvascular occlusion that is believed to lead to end-organ damage. Although the sickled red blood cell is the inciting factor in the pathogensis of SCD, the exact mechanism of vaso-occlusion is unknown. Interactions between white blood cells, platelets, and vascular endothelial cells are also believed to contribute to vaso-occlusion is sickle cell disease. Vaso-occlusion leads to downstream tissue ischemia, that eventually resolves and reperfusion to the tissue returns. It is known that ischemia-reperfusion injury triggers an inflammatory cascade that is initiated by the activation of CD1d-restricted iNKT cells and can be inhibited by anti-CD1d or adenosine A_{2A} receptor ($A_{2A}R$) agonist treatment.

iNKT cells are known to release copious amounts of cytokines when activated, including IFN-γ. Compared to controls (C57BL/6), SCD mice (NY1DD) have more numerous and activated pulmonary iNKT cells and increased pulmonary levels of IFN-γ. IFN-γ is known to recruit effector lymphocytes to areas of inflammation via the IFN-γ inducible chemokine – CXCR3 axis. NY1DD mice were found to have increased levels of IFN-γ inducible chemokines and elevated numbers of lymphocytes expressing the chemokine receptor CXCR3.

Strikingly, treating NY1DD mice with anti-CD1d antibody to inhibit iNKT cell activation for only two days reverses baseline pulmonary dysfunction. Anti-CD1d antibodies decrease pulmonary levels of IFN-γ and CXCR3 chemokines. Crossing NY1DD to lymphocyte-deficient $Rag1^{-/-}$ mice decreases pulmonary dysfunction. This is reversed by the adoptive transfer of 1 million NKT cells. Similar to mice, humans with

SCD have increased numbers of activated circulating iNKT cells expressing CXCR3. Another method for inhibiting iNKT cells is treatment with adenosine A_{2A} receptor ($A_{2A}R$) agonists. Treating NY1DD mice a selective $A_{2A}R$ agonist, decreased pulmonary injury.

The results of this study provide the basis for a new paradigm to understand the pathogenesis of pulmonary inflammation and vaso-occlusion in SCD and have important translational therapeutic implications. Together, these data indicate that iNKT cells play a pivotal role in sustaining inflammation in NY1DD mice and that this mechanism may translate to human disease. By inhibiting CD1d-restricted NKT cell activation, it may be possible to reduce end-organ damage in SCD.

List of Abbreviations

α-GalCer	Alpha-galactosyl ceramide
A_{2A}R	Adenosine A_{2A} receptor
ADA	Adenosine deaminase
ALT	Alanine transaminase
AMP	Adenosine monophosphate
ANOVA	Analysis of variance
APC	Antigen presenting cell
ATP	Adenosine triphosphate
BALF	Bronchoalveolar lavage fluid
BCR	B-cell receptor
BM	Bone marrow
cAMP	Cyclic adenosine monophosphage
CCR	Chemokine (C-C motif) receptor
CRP	C-reactive protein
CXCL	Chemokine (C-X-C motif) ligand
CXCR	Chemokine (C-X-C motif) receptor
DC	Dendritic cell
DM	Diabetes mellitus
DMSO	Dimethyl sulfoxide
EAE	Experimental autoimmune encephalomyelitis
EBD	Evans blue dye
EBV	Epstein barr virus

EC	Endothelial cell
EpiC	Epithelial cell
FBS	Fetal bovine serum
FEV	Forced expiratory volume
FOB	Frequency of breath
FVC	Forced vital capacity
GVHD	Graft versus host disease
Hb	Hemoglobin
H&E	Hematoxylin and eosin
H/R	Hypoxia reoxygenation
IFN	Interferon
iGB3	Isoglobotrihexosylceramide
IL	Interleukin
iNKT	Invariant NKT cell
IP-10	Interferon inducible protein 10
IRI	Ischemia reperfusion injury
ITAC	Interferon inducible T-cell alpha chemoattractant
LPS	Lipopolysaccharide
MAPK	Mitogen activated protein kinase
MCP	Monocytes chemoattractant protein
MHC	Major histocompatibility complex
MI	Myocardial infarction
MIG	Monokine induced by gamma interferon

MS	Multiple sclerosis
NADPH	Nicotinamide adenine dinucleotide phosphate
NSAID	Non-steroidal anti-inflammatory drug
PAF	Platelet activating factor
PDE	Phosphodiesterase
PMN	Polymorphonuclear
PtdEtN	Phosphatidylethanolamine
RBC	Red blood cell
RT-PCR	Reverse transcription polymerase chain reaction
SCD	Sickle cell disease
SDF	Stromal cell derived factor
sICAM	Soluble intercellular adhesion molecule
SLE	Systemic lupus erythematosus
SO_2	Oxygen saturation
sRBC	Sickled red blood cell
sVCAM	Soluble vascular cell adhesion molecule
TCR	T-cell receptor
TLR	Toll-like receptor
TNF	Tumor necrosis factor
TV	Tidal volume
UC	Ulcerative colitis
VEGF	Vascular endothelial growth factor
WBC	White blood cell

Table of Contents

Figures

Tables

Dedication Page

I would like to dedicate this work to my family and the Linden laboratory.

1. Introduction

1.1. Sickle cell disease

1.1.1. Background

Sickle cell disease is an inherited disorder arising from at least one mutant beta hemoglobin (*HBB*) allele that results in the formation of sickle hemoglobin (HbS), alone or in combination with another mutation in hemoglobin (Table 1). Sickle cell disease consists of all genotypes containing at least one sickle gene, in which HBS makes up at least half the hemoglobin present. Most individuals with sickle cell disease are homozygotic for the sickle *HBB* mutation and present clinically defined with sickle cell anemia (HbSS). Five other major sickle genotypes are also linked to the disease (Table 1). Sickle cell disease is an inherited autosomal recessive trait. Among African Americans, about 1 in 400 births result in the homozygous state, sickle cell anemia. Since individuals with sickle cell anemia make up the majority of sickle cell disease, the literature frequently uses the terms sickle cell disease and sickle cell anemia interchangeably. While all individuals with sickle cell disease have similar clinical symptoms, such as anemia and shortness of breath, these symptoms can differ greatly in severity depending on the subtype. This project focuses on the pathophysiology and treatment of sickle cell anemia in the context of sickle cell disease.

Sickle cell disease	Genotype	Phenotype
Sickle cell anemia (HbSS)	Homozygous for sickle *HBB* mutation	Moderate – severe
HbS/β^o thalassemia	Double heterozygous for sickle *HBB* and β^o *HBB* (point mutation that results in no beta hemoglobin chains) mutations	Moderate – severe
HbSC	Heterozygous for sickle *HBB* mutation and *HBB* mutation that results in formation of HbC	Intermediate
HbS/β^+ thalassemia	Double heterozygous for sickle *HBB* and β^+ *HBB* (point mutation that results in some beta hemoglobin chain) mutations	Mild – moderate
HBS/HBE Syndrome	Heterozygous for sickle *HBB* and *HBB* mutation that results in formation of HbE	Very mild

Table 1. Variant sickle cell syndromes

1.1.2. Molecular context

Hemoglobin is a tetramer of globins, which change throughout development. Fetal hemoglobin (HbF), which has been shown to be protective in sickle cell disease, is a tetramer of α- and ζ- globins ($\alpha_2\zeta_2$) (Watson J et al., 1948). The switch from HbF to adult hemoglobin (HbA, $\alpha_2\beta_2$) occurs around six weeks after birth, at which time individuals typically develop clinical signs and symptoms of sickle cell disease (Bainbridge et al., 1985). Sickle hemoglobin (HbSS, $\alpha_2\beta^S{}_2$) is caused by a point mutation (GAG → GTG) in the β-globin gene (*HBB*) that changes the sixth amino acid from glutamine to valine. The abnormal position of the β-6 valine on the outside of the β tetramer allows it to adhere to the β-85 phenylalanine and the β-88 leucine on adjacent β tetramers. HbS is poorly soluble when deoxygenated and in hypoxic conditions HbS polymerizes reversibly to form a gelatinous network of fibrous polymers that stiffen the erythrocyte membrane, increase viscosity, and cause dehydration due to potassium leakage and calcium influx (Figure 1) (White, 1974).

While the generation of mutant HbS is a monogenetic event, the phenotype of sickle cell disease is multigenic (Bainbridge et al., 1985; Cohen et al., 2004). Since the severity of the disease varies greatly between individuals with sickle cell disease and between those individuals who have the same sickle cell disease subtype, it is believed that additional genes participate in the pathology of the disease, possibly including genes that regulate cytokine production, endothelial adhesion, and platelet activation. It has been proposed that after these pleiotropic genes are located, specific polymorphisms may be identified that will help to define an individual's risk (Stuart and Nagel, 2004).

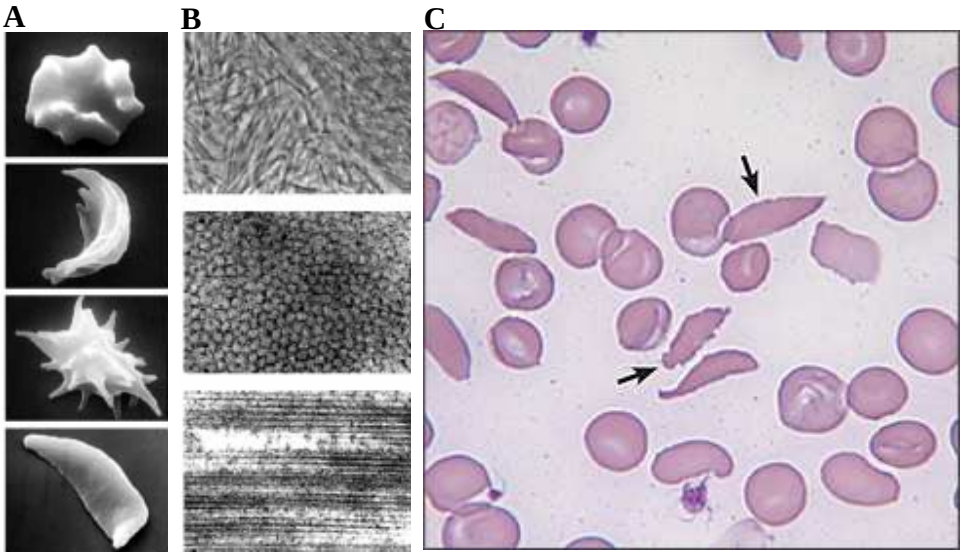

Figure 1. Sickle red blood cell characteristics

(**A**) Sickled red blood cells showing various morphologies (top to bottom): granular, classic sickle, holly shaped, irreversibly sickled (White, 1974). (**B**) Electron microscopy of a sickled red blood cell reveals highly ordered polymer domains, as seen from the side (bottom) and on the end (middle) or highly disorganized domains (top) (White, 1974). (**C**) Blood smear from an individual with sickle cell disease. *Arrows* indicate sickled red blood cells.

1.1.3. Clinical manifestations

The predominant clinical features of sickle cell disease include hemolytic anemia, episodic painful events (vaso-occlusive crisis), chronic organ deterioration, and various acute complications (Hebbel, 2005). The clinical manifestations of sickle cell disease vary greatly between and among the major sickle cell disease subtypes. Virtually every organ system in the body is subject to vaso-occlusion, which accounts for the characteristic acute and chronic multisystem failure of this disease.

Chronic hemolytic anemia is one of the hallmarks of sickle cell disease. Sickled red blood cells have a lifespan of 17 days (normal lifespan is 120 days) and are destroyed randomly (McCurdy, 1969). A constant degree of hemolytic anemia may be exacerbated by additional events, such as exercise, aplastic crises (transient arrests of erythropoiesis due to parvovirus B19), acute splenic sequestration (hyperslenism and autoinfarction), acute hepatic sequestration, chronic renal disease (decreased erythropoietin), bone marrow necrosis, deficiency of folic acid or iron, and delayed hemolytic transfusion reactions (Hebbel, 2005; Stuart and Nagel, 2004).

An episode of acute pain in a patient with sickle cell disease is called "sickle cell crisis," coined in 1965 by Diggs, who used the expression "crisis" to refer to any new rapidly developing syndrome in a patient with sickle cell disease (Diggs, 1965). Vaso-occlusive crisis is due to episodic microvessel occlusion at one or many sites that causes pain and is accompanied by local inflammation (Stuart and Nagel, 2004). The basic mechanism is believed to be vaso-occlusion of the bone marrow vasculature, causing bone infarction, which in turn causes the release of inflammatory mediators that activate afferent nociceptors (Bunn, 1997). Clinical studies have shown that individuals with

sickle cell disease who have high pain rates tend to die earlier than those with low pain rates (Stuart and Nagel, 2004).

Virtually every organ system is affected by chronic and acute complications of sickle cell disease. Since pulmonary pathophysiology in sickle cell disease is the focus of this document, a complete review of organ dysfunction is beyond the scope of this chapter. Briefly, renal involvement is a common manifestation of sickle cell disease. The medullary environment has low oxygen tension and high osmolality, both of which contribute to osmotic dehydration of the red blood cells causing polymerization of HbS, sickling, and vaso-occlusion (Pham et al., 2000). The various nephropathies that affect individuals with sickle cell disease are believed to be the result of repeated ischemia-reperfusion episodes to the microvasculature in the kidney (Molitierno, Jr. and Carson, III, 2003).

Also, hepatic dysfunction exists in individuals with sickle cell disease. Chronic hemolytic anemia contributes to the formation of pigmented gallstones, which are eventually found in approximately 70 % of individuals (Rennels et al., 1984). Acute hepatic crisis is associated with liver ischemia and is associated with a poor prognosis (Rosenblate et al., 1970a; Sheehy et al., 1980). Chronic liver disease is thought to be caused by intrahepatic trapping of sickled red blood cells leading to hepatomegaly, liver dysfunction, and cirrhosis (Rosenblate et al., 1970a).

1.1.3.1. Pulmonary complications

Pulmonary disease is the leading cause of death in sickle cell disease (Platt et al., 1994). Since the pulmonary arterial circulation has low oxygen tension and pressure, low

blood velocity, and constricts in response to hypoxia, the lung environment facilitates the polymerization of HbS and is highly vulnerable to ischemic injury (Platt et al., 1994). Both acute and chronic pulmonary complications are common in sickle cell disease. Acute chest syndrome presents as the radiological appearance of new pulmonary infiltrate, which can be accompanied by changes in breathing patterns (dyspnea, tachypnea), chest pain, fever, and leukocytosis (Stuart and Nagel, 2004). Acute chest syndrome is predominantly caused by vaso-occlusion or infection (Vichinsky et al., 1997). Both hypoxia and vasoconstriction contribute to HbS polymerization and red blood cell sickling that leads to vaso-occlusion of the microvascular beds and further HbS deoxygenation and sickling. The major danger of acute chest syndrome is systemic hypoxia, which can cause widespread red blood cell sickling and vaso-occlusion leading to end-organ damage (Stuart and Nagel, 2004). Chronic pulmonary complications are associated with a poor prognosis and can include interstitial fibrosis, restrictive lung disease, obstructive lung disease, and pulmonary hypertension (Aquino et al., 1994; Platt et al., 1994). Chronic complications are more common in individuals with sickle cell disease with a history of multiple episodes of acute chest syndrome (Powars et al., 1988).

1.1.4. Pathophysiology

Historically, sickle cell disease has been viewed as a disease of red blood cell abnormalities. For almost a century, sickle cell disease was viewed as a direct result of HbS polymerization, in which sequential deoxygenation, sickling, and rigidification of sickled red blood cells, stasis of microvascular blood flow, and additional sickling led to painful microvascular occlusion, this was the dogma that drove sickle cell disease

research for decades (Embury, 2004). Recently, novel discoveries of polymerization-independent mechanisms have placed sickle cell disease into the broader classification of vascular disease. In particular, a new paradigm has emerged that suggests that the wide spectrum of clinical manifestations of sickle cell disease result in part from chronic inflammation with abnormal endothelial activation and coagulation (Figure 2) (Chies and Nardi, 2001; Platt, 2000).

The first indication that inflammation was associated with sickle cell disease was the discovery that individuals at steady state had moderate leukocytosis, which has further been shown to be a risk factor for mortality, cerebrovascular incident, and acute chest syndrome (Balkaran et al., 1992; Buchanan and Glader, 1978; Castro et al., 1994; Platt et al., 1994). Also, individuals with sickle cell disease at steady state have elevated levels of C-reactive protein (CRP), fibrinogen, tumor necrosis factor-α (TNF-α), interleukin-1 (IL-1), interferon-γ (IFN-γ), interleukin-2 (IL-2), interleukin-6 (IL-6), thrombin, endotoxin, soluble vascular cell adhesion molecule-1 (sVCAM-1), and circulating endothelial cells, all of which contribute to the pro-inflammatory hypothesis (Singhal et al., 1993; Stuart et al., 1994). It has also been observed that individuals with sickle cell disease with a predominantly Th1 inflammatory response are more susceptible to developing severe clinical manifestations then those individuals with sickle cell disease whose immune system is directed towards a Th2 pattern (Taylor et al., 1997; Taylor et al., 1999). It has been suggested that measuring these cytokines and inflammatory biomarkers may be used as a measure of clinical severity (Schnog et al., 1998).

There is also evidence that individuals with sickle cell disease have a chronically active coagulation system, which has been shown to increase during vaso-occlusive crisis (Francis and Hebbel, 1994). Clinical evidence has demonstrated that individuals with sickle cell disease have increased thrombin generation and platelet activation (Tomer et al., 2001). Tissue factor has also been found to be abnormally expressed on monocytes and on circulating endothelial cells in individuals with sickle cell disease, supporting the concept of a hypercoaguable state (Solovey et al., 1998). This pro-coagulatory phenotype results in conditions that favor vaso-occlusion.

The vascular endothelium has also been found to contribute to the pathogenesis of vaso-occlusion. *In vitro* and *in vivo* assays have demonstrated the abnormal adhesive properties of sickled red blood cells to the vascular endothelium (Sultana et al., 1998; Swerlick et al., 1993). It has been postulated that sickled red blood cell adhesion to the vascular endothelium may lead to the production of oxygen free radicals and activation of the transcription factor nuclear factor-κβ (NF-κβ) (Sultana et al., 1998). In turn, NF-κβ has been shown to upregulate the transcription of various inflammatory mediators, such adhesion molecules (E-selectin, VCAM-1, and ICAM-1), all of which have important roles in leukocyte adhesion to the endothelium (Collins et al., 1995). Therefore, current evidence suggests that vaso-occlusion is mediated by endothelial cell, sickled red blood cell, and leukocyte interactions, which can lead to blood flow abnormalities and ischemic episodes (Frenette, 2004).

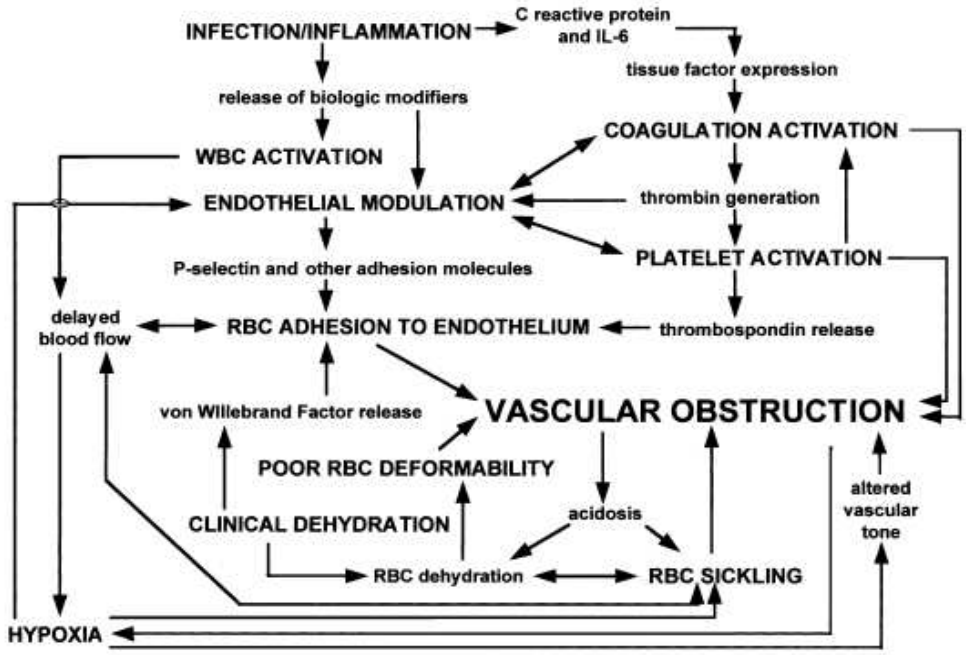

Figure 2. The interrelationships of the risk factors for sickle cell vaso-occlusion

(Embury, 2004)

1.2. Ischemia-reperfusion injury

1.2.1. Background

It is well known that ischemic injury, which is the cessation of blood flow with immediate oxygen deprivation of cells (i.e. hypoxia with accumulation of metabolic products), results in cellular dysfunction, tissue injury, and eventually cell death. Ischemia is a common and important clinical problem seen in many different organ systems: myocardial infarction (MI), stroke, acute kidney injury, shock liver, mesenteric ischemia, and systemic shock. Ischemia is also common in all solid organ transplants. Historically, it was believed that ischemia and the subsequent lack of oxygen was driving tissue damage and the main goal of therapy was to restore blood flow as rapidly as possible. However, it is now believed that restoration of blood flow to the ischemic tissue is often accompanied by secondary injury, which is known as reperfusion injury. In 1975, Cerra *et al.* were among the first groups to describe reperfusion injury in a canine model of myocardial infarction (Cerra et al., 1975). They noted hemorrhagic necrosis when normal coronary artery perfusion was resumed after various lengths of ischemia. Ischemia-reperfusion injury is now recognized as a highly complex cascade of events that includes interactions between vascular endothelium, interstitial compartments, circulating cells, and numerous biochemical entities. Furthermore, ischemia-reperfusion injury can be divided into two phases: one, the initial phase that occurs during ischemia; and two, the secondary phase that occurs during reperfusion and is accompanied by inflammation. Currently, the exact mechanisms of ischemia-reperfusion injury are still being elucidated. While a complete discussion is beyond the scope of this chapter, some of the principal mediators will be discussed.

1.2.2. Mechanisms of ischemia-reperfusion injury

1.2.2.1. Oxidative stress

Ischemia-reperfusion injury is characterized by the production of oxygen-derived free radicals during the initial phase of reperfusion. Oxidative stress is characterized by the formation of reactive oxygen species such as superoxide anion, hydrogen peroxide, and hydroxyl radical (McCord, 1985). These molecules, in particular the hydroxyl radical, are highly unstable and react with the first structure they encounter, usually the lipid component of the cell membrane. Cell injury produced by lipid peroxidation can range from increased permeability to cell lysis. There are several mechanisms that lead to the production of reactive oxygen species (Figure 3). In one mechanism, periods of ischemia drive the degradation of adenosine triphosphate (ATP), which results in the accumulation of hypoxanthine and the conversion of the enzyme xanthine dehydrogenase into xanthine oxidase. During ischemia, xanthine oxidase is inhibited due to a lack of molecular oxygen substrate. However, upon reperfusion this enzyme rapidly catalyzes the oxidation of hypoxanthine into superoxide (Kuppusamy and Zweier, 1989; Parks and Granger, 1986; Parks et al., 1988).

Another mechanism depends on the NADPH oxidase system, which is present on the membrane surface of monocytes/macrophages, neutrophils, and endothelial cells, and catalyzes the reduction of oxygen into hydrogen peroxide and superoxide anion (during the reperfusion stage) (Badwey and Karnovsky, 1980). Tissue resident macrophages have been shown to be sources of reactive oxygen species. For example, Kupffer cells (resident liver macrophages) isolated from post-ischemic livers demonstrated increased superoxide generation *in vitro* (Caldwell-Kenkel et al., 1991). Neutrophils have also been implicated

in ischemia-reperfusion injury. Neutrophils have been observed in post-ischemic tissue and it has been demonstrated that blocking infiltration or depletion of these cells has a protective effect in various models of ischemia-reperfusion injury (Hansen, 1995; Ma et al., 1991; Ma et al., 1993; Winn et al., 1993). The adhesion of neutrophils to vascular endothelium is accompanied by an oxidative burst, which is a mechanism by which neutrophils release myeloperoxidase (MPO) and produce superoxide anion by the NADPH-dependent oxidase (Chen et al., 1995; Jaeschke et al., 1992; Weiss, 1989). Endothelial cells are highly sensitive to physical forces resulting from blood flow variation and are able to transform these mechanical forces into electrical and biochemical signals (mechanotransduction) (Lansman, 1988). The absence of the mechanical component of flow during lung ischemia stimulates membrane depolarization of endothelial cells with the activation of NADPH oxidase, NF-κβ, and calcium/calmodulin-dependent nitric oxide synthase (Al-Mehdi et al., 1998).

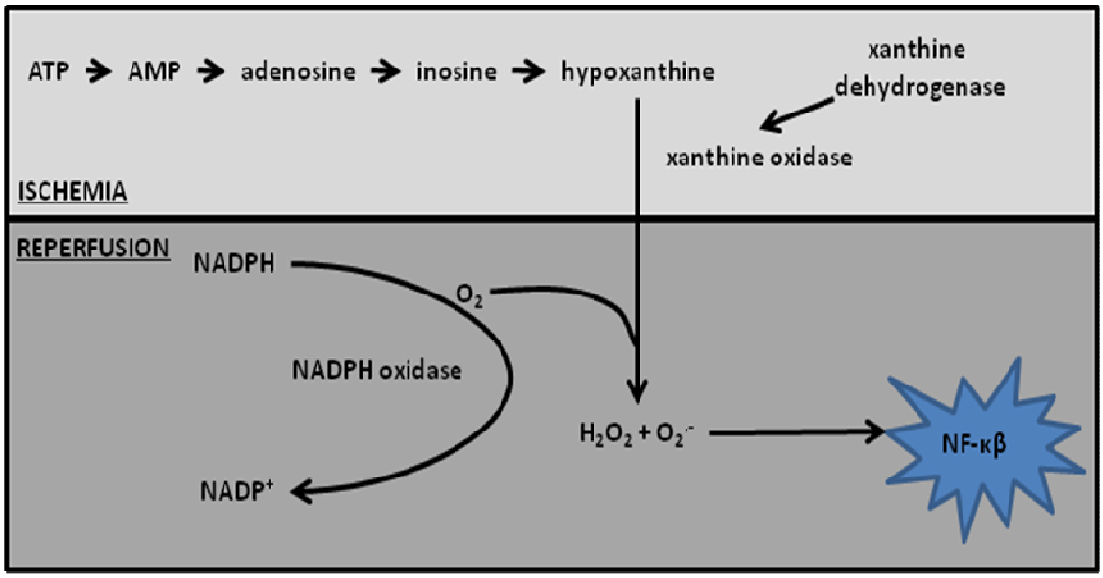

Figure 3. Formation of reactive oxygen species during ischemia-reperfusion injury and subsequent activation of NF-κβ

1.2.2.2. Release of pro-inflammatory mediators

Clinical and experimental studies have shown that ischemia-reperfusion of solid organs such as the kidney, liver, heart, and lung induces a rapid release of pro-inflammatory cytokines, (Table 2) (Gerlach et al., 1999; Lemay et al., 2000; Oz et al., 1995; Serrick et al., 1994). A potential mechanism for cytokine involvement in ischemia-reperfusion injury is upregulation of NF-κβ transcription of pro-inflammatory genes. NF-κβ is known to be activated in response to oxidative stress and it has been observed that levels of pro-inflammatory cytokines are elevated after reperfusion (Kaul and Forman, 1996; Sun and Oberley, 1996). NF-κβ is a member of the early immediate gene family and is a primary activator of pro-inflammatory cytokine transcription (including TNF-α, IL-1, IL-6, IL-8, PAF, and IFN-γ). The activity of these pro-inflammatory cytokines in ischemia-reperfusion injury is varied and complex, but they are postulated to propagate the initial xanthine oxidase driven reactive oxygen species response and the accompanying increase in vascular permeability and subsequent cell death (Herskowitz et al., 1995; Suzuki and Toledo-Pereyra, 1994).

The generation of bioactive lipids, which can serve as both intra- and extracellular mediators, has also been implicated in ischemia-reperfusion injury. Phospholipase A_2, which plays a pivotal role in the generation of these lipid mediators, has been detected in a wide variety of inflammatory conditions such as ischemia-reperfusion injury (Koike et al., 2000). The activation of phospholipase A_2 during ischemia-reperfusion injury induces the production of platelet-activating factor (PAF), an extraordinarily potent mediator of inflammation, and mobilizes arachidonic acid from the membrane lipid pool, which will

then be degraded by two major pathways into eicosanoids (Kim et al., 2000; Stammberger et al., 1999).

Cytokine	Cell Source	Function
TNF-α	Macrophages, lymphocytes	Pro-inflammatory
IFN-γ	Lymphocytes	Pro-inflammatory
MCP-1	Immune cells, lung epithelial cells	Macrophage chemotaxis
IL-1β	Macrophages, fibroblasts	Pro-inflammatory
IL-2	Lymphocytes	T-cell proliferation
IL-6	Macrophages, endothelial cells, epithelial cells	Pro-inflammatory
IL-8	Macrophages, epithelial cells, fibroblasts	Neutrophil chemotaxis
IL-10	Macrophages, lymphocytes	Anti-inflammatory
IL-12	Macrophages	T-cell activation
IL-18	Macrophages	T-cell activation

Table 2. Source and function of cytokines potentially involved in ischemia-reperfusion injury

IL: interleukin; MCP-1: macrophage chemoattractant protein-1; TNF: tumor necrosis factor

1.2.3. T-Cells in ischemia-reperfusion injury: experimental evidence

Historically, the inflammatory response to acute ischemia was believed to be directed by predominantly an innate immune response. B- and T-cells constitute the major mediators of the adaptive immunity and were not thought to play a role in the pathogenesis of ischemia-reperfusion injury. Recent data suggests that this is not the case and clearly lymphocytes have a significant role in the response to ischemia-reperfusion injury in a variety of organ systems. Since there is an overwhelming body of literature that has implicated T-cells in ischemia-reperfusion injury pathology, we will only discuss the major contributions to the field.

In 1994, Schroeter *et al.*, identified an influx of T-cells into the post-ischemic brain within 24 hours of reperfusion (Schroeter et al., 1994). To demonstrate that these cells were the mediators of brain ischemia-reperfusion injury, $Rag1^{-/-}$ mice (no mature T- or B-cells) have been utilized in many models. In 2006, Yilmaz *et al*. demonstrated that $Rag1^{-/-}$ mice, subjected to middle cerebral artery occlusion had significantly reduced cerebral infarct size and neurologic damage compared to wild-type mice (Yilmaz et al., 2006). Furthermore, they showed that this injury could be reconstituted with splenocytes from wild-type mice. In the same study, the authors also showed that mice deficient of $CD8^+$ T cells, $CD4^+$ T cells, and interferon (IFN)-γ had reduced volume of cerebral infarct compared to wild-type mice.

T-cells have also been implicated in lung ischemia-reperfusion injury. Using a syngeneic lung transplant model in Lewis rats, de Perrot *et al.* demonstrated that recipient $CD4^+$ T cells infiltrated lung grafts within 1 hour of reperfusion (de et al., 2003). Furthermore, they demonstrated that T-cell deficient nude rats (rnu/rnu) were protected

from developing lung ischemia-reperfusion injury. When compared to the nude rats, wild-type rats had a more severe injury as indicated by decreased oxygenation, increased peak airway pressures, and higher levels of IFN-γ. In the same study, nude rats that were reconstituted with T-cells from wild-type rats developed the same injury pattern seen in wild-type rats after 12 hours of reperfusion.

T-cells have also been demonstrated to be pathogenic during myocardial ischemia-reperfusion injury. Yang *et al.* evaluated myocardial infarct size in $Rag1^{-/-}$ mice and controls following 45 minutes of left anterior descending coronary artery occlusion (Yang et al., 2006). $Rag1^{-/-}$ mice had significantly smaller infarct size compared to that of control mice. After the adoptive transfer of $CD4^+$ T-cells, but not $CD8^+$ T-cells, into $Rag1^{-/-}$ mice, the infarct size was significantly greater than that of the control $Rag1^{-/-}$ mouse. Furthermore, $Rag1^{-/-}$ mice reconstituted with $CD4^+$ T-cells from IFN-$\gamma^{-/-}$ mice showed no increase in infarct size indicating that this cytokine might be an important mediator of ischemia-reperfusion injury.

T-cells have also been implicated in hepatic ischemia-reperfusion injury. In 1997, Zwacka *et al.* demonstrated that T-cell deficient (nu/nu) mice had significantly reduced injury post-lobar hepatic ischemia-reperfusion as compared to control BALB/c mice (Zwacka et al., 1997). They also showed that *in vivo* depletion of $CD4^+$ T-cells in wild-type mice also resulted in decreased injury, and that the adoptive transfer of $CD4^+$ T-cells, but not $CD8^+$ T-cells, into the nu/nu mice restored the injury.

Various studies have also implicated T-cells in renal ischemia-reperfusion injury. In 2001, Burne *et al.* examined the effects of renal ischemia-reperfusion injury on T-cell-deficient mice (nu/nu), CD4-deficient mice ($CD4^{-/-}$), and CD8-deficient mice ($CD8^{-/-}$)

(Burne et al., 2001). Both the nu/nu mice and $CD4^{-/-}$, but not the $CD8^{-/-}$, mice had significantly less injury as compared to wild-type mice. Adoptive transfer with T-cells from wild-type mice into nu/nu mice or with $CD4^{+}$ T-cells into the $CD4^{-/-}$ mice reconstituted the renal ischemia-reperfusion injury phenotype. Taken together, this body of work suggests that $CD4^{+}$ T-cells are the mediators of tissue ischemia-reperfusion injury perhaps through an IFN-γ cytokine driven path.

1.2.4. Ischemia-reperfusion injury in sickle cell disease

As stated above, the pathophysiology of sickle cell disease is believed to be due to chronic ischemia-reperfusion injury. It has been postulated that vaso-occlusion leads to the production of oxygen free radicals and activation of the transcription factor NF-κβ, which in turn up-regulates the transcription of various inflammatory mediators. In sickle cell disease, oxidative damage to the blood vessel wall is likely a critical component of the pathogenesis of vaso-occlusion (Kaul and Hebbel, 2000; Osarogiagbon et al., 2000). Proposed mechanisms of oxidative damage include the release of xanthine oxidase from livers damaged by acute episodic sickling-induced ischemic injury, sickle red blood cells that generate reactive oxygen species, and mononuclear cell production of superoxide anion, which inactivates nitric oxide (Aslan et al., 2001; Dias-Da-Motta et al., 1996; Hebbel et al., 1982). The pro-inflammatory, pro-coagulatory, and pro-adhesive phenotype observed in individuals with sickle cell disease and transgenic mouse models results in conditions that favor vaso-occlusion and perpetuation of ischemia-reperfusion injury, which eventually leads to end-organ damage. Current evidence suggests that vaso-

occlusion in sickle cell disease is mediated by endothelial cell, sickled red blood cell, and leukocyte interactions, which can lead to blood flow abnormalities and ischemic episodes. Therefore, sickle cell disease can be thought of as a disease of ischemia-reperfusion injury and the mechanisms and treatments for ischemia-reperfusion injury may be applied to sickle cell disease.

1.3. NKT Cells

1.3.1. Background

In normal individuals, NKT cells comprise a relatively minor subset of lymphocytes (~0.5 % of the T-cell population in the blood and peripheral lymph nodes, ~2.5 % of T-cells in the spleen, mesenteric, and pancreatic lymph nodes, and up to 30 % of T-cells in the liver) (Bendelac et al., 2007). In the mouse, the greatest numbers of NKT cells are found in the liver, bone marrow, and thymus; intermediate numbers in the lung, spleen, and blood; and the lowest numbers in the lymph node (Eberl et al., 1999; Matsuda et al., 2000). In a normal inflammatory response against pathogens it is believed that NKT cells bridge the innate and adaptive immune system by their ability to promptly release copious amounts of cytokines (Th1 or Th2) and interact with a variety of cells from the innate immune system. For example, although the mechanism is unknown it has been reported that NKT cells provide an early host protection against *Streptococcus pneumonia* by promoting the trafficking of neutrophils into airways (Kawakami et al., 2003). Along with contributing to a normal antimicrobial response, NKT cells have been shown to participate in antitumor immunity and the balance between tolerance and autoimmunity (Brigl and Brenner, 2004).

iNKT cells, also known as type I, express a restricted TCR [Vα14-Jα18 (murine) or Vα24-Jα18 (human)] that is activated by lipid antigen presentation by CD1d (an MHC-I like molecule) found on antigen presenting cells (APCs) (Brigl and Brenner, 2004; Trobonjaca et al., 2001). It is believed that CD1d is present on resting APCs at all times allowing CD1d and iNKT cells to function at early points during host response to infection or other challenges. While resting myeloid lineage cells express low levels of CD1d, circulating and splenic B-cells express very high levels. Furthermore, CD1d is also expressed on epithelial cells, parenchymal cells, and vascular smooth muscle cells. Within minutes of engagement of the CD1d-lipid to the invariant TCR and co-stimulatory molecules, iNKT cells become activated and secrete large amounts of cytokines (Brigl and Brenner, 2004). The most well characterized CD1d-restricted ligand is α-galactosylceramide (α-GalCer), a marine sponge-derived glycolipid that specifically activates iNKT cells. CD1d activation has also been hypothesized to occur as a result of presentation of host lipids that are byproducts of the degradation of necrotic or apoptotic cells (Boyton, 2008). Type II NKT cells express more diverse lipid-binding TCRs and are CD1d restricted but unresponsive to α-GalCer; type III NKT cells have diverse TCRs (Taniguchi et al., 2003).

Upon TCR activation, iNKT cells rapidly release large quantities of cytokines including IL-4, IL-2 and IFN-γ, which promote activation of dendritic cells (DCs), NK cells, B cells, and conventional $CD4^+$ and $CD8^+$ T-cells (Kinjo et al., 2005; Kronenberg and Gapin, 2002; Mattner et al., 2005; Zhou et al., 2004). Furthermore, IFN-γ can stimulate endothelial, epithelial, neuronal, and lymphoid cells to release IFN-γ inducible CXC chemokines (MIG/CXCL9, IP-10/CXCL10, and ITAC/CXCL11), which are potent

chemoattractants for mononuclear cells that express CXCR3 (i.e. activated NKT, T-, and NK cells) (Agace et al., 2000; Gasperini et al., 1999; Sauty et al., 1999; Singh et al., 2007; Thomas et al., 2003).

1.3.2. iNKT cells and disease

iNKT cells have been implicated in a wide variety of disease conditions. However, at present, the mechanism of iNKT cell involvement in these diseases has yet to be determined. Although controversial, iNKT cells have been reported to play a role in mediating type 1 diabetes, systemic lupus erythematosus, cancer, asthma, and atherosclerosis (Forestier et al., 2005; Gombert et al., 1996; Lisbonne et al., 2003; Tahir et al., 2001; Tupin et al., 2004). Also recently, iNKT cells have been implicated in ischemia-reperfusion injury. In 2006, Lappas *et al.* demonstrated the role of CD1d restricted NKT cells in mediating liver ischemia-reperfusion injury (Lappas et al., 2006). Mice pre-treated with anti-CD1d (inhibits CD1d-restricted NKT cell activation) were found to have decreased liver injury as compared to isotype treated mice. Furthermore, they demonstrated that the adoptive transfer of iNKT cells into $Rag1^{-/-}$ mice was sufficient to reconstitute liver ischemia-reperfusion injury. Furthermore, in 2007, Li *et al.* implicated iNKT cells in renal ischemia-reperfusion injury (Li et al., 2007). They demonstrated protection from renal ischemia-reperfusion injury in mice pre-treated with anti-CD1d or in transgenic mice that lack iNKT cells ($J\alpha18^{-/-}$).

1.4. Adenosine

1.4.1. Background

Under normal conditions, adenosine is a constitutively active purine nucleoside that is released from various cells, including fibroblasts, epithelial cells, endothelial cells, platelets, and muscle cells, or it is formed extracellularly by the metabolism of released purine nucleotides (Figure 4). Intracellular adenosine production occurs primarily as a result of the breakdown of adenosine triphosphate (ATP) in response to cellular energy demands, with the rate-limiting step being the dephosphorylation of adenosine monophosphate (AMP) by CD73, a 5'-nucleotidase that exists as a soluble cytoplasmic enzyme and as an ectoenzyme (Dunwiddie et al., 1997; Zimmermann, 2000). Upon release, adenine nucleotides can be rapidly dephosphorylated by membrane bound ectonucleotidases (the apyrase, CD39, and CD73) into adenosine. Adenosine is transported between extracellular and intracellular stores by both equilibrative transporters (ENTs), which mediate the equilibrium of adenosine concentrations by facilitated transport, and concentrative transporters (CNTs), which allow for the preservation of adenosine concentration gradients across cell membranes (Anderson et al., 1996; Huang et al., 1994; Williams and Jarvis, 1991). Adenosine is very rapidly metabolized by extracellular or intracellular adenosine deaminase, resulting in the production of inosine, or phosphorylated by intracellular adenosine kinase to form AMP (Arch and Newsholme, 1978; Lloyd and Fredholm, 1995). Adenosine concentrations vary greatly by tissue and physiological state. Levels can increase dramatically (100-fold) during metabolically demanding conditions of oxidative stress, hypoxia, exercise, or inflammation (Latini et al., 1999a; Latini et al., 1999b; Rudolphi et al., 1992b; Rudolphi

et al., 1992a; Vizi et al., 2002). In particular, hypoxia has been shown to inhibit adenosine kinase, which converts adenosine into AMP (Decking et al., 1997).

Extracellular adenosine binds to a G-protein coupled family of cell surface receptors known as adenosine receptors (A_1, A_{2A}, A_{2B}, and A_3) (Fredholm et al., 2001). All four types of adenosine receptors have seven membrane spanning α-helices with an extracellular amino terminus and an intracellular carboxy terminal tail (Fredholm et al., 2001). Due to the large size of the adenosine receptors and their interactions with membrane lipids, it has proven difficult to obtain much structural information. However, studies with mutated receptors indicate that receptor-ligand interactions occur in helices 3, 5, 6, and 7 (Fredholm et al., 2001). Adenosine receptor expression and effects varies widely by tissue and subtype (Table 3).

It has been shown that endogenous adenosine has protective actions for many organ systems, such as the heart, brain, kidney, skeletal muscle, and adipose tissue (Hasko and Cronstein, 2004). This evidence led Newby to hypothesize that adenosine acts as a "retaliatory metabolite" that protects the cell against excessive external stimulation (Newby et al., 1985). Therapeutically, adenosine itself has been used to terminate supraventricular tachyarrhythmias and as a coronary vasodilator for pharmacological stress imaging. However, due to its short half-life and non-specific binding to all four adenosine receptors, the development of new pharmacological agents to specific receptors has recently become an interesting therapeutic topic for multiple conditions, specifically in the treatment of CNS disorders, cardiovascular disease, ischemia-reperfusion injury, and inflammatory diseases.

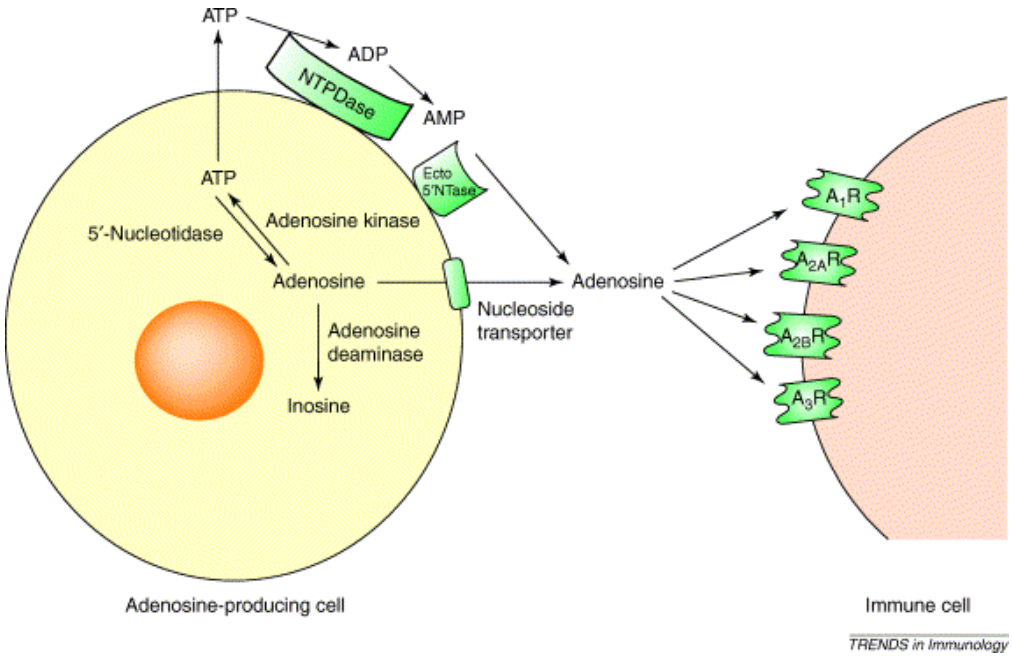

Figure 4. Major pathways involved in adenosine metabolism

(Hasko and Cronstein, 2004)

Receptor	Coupling	Location	Agonist Effect
A_1R	G_i/G_o	Brain	Sedation
		Kidney	Anti-diuresis
		Heart	Negative inotropic, preconditioning
$A_{2A}R$	G_s	Striatum	Inhibition of locomotion
		Vascular smooth muscle	Dilation
		Inflammatory cells	Anti-inflammatory
$A_{2B}R$	G_s/G_q	Mast cells	Degranulation, pro-inflammatory
		Endothelium	Dilation, angiogenesis
		Gut epithelium	Water secretion
		Muscle, liver	Glucose formation
A_3R	G_i	Eosinophils	Degranulation, pro-inflammatory
		Rodent mast cells	Degranulation

Table 3. Adenosine receptor subtype expression and function

(Fredholm et al., 2001)

1.4.3. $A_{2A}R$ agonists and inflammation

Recently, it has been shown that adenosine protects through modulation of the immune system. The $A_{2A}R$ is expressed on virtually all inflammatory cells including neutrophils, monocytes, eosinophils, and lymphocytes, as well as epithelial and endothelial cells (Gessi et al., 2000). In particular, studies have shown that activation of $A_{2A}R$ reduces ischemia-reperfusion injury in the heart, lung, liver, and kidney by decreasing neutrophil accumulation, superoxide generation, endothelial adherence, and the expression of adhesion molecules (Harada et al., 2000; Jordan et al., 1997; Okusa et al., 2000; Ross et al., 1999; Thiel et al., 2003). In addition, $A_{2A}R$ agonists have been shown to inhibit the phosphorylation of ZAP70, a critical step in T-cell activation, and suppress perforin and FASL-mediated cytotoxicity in NK cells (Raskovalova et al., 2006; Sevigny et al., 2007).

During a response to infection, it is vital to have an active immune response. However, inappropriately high or prolonged activity can result in host tissue destruction. It is believed that adenosine, which is released from damaged tissues, signals through $A_{2A}R$ to inhibit further inflammatory activity and thereby act as an endogenous regulator of inflammation. Therefore, the development of specific $A_{2A}R$ agonists as anti-inflammatory compounds has been of great interest to many groups and many agonists have been synthesized (Figure 5). The potent and selective $A_{2A}R$ agonist ATL146e (4-{3-[6-Amino-9-(5-ethylcarbamoyl-3,4-dihydroxy-tetrahydro-furan-2-yl)- 9H-purin-2-yl]-prop-2-ynyl}-cyclohexanecarboxylic acid methyl ester) has been shown *in vivo* to exert protective effects in various models of inflammation, including lung transplant, arthritis, sepsis, and ischemia-reperfusion injury in the liver, kidney, and lung (Cohen et al., 2004;

Day et al., 2003; Day et al., 2004; Gazoni et al., 2008; Reece et al., 2005; Sullivan et al., 2004).

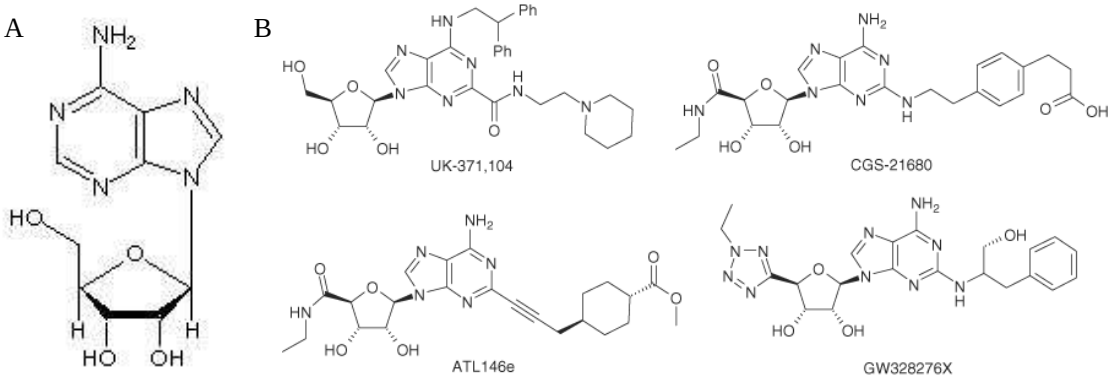

Figure 5. Adenosine and prototypical $A_{2A}R$ agonists

(**A**) Adenosine (**B**) Specific $A_{2A}R$ agonists

1.4.3.1. Lung inflammation and the role of A_{2A}Rs: experimental evidence

Many studies have demonstrated the use of A_{2A}R agonists in inhibiting lung inflammation. In 2002, Fozard *et al.*, were the first to report that A_{2A}Rs were important in regulating lung inflammation. Following sensitization and challenge with ovalbulmin, rats received intra-tracheal injections of A_{2A}R agonists (Fozard et al., 2002). They showed a decrease in the number of eosinophils and neutrophils in the bronchial alveolar lavage fluid (BALF) in rats treated with the A_{2A}R agonists and that this effect was blocked by A_{2A}R antagonists. Bonneau *et al*., in 2006, treated ovalbumin sensitized and challenged mice with inhaled A_{2A}R agonists and found decreased infiltration of neutrophils, eosinophils, macrophages, and lymphocytes into the BALF (Bonneau et al., 2006). Further supporting the role of A_{2A}Rs in lung inflammation has been the use of $A_{2A}R^{-/-}$ mice. In 2007, Reutershan *et al*. demonstrated that A_{2A}R agonists inhibited LPS-induced neutrophil infiltration into the BALF and that $A_{2A}R^{-/-}$ mice treated with A_{2A}R agonists were not protected (Reutershan et al., 2007). Also in 2007 Nadeem *et al*., showed that ragweed-sensitized $A_{2A}R^{-/-}$ mice had increased airway reactivity over wild-type mice as demonstrated by increased lymphocytes, eosinophils, and neutrophils in the BALF (Nadeem et al., 2007). Taken together, this experimental evidence demonstrates a role of A_{2A}R in controlling inflammation in the lung: first, selective A_{2A}R agonists inhibit inflammation; second, lung inflammation is increased in $A_{2A}R^{-/-}$ animals; and third, $A_{2A}R^{-/-}$ animals are not protected by A_{2A}R agonists.

1.4.4. Mechanisms of anti-inflammatory effects of $A_{2A}R$ agonism

Four main mechanisms have been proposed to explain the anti-inflammatory effects of $A_{2A}R$ agonists: increases in oxygen supply/demand ratio, ischemic pre-conditioning and post-conditioning, anti-inflammatory responses, and angiogenesis (Linden, 2005). At present, very few of these mechanisms have been studied in the lung. The anti-inflammatory effects can be discussed under two broad categories: one, the biochemical mechanisms; and two, the target cells responsible for the anti-inflammatory actions.

Biochemically, the $A_{2A}R$ is linked to Gs, a signaling protein that when activated stimulates the formation of cAMP. The downstream signaling pathways used by $A_{2A}Rs$ vary with the type of cell and the signaling machinery that the cell possesses. Activation of $A_{2A}Rs$ is known to increase mitogen-activated protein kinases (MAPK), which are serine/threonine specific protein kinases that respond to extracellular stimuli and regulate various cellular activities (gene expression, mitosis, differentiation, and cell survival). Also, regulation of NF-κβ activity has been proposed as one potential anti-inflammatory biochemical mechanism. Nadeem *et al*. demonstrated that $A_{2A}R^{-/-}$ mice had increased phosphorylation of lung Iκβα (inhibitor of NF-κβ nuclear translocation when dephosphorylated), which resulted in increased lung levels of NF-κβ transcription of pro-inflammatory genes (Nadeem et al., 2007). Supporting this data, splenocytes from $A_{2A}R^{-/-}$ mice challenged with LPS were shown to have increased mRNA levels of NF-κβ associated pro-inflammatory cytokines, and wild-type animals challenged with LPS pre-treated with $A_{2A}R$ agonists inhibited LPS-induced mRNA cytokine expression (Lukashev et al., 2004).

Understanding of the potential target cell mediators involved in the anti-inflammatory mechanism of $A_{2A}R$ agonists is derived mainly from studies involving ischemia-reperfusion injury. Ischemia-reperfusion injury is associated with tissue damage during ischemia and further damage upon reperfusion. During reperfusion, tissues damage is believed to be mediated by a combination of reactive oxygen species, nitric oxide, inflammatory cells, cytokines, eicosanoids, the complement cascade, endothelial cells, and adhesion molecules. Numerous studies have demonstrated that the anti-inflammatory actions of $A_{2A}R$ agonists on ischemia-reperfusion injury are due to effects on $CD4^+$ T-cells (Day et al., 2003; Lappas et al., 2006; Yang et al., 2006). Importantly, in 2006, Lappas *et al*. noted that the rapid induction of reperfusion injury was not consistent with the known time course for activation of conventional $CD4^+$ T-cells and that injury must be mediated by a rapidly activated T-cell subset (Lappas et al., 2006). Their studies demonstrated that CD1d restricted NKT cells were the initiators of reperfusion injury as well as the target cell of the anti-inflammatory effects of $A_{2A}R$ agonists.

1.5. Current treatment strategies to limit sickle cell disease pathophysiology

Treatment strategies for individuals with sickle cell disease are quite complex and require close monitoring by health care workers. Briefly, current treatment includes prophylactic and liberal use of antibiotics during infections, transfusion therapy, pain management, and hydroxyurea (Hebbel, 2005). Liberal use of antibiotics has been shown to significantly reduce the risk of infection and death. However, since the early 1990s, antibiotic-resistant strains of various bacteria have emerged (Adamkiewicz et al., 2003). Repeated transfusion complications include iron overload and viral transmission, and

transfusion therapy has been shown to have limited value (Hebbel, 2005). The mainstays for pain treatment include NSAIDs and opiods, however it has been well documented that continual use of narcotics can lead to addiction by individuals with sickle cell disease and undertreatment by healthcare providers (Kirsh et al., 2002).

Although studies have shown an overall benefit of hydroxyurea in sickle cell disease (postulated via stimulation of HbF production), 10-50 % of individuals do not respond to treatment (Charache et al., 1995). Due to the mechanism of action of hydroxyurea (inhibition of ribonucleotide reductase that inhibits DNA synthesis and repair, which ultimately leads to S-phase cell death), a major concern is that long-term hydroxyurea therapy may be carcinogenic or leukemogenic, which has already been documented in individuals treated with hydroxyurea for polycythemia vera (Dalton et al., 2005). While these therapies have increased the lifespan of individuals with sickle cell disease, morbidity and mortality still remain relatively high with most individuals dying prematurely. Therefore, there is a pressing need for new treatments with minimal side effects.

1.6. Project rationale

As described above there is a plethora of evidence that exists to support the concept that the pathophysiology of sickle cell disease is due to chronic ischemia-reperfusion injury. The pro-inflammatory, pro-coagulatory, and pro-adhesive phenotype observed in individuals with sickle cell disease and transgenic mouse models results in conditions that favor vaso-occlusion and perpetuation of ischemia-reperfusion injury, which eventually caused end-organ damage. Current evidence suggests that vaso-

occlusion in sickle cell disease is mediated by endothelial cell, sickled red blood cell, and leukocyte interactions, which can lead to blood flow abnormalities and ischemic episodes and sickle cell disease can be thought of as a disease of ischemia-reperfusion injury. However, the exact mechanism of vaso-occlusion and ischemia-reperfusion injury in sickle cell disease is unknown. As noted above, recent data suggests that iNKT cells are the upstream mediators of ischemia-reperfusion injury. Also, $A_{2A}R$ agonists have recently been shown to decrease ischemia-reperfusion injury by inhibiting iNKT cell activation. Taken together, these data suggest that iNKT cells may be involved in ischemia-reperfusion injury in sickle cell disease and that $A_{2A}R$ agonists may be useful in inhibiting iNKT cell mediated injury. Therefore, in the following pages we will explore the mechanism of iNKT cells and $A_{2A}R$ agonists in sickle cell disease.

2. Methods

2.1. Mouse model

Many murine genetic models of sickle cell disease exist (Nagel and Fabry, 2001). There is no single best model and the model you choose depends on the questions asked. In this study, since were interested in investigating sickle cell disease pulmonary dysfunction at baseline, we needed to utilize a model of moderate disease. A well characterized experimental model of moderate sickle cell disease is the NY1DD mouse ($\alpha^{H}\beta^{S}[\beta^{MDD}]$), which was created by Fabry in 1992 and is homozygous for a spontaneous deletion of mouse β^{major}-globin locus (β^{MDD}) and carries a human α- and β^{S}-globin transgene ($\alpha^{H}\beta^{S}$) (Fabry et al., 1992a; Fabry et al., 1992b). Like individuals with sickle cell disease at baseline, NY1DD mice exhibit a pro-inflammatory phenotype that is believed to contribute to morbidity and mortality (Belcher et al., 2003; Hofstra et al., 1996; Platt, 2000).

Two locus control regions (LCR), one containing the human α-globin gene and the other containing the human β^{S}-globin gene, were constructed. These constructs were purified and co-injected into fertilized eggs of FVB/N mice. The founders, containing copies of both human genes, were bred with wild-type FVB/N mice and the F1 offspring were screened for the inheritance of the transgenes. The founders that were able to transmit both of the transgenes ($\alpha^{H}\beta^{S}$) were used to make a transgenic line. However, only 36 % of all β-globins expressed were human β^{S}. In order to increase the expression of human β^{S} the FVB/N $\alpha^{H}\beta^{S}$ mice were crossed with mutant DBA/2J mice carrying a spontaneous mouse β^{major}-globin gene deletion ($Hbb^{d3[th]}$). Previous to the cross with the FVB/N $\alpha^{H}\beta^{S}$ the $Hbb^{d3(th)}$ mice were back crossed for 8 generations with C57BL/6J mice

and then bred to homozygosity for *Hbb*$^{d3(th)}$. Of the resulting offspring, mice heterozygous for the β^{major} deletion ($\alpha^{H}\beta^{S}[\beta^{MD}]$; MD, mouse deletion) had 54 % β^{S} expression and mice homozygous for the β^{major} deletion ($\alpha^{H}\beta^{S}[\beta^{MDD}]$) had 72.5 % β^{S} expression. Furthermore, mice homozygous for the human $\alpha^{H}\beta^{S}$ transgene were not observed, indicating a lethal combination.

Two NY1DD breeding pairs were provided as a gift from Dr. Robert Hebbel (Department of Medicine, University of Minnesota Medical School, Minneapolis, MN). The NY1DD mice, heterozygous for the human $\alpha\beta^{S}$ transgene and homozygous for the mouse β^{major}-globin deletion, were phenotyped by their hemoglobin iso-electric pattern. The observed offspring from breeding mice with the same hemoglobin iso-electric patterns are 33 % β-thalassemic (β^{MDD}) and 66 % heterozygous ($\alpha^{H}\beta^{S}[\beta^{MDD}]$). The heterozygous mice are used for experimentation (12- to 16-weeks-old) and breeding and the β-thalassemic mice are euthanized. Congenic 12- to 16- week-old wild-type C57BL/6J mice (Jackson Laboratory) are used as controls for experimentation.

NY1DD x Rag1$^{-/-}$ and NY1DD x $A_{2A}R^{-/-}$ mice were created by crossing NY1DD mice with either Rag1$^{-/-}$ or $A_{2A}R^{-/-}$ mice, both on a C57BL/6J background and identified by PCR for the NY1DD human β^{S}-globin transgene, mouse B^{major} deletion, and the Rag1$^{-/-}$ or $A_{2A}R^{-/-}$ deletion (Table 4). All animal protocols were approved by the Institutional Animal Care and Use Committee of the University of Virginia.

Gene	Primer	Sequence (5' – 3')
Human β^S (*HBB)*	Forward	CATGTGGAGACAGAGAAGACTC
	Reverse	CGAGCTTAGTGATACTTGTGGG
Murine β^{major} (*Hbb-b1*)	Forward	CCCTCTACGGAATGTTATGGTC
	WT Reverse	GAGCCAAGTAGGAAGAAGGTAG
	DAI Reverse	GTGATTAAGCAAAAAGAATTTTTAAGTGTAAATTT
Murine *Rag-1*	Forward	GAGGTTCCGCTACGACTCTG
	WT Reverse	TGGATGTGGAATGTGTGCGAG
	KO Reverse	CCGGACAAGTTTTTCATCGT
Murine $A_{2A}R$ (*Adora2a*)	Forward	GGGCTCCTCGGTGTACAT
	WT Reverse	CCCACAGATCTAGCCTTA
	KO Reverse	TGTCACGTCCTGCACGAC

Table 4. PCR primers for identification of NY1DD backcrosses

DAI: Deletion associated insertion; WT: wild-type; KO: knock-out.

2.2. Human subjects

Blood samples were obtained from individuals with sickle cell disease (HbSS), ages 19 years and older, as well as age and race matched controls. Samples were taken from individuals with sickle cell disease during a routine office visit to the Adult Hemoglobinopathy Clinic at Washington University when the participant reported no more than typical pain. Sickle cell disease diagnoses were confirmed by hemoglobin analysis. Age matched African American controls were healthy employees of Washington University, who were also appropriately consented for study participation. All human protocols were approved by the Institutional Review Board at Washington University and the University of Virginia.

2.3. Vascular permeability

Pulmonary vascular permeability was evaluated by measurement of Evans blue dye extravasation. Evans blue dye (30 mg/kg body weight, 200 µl) was injected i.v. in anesthetized mice and allowed to circulate for 30 min. The chest was opened, the inferior vena cava transected, and the pulmonary vasculature flushed with 10 ml of saline via the right ventricle to remove excess intravascular dye. The lung lobes were removed, weighed, homogenized, and incubated in 100 % formamide at 37 ^{o}C for 24 hours to extract Evans blue dye. The concentration of Evans blue dye extracted was analyzed by spectophotometry. Correction of optical densities (*E*) for contaminating heme pigments was performed as previously described, using the equation: E_{620}(corrected) = E_{620} – (1.426 X E_{740} + 0.03) (Wang et al., 2001). Data is presented as µg Evans blue dye per g lung.

2.4. Arterial oxygen saturation (% SO_2)

Animals were anesthetized and the skin and musculature over the left chest were dissected. A left ventricular heart puncture was performed with a heparinized syringe and 150 µl of arterial blood collected for gas analysis (Osmetech OPTI^{TM} CCA).

2.5. Pulmonary immunohistochemistry and histopathological grading

Mice were sacrificed, the chest opened, the inferior vena cava transected, the pulmonary vasculature flushed with 10 ml of saline via the right ventricle. The lungs were inflation fixed with 1 % paraformaldehyde-lysine-periodate (PLP) at a height of 25 cm. Five µm paraffin sections were stained with hematoxylin and eosin (H&E). Sections were hydrated and incubated with Antigen Unmasking Solution (Vector) for antigen retrieval and counter stained with hematoxylin. Analysis of histopathological changes was performed by a blinded pathologist using a modified histological scoring system as previously described (Belperio et al., 2002a; Imanaka et al., 2001). Two criteria were used for scoring: capillary congestion and alveolar wall thickness. Sections were graded by assigning a score: 0, absent; 1, mild; 2, moderate; 3, severe; and 4, very severe. The individual scores were combined to obtain an overall score ranging from 0 to 8. The mean was generated for each group of animals (three sections from each lung, four lungs per group) to generate a cumulative histological score.

2.6. Unrestrained whole body plethysmography

Frequency of breathing and tidal volume were evaluated using unrestrained whole body plethysmography. Mice were placed into calibrated plexiglas chambers that were connected to a direct airflow sensor (Buxco Max II, Buxco Electronics, Inc). Airflow through the chambers was maintained at 70 ml/min. The flow signals were recorded using IOX software (EMKA Technologies). Respiratory function was recorded for 20 min and averaged following a 20 min adjustment period.

2.7. Peripheral blood smear

Blood was obtained via retro-orbital bleeding and one drop was placed onto the end of a glass slide. Quickly a blood smear (1 cell layer thick) was created by passing another glass slide over the blood droplet (Figure 6).

2.8. Tissue preparation

Animals were anesthetized, the chest wall opened, and the inferior vena cava was transected. The mouse was perfused with 15 ml saline via the left ventricle to remove non-adhered intravascular cells. Organs were removed and minced. Lungs and livers were incubated in digestion buffer (1 mg/ml collagenase type Ia, 60 U/ml hyaluronidase type I-s, 60 U/ml DNase1, 2 µl/ml BD GolgiPlug™) for 45 min at 37 ^{o}C. Single cell suspensions were created by passing tissue through a 40 µm cell strainer.

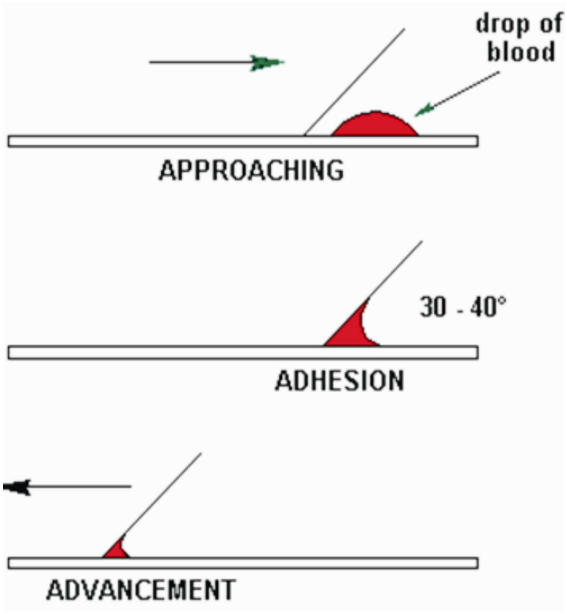

Figure 6. Peripheral blood smear technique

2.9. Immunostaining of cells for flow cytometry

Purified murine cells were washed twice (1 % BSA in PBS) and erythrocytes were lysed (Biolegend). Cells were washed and resuspended at 1 X 10^6 cells/ml in 100 µl of staining buffer (1 % BSA, 0.1 % sodium azide in PBS). Non-specific Fcγ receptor binding of labeled antibodies was blocked by incubation with CD16/32 (clone 93) for 10 min prior to primary antibody staining. iNKT cells were stained first with the anti-mouse αGalCer-analog (PBS57) loaded CD1d tetramer (controls were stained with unloaded CD1d tetramer) for 30 min at room temperature in the dark. Other leukocytes were then incubated for 30 min at 4 ^oC with various cell surface markers and a fixable LIVE/DEAD® stain was used for viability (Invitrogen). Cells were then washed, fixed, and permeabilized for intracellular staining.

Alternatively, 100 µl of whole human blood was stained. iNKT cells and other markers were stained as described above. However, immediately after non-bound cell surface markers and the fixable LIVE/DEAD ® stain were washed off, red blood cells were lysed. Cells were then washed, fixed, and permeabilized for intracellular staining.

Fluorescence intensity was measured with a CyAn™ ADP LX 9 Color analyzer (DakoCytomation) with 405 (450/50, 530/40 emitter filters), 488 (530/40, 575/25, 613/20, 680/30, 750LP emitter filters), and 642 (665/20, 750LP emitter filters) nm excitation lasers. Data analyses were performed with FlowJo software (Tree Star, Inc.). Gates to determine mouse leukocyte populations were created based upon fluorescence minus one staining and isotype staining of single (low pulse width), live ($Aqua^-$), and CD45-$PerCP^+$ (BD; 30-F11) cells. Murine, neutrophils were identified as anti-neutrophil-$FITC^+$ (Serotec; 7/4), CD11b-APC-$AF750^+$ (EBioscience; M1/70), and Ly-6G/GR1-

Pacific Blue^{+} (EBioscience; RB6-8C5). Murine NK cells were identified as NKp46-FITC^{+} (R&D; polyclonal) and CD3ε-Pacific Blue^{-} (EBioscience; 500A2). Murine iNKT cells were identified as CD1d-tetramer-AF647^{+} (NIH tetramer facility) and CD3ε-Pacific Blue^{+}. Murine CD4 T-cells were identified as CD1d-tetramer-AF647^{-}, CD3ε-Pacific Blue^{+}, and CD4-PEAF610^{+} (Caltag; L3T4). Murine CD8 T-cells were identified as CD1d-tetramer-AF647^{-}, CD3ε-Pacific Blue^{+}, and CD8α-APCAF750^{+} (EBioscience; 53-6.7) (Figure 7). Additional surface and intracellular activation markers used: CD69-PE (EBioscience; H1.2F3), IFN-γ-PE (EBioscience; XMG1.2), CXCR3-PE (R&D; 220803). Human iNKT cells were identified as: single (low pulse width), live (Aqua^{-}), and CD45-APCAF750^{+} (EBioscience; RAB-6B2), CD3-PEAF610^{+} (Caltag; S4.1), and CD1d-tetramer-APC^{+} (NIH tetramer facility) (Figure 8). Additional surface and intracellular activation markers used: CD69-PE (EBioscience; FN50), IFN-γ (EBioscience; 4S.B3), CXCR3-FITC (R&D; 49801).

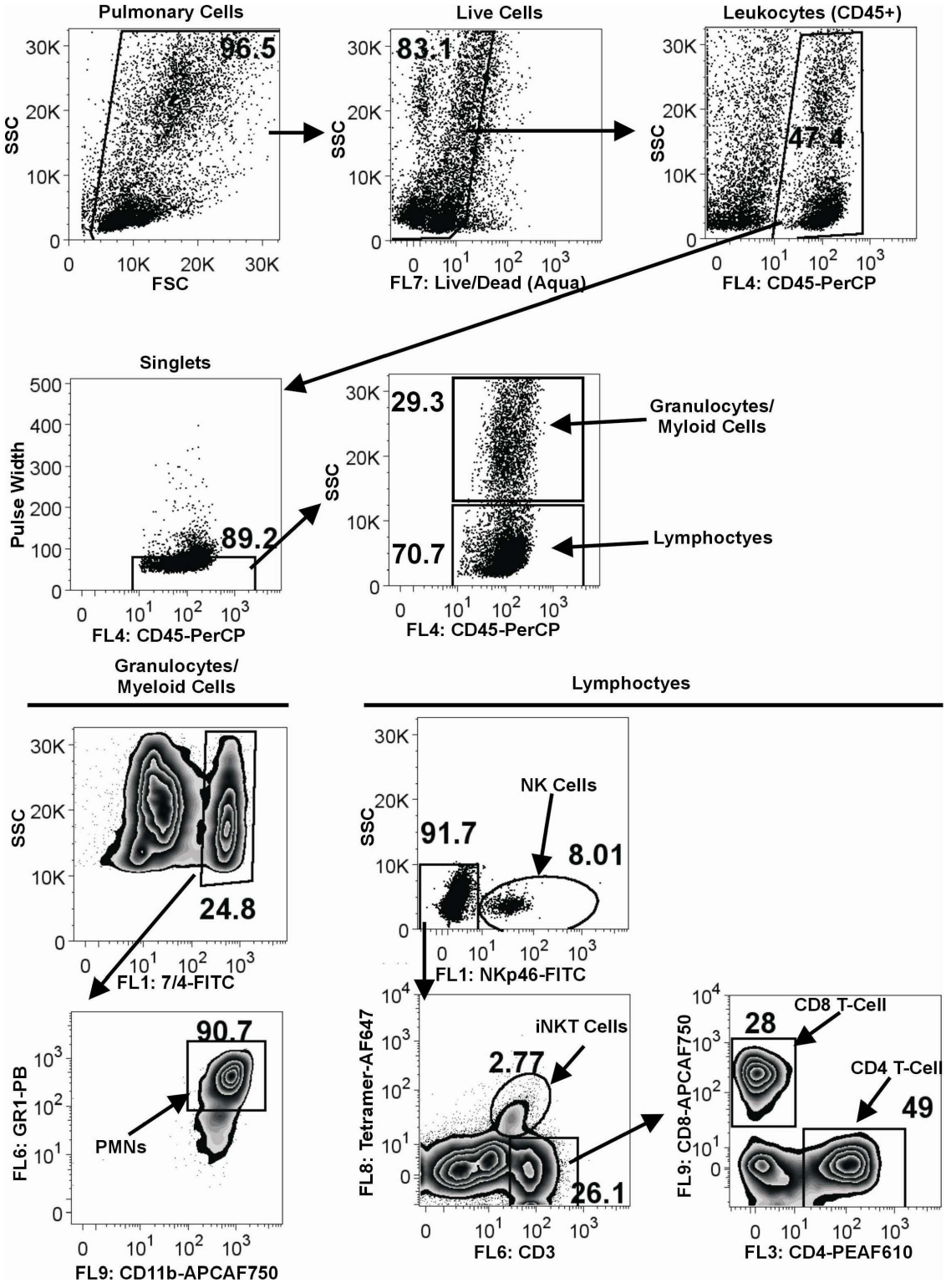

Figure 7. Flow cytometric analysis of murine pulmonary lymphocytes

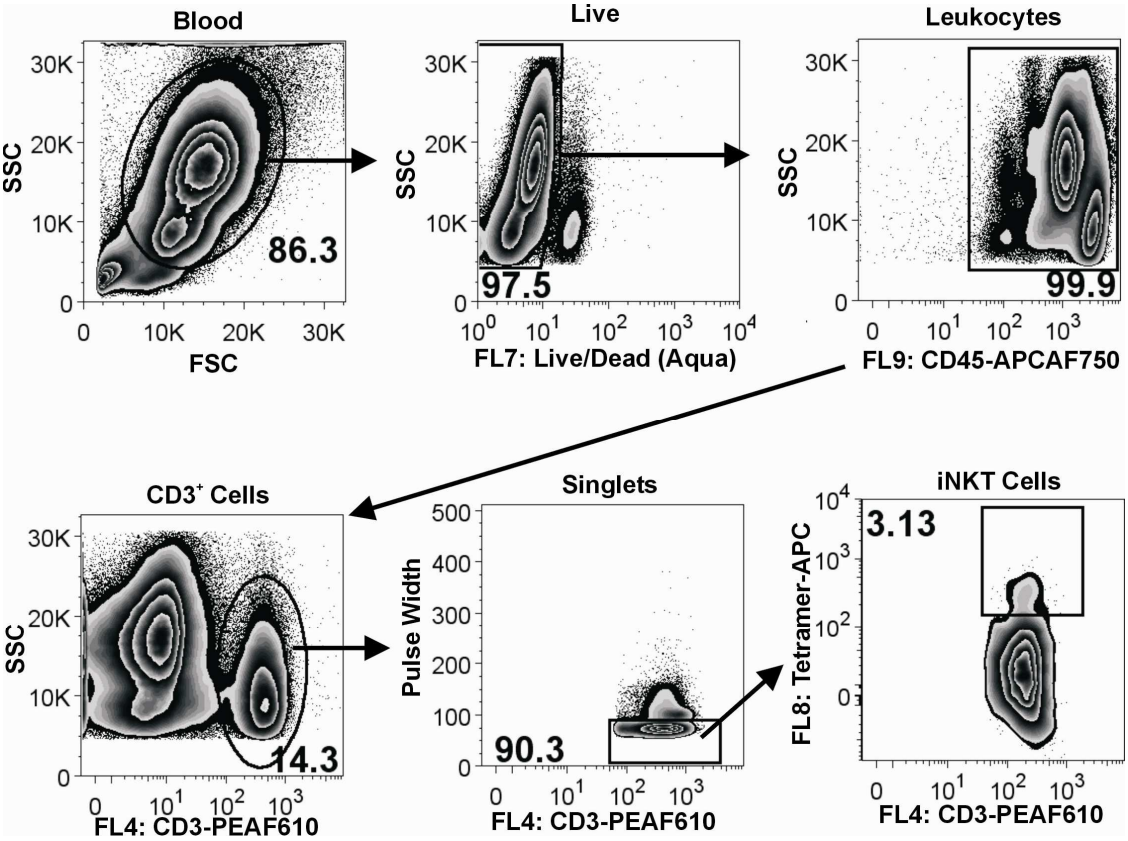

Figure 8. Flow cytometric analysis of human blood

2.10. Determination of absolute numbers of leukocytes

Counting beads (Invitrogen) were added to each sample before flow cytometric analysis. After analysis, the absolute number of pulmonary leukocytes was determined from the following formula:

Total # cells per lung = [(# events in gate)*(total # beads added)/(# beads collected)]*dilution of sample

2.11. Cell sorting and quantitative RT-PCR for $A_{2A}R$

Live ($DAPI^-$) leukocytes ($CD45^+$) were sorted (FACSVantage SE Turbo Sorter) based upon cell surface antigens: iNKT cells (CD1d-$tetramer^+$, $CD3^+$), NK cells ($NKp46^+$, $CD3^-$), and T-cells (CD1d-$tetramer^-$, $CD3^+$). Cells were resuspended in Tri-reagent (Ambion). RNA was extracted and cDNA was reverse transcribed following the manufacturer's instructions (iScript cDNA Synthesis kit; Bio-Rad). Quantitative PCR was performed using the Quantitect SYBR® Green PCR kit (Qiagen). Real-time PCR was performed using the iCycler iQ Real-Time PCR Detection System from Bio-Rad using the supplied software. The thermal cycler tracks fluorescence levels over 40 amplification cycles. A melt curve was performed at the end of each run to verify that there was a single amplification product and a lack of primer dimers. All samples were normalized to the amount of cyclophilin mRNA present in the sample. Data are represented as fold change compared to C57BL/6 mRNA expression.

$A_{2A}R$ primers:

Forward: 5´-TGGCTTGGTGACGGGTATG-3´

Reverse: 5´-CGCAGGTCTTTGTGGAGTTC-3´

2.12. Hypoxia-reoxygenation

Mice were subjected to 3 hours of hypoxia (8 % oxygen). After hypoxic periods mice were returned to normoxic conditions for 4 - 18 hours (Kaul and Hebbel, 2000).

2.13. Antibody treatments

2.13.1. iNKT cell inhibition (anti-CD1d)

CD1d was blocked by two intra-peritoneal injections separated by 24 hours of anti-mouse CD1d mAb (1B1) at 10 μg/g (isotype controls were treated with $rIgG_{2b}$). Mice were sacrificed either 1 day or 5 days after the last injection. Anti-CD1d (clone 1B1) and isotype controls were purified from hybridomas in the University of Virginia hybridoma core.

2.13.2. CXCR3 neutralization

CXCR3 was neutralized by daily 1 ml subcutaneous injections of goat polyclonal anti-mouse CXCR3 for 7 days. Normal goat serum was used as a control. The production, characterization, and *in vivo* efficacy of this anti-CXCR3 serum in mouse models have been previously described (Belperio et al., 2002b).

2.14. Measurement of pulmonary cytokines and chemokines

Lungs were perfused, removed, and snap frozen. Tissue was homogenized in Complete media and IFN-γ (EBioscience), MIG/CXCL9, IP10/CXCL10,

ITAC/CXCL11, and SDF-1 (CXCL12) were measured by ELISA according to the manufacturer's protocol (R&D).

2.15. Isolation and adoptive transfer of NKT cells

Ubiquitously GFP labeled C57BL/6 animals (Jackson Laboratories) were injected with polyclonal anti-Asialo-GM1 (40 µl/day; 2 days) prior to isolation of splenocytes to deplete NK cells without affecting NKT cells. After isolation of splenocytes, cells were passed over a T-cell enrichment column (R&D) and eluted cells were incubated with anti-NK1.1-PE. The cells were washed to remove unbound antibody and NK1.1-PE-labeled NKT cells were incubated with magnetic anti-PE beads (Miltenyi Biotech) and purified by magnetic isolation. By flow cytometric analysis 85 % of the resulting cells were NKT cells. Based on CD69 expression, the purified cells were not activated.

Cells were either left untreated, incubated with the $A_{2A}R$ alkylating agent, FSPTP (200 µM) (5-amino-7-[2-(4-fluorosulfonyl)phenylethyl]-2-(2-furyl)-pryazolo[4,3-e]-1,2,4-triazolo[1,5-c]pyrimidine), for 30 min, or incubated with vehicle (saline, 2 % DMSO) (Shryock et al., 1998). One million cells were injected retro-orbitally 1 day prior (FSPTP treatment) or 4 days prior to experimentation. Successful transfer was confirmed by flow cytometric analysis for GFP positive cells.

2.16. $A_{2A}R$ agonist treatment

Three day or 7 day Alzet®-mini pumps containing ATL146e (1 ng/kg/min, 10 ng/kg/min, 30 ng/kg/min) or vehicle (saline, 0.2 % DMSO) were implanted

subcutaneously at the mid-scapular level into C57BL/6J, NY1DD, NY1DD x Rag1$^{-/-}$, and NY1DD x $A_{2A}R^{-/-}$ mice. Animals were sacrificed at various time points and analyzed for pulmonary inflammation.

2.17. Measurement of intracellular cAMP

Purified cells were suspended in RPMI 1640 medium supplemented with 10 % heat-inactivated FBS and 1 % antibiotic-antimycotic (Invitrogen). Cells were incubated at 37 °C for 10 min with 1 U/ml adenosine deaminase ([ADA], irreversibly deaminates adenosine to inosine) and vehicle or 1 µM rolipram, a selective inhibitor of phosphodiesterase IV ([PDE4], inhibits the breakdown of intracellular cAMP), and in the presence or absence of 100 nM ATL146e (Sullivan et al., 1995; Sullivan et al., 2001). Cells were then lysed, and intracellular cAMP levels were measured using the chemiluminescent immunoassay system for the quantitation of cAMP from mammalian cells, cAMP-Screen System, according to the manufacturer's protocol (Applied Biosystems).

2.18. Platelet depletions

Platelets were depleted either by chronic (busulfan) or acute (anti-platelet serum) treatments. Busulfan (20 mg/kg) was injected intra-peritonealy on days 1 and 4 (vehicle: polyethylene glycol). Circulating platelet counts were determined on days 7 and 14. By day 14, 85 % of platelets were depleted. Anti-platelet serum (25 µl / day; 1 day) was injected intra-peritonealy (vehicle: normal goat serum) and circulating platelets were

counted 24 hours later. Anti-platelet serum treatment resulted in 85 % depletion of circulating platelets.

2.19. Total soluble collagen (Sircol)

Lungs were perfused, removed, and snap frozen. Tissue was homogenized in Complete media and total soluble collagen was measured by the Sircol collagen assay following the manufacturer's protocol (Biocolor).

2.20. Statistics

Prism software (GraphPad) was used for all statistical analyses. An unpaired *t*-test was used to compare two experimental groups. One-way analysis of variance (ANOVA) with Neuman-Keuls post-testing was used to compare multiple experimental groups. Two-way ANOVA with Bonferroni post-testing was used to compare experimental groups to each other and over time. Histological grading was analyzed with either a nonparametric *t*-test (Mann-Whitney) or a nonparametric Kruskal-Wallis test with Dunns post-testing. A *P*-value of <0.05 was accepted as being significant.

3. Results

3.1. NY1DD mice have baseline organ dysfunction

Several murine models of sickle cell disease with phenotypes that vary in severity have been developed to model human disease. In this study we used the well characterized NY1DD model that expresses 75 % human β^S-globin and 56 % human α-globin (Fabry et al., 1992a). While these mice have been previously described as having a relatively mild hematological pathology (i.e. they have a normal hematocrit), they have been shown to exhibit baseline organ damage to lung, liver, spleen, and kidney (Fabry et al., 1992a). At baseline, individuals with sickle cell disease have various degrees of organ dysfunction that is often punctuated by periodic exacerbations referred to as sickle "crises." A disease exacerbation, or crisis, can also be produced in mice exposed to endotoxin or transient hypoxia (Fabry et al., 1992b; Holtzclaw et al., 2004). In the current study we chose to study pulmonary sickle cell disease at baseline rather than during crisis for several reasons: 1) recent findings suggest that transient microvascular occlusion occurs chronically in a sub-clinical manner in individuals with sickle cell disease, and that end-organ damage and short life-span in sickle cell disease are often due to the cumulative effects of repeated bouts of minor ischemic events; 2) relatively little attention has been paid to evaluating the natural progression of chronic organ injury in this model; and 3) the baseline sickle cell disease pulmonary phenotype is more stable and amenable to investigation than are crisis phenotypes.

3.1.1. NY1DD mice have gross pathological end-organ damage

Like humans with sickle cell disease at baseline, NY1DD mice exhibit a pro-inflammatory phenotype (increased circulating WBCs, pro-inflammatory cytokines, adhesion molecules, and platelet activation) that is believed to contribute to morbidity and mortality (Belcher et al., 2003; Hofstra et al., 1996; Platt, 2000). To explore end-organ damage, we grossly examined NY1DD lung, spleen, liver and kidney for size and weight as compared to C57BL/6 controls at 8 weeks (Figure 9A-F). Similar to individuals with sickle cell disease, NY1DD mice displayed hypertrophied livers and kidneys. Unlike individuals with sickle cell disease, NY1DD mice have significantly larger spleens. This is due to the fact that unlike in humans, in mice extra-medullary hematopoesis occurs in the spleen causing it to become hypertrophied.

3.1.2. NY1DD mice have hematologic complications

Individuals with sickle cell disease have increased circulating WBCs that is believed to correlate with poor prognosis. NY1DD mice also displayed increased circulating WBCs (Table 5). However, unlike individuals with sickle cell disease NY1DD mice were not severely anemic as their red blood cell parameters fell within normal limits. Upon examination of NY1DD peripheral blood smears various red blood cell morphologies were found, including sickled, target, tear drop, stomatocyte, elliptocyte, and reticulocyte (Figure 10). Also, aggregates of red blood cells were found (Figure 10).

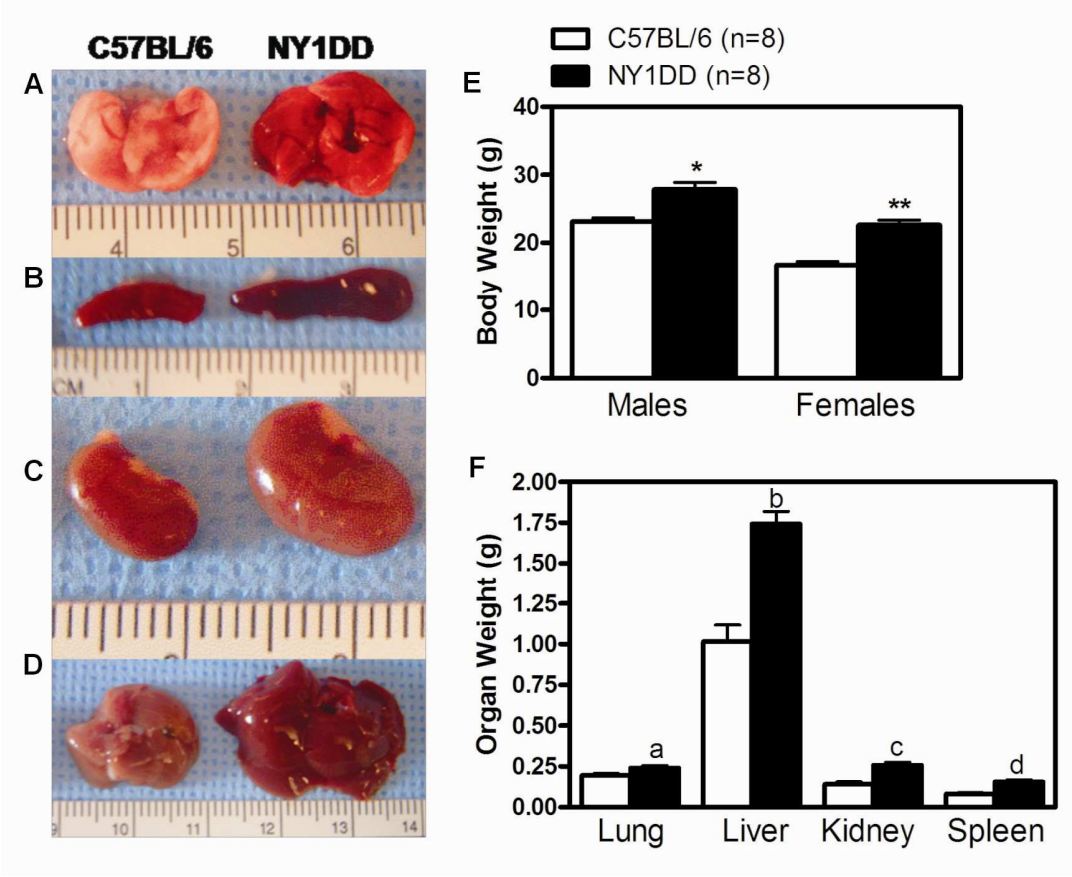

Figure 9. NY1DD mice have gross pathological end-organ damage

Representative images of (**A**) lungs, (**B**) spleen, (**C**) kidney, and (**D**) liver from 8 week old C57BL/6 and NY1DD male mice. (**E**) NY1DD animals weigh significantly more than C57BL6 mice at 8 weeks of age. (**F**) 8 week old NY1DD animals have significantly heavier organs than age matched C57BL/6 mice. Data were analyzed by an unpaired *t*-test. *, P=0.001; **, P <0.0001; a, P =0.036; b, P =0.0002; c, P =0.0005; d, P =0.0004.

	C57BL/6 ***(n=17)***	**NY1DD** **(*n=13)***	***P*-value**
Total Leukocytes (10^3/µl)	3.22 (0.19)	7.17 (0.32)	<0.0001
Neutrophils (10^3/µl)	0.73 (0.06)	2.00 (0.11)	<0.0001
Lymphocytes (10^3/µl)	2.08 (0.15)	4.74 (0.28)	<0.0001
Monocytes (10^3/µl)	0.07 (0.01)	0.40 (0.04)	<0.0001
Red Blood Cells (10^6/µl)	9.60 (0.17)	10.28 (0.26)	0.043
Hemoglobin (g/dl)	15.32 (0.17)	14.06 (0.43)	0.0088
Hematocrit (%)	45.34 (0.28)	39.66 (0.99)	0.0055
Mean Corpuscle Volume (fl)	43.50 (0.17)	38.62 (0.21)	<0.0001
RBC Distribution Width (%)	17.26 (0.15)	21.28 (0.15)	<0.0001
Platelets (10^3/µl)	830.8 (32.5)	950.6 (40.3)	0.028
Mean Platelet Volume (fl)	4.44 (0.05)	5.15 (0.06)	<0.0001

Table 5. Baseline hematological parameters in NY1DD mice

EDTA anti-coagulated blood was analyzed for complete blood counts with differential (Hemavet). Data represents mean (standard error of the mean). Data were analyzed by an unpaired *t*-test. RBC: red blood cell.

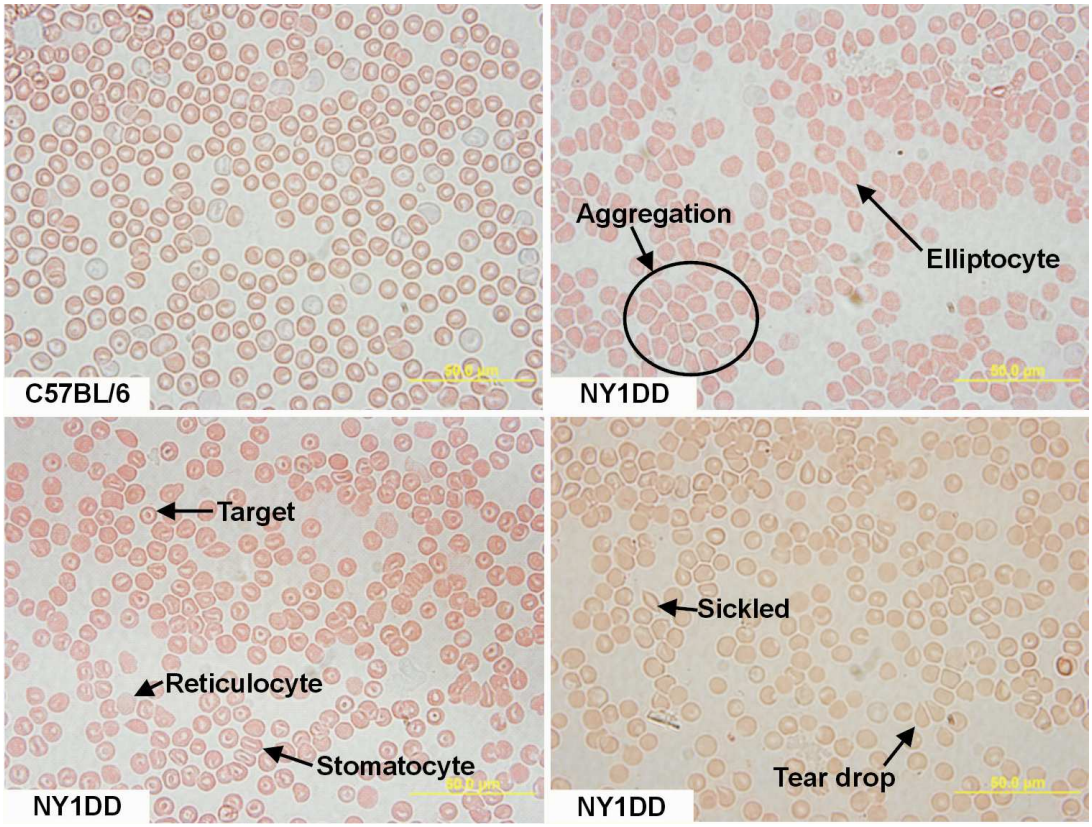

Figure 10. NY1DD mice have abnormal red blood cell morphologies

Peripheral blood smear from a control C57BL/6 mouse with normal appearing red blood cells (bi-concave discs). Peripheral blood smears from three NY1DD mice depicting abnormal red blood cell morphologies: sickle, elliptocyte, target, stomatocyte, tear drop, and reticulocyte. Also indicated is an area of red blood cell aggregation.

3.1.3. NY1DD mice have pulmonary dysfunction and inflammation

Pulmonary disease is the leading cause of death in sickle cell disease (Platt et al., 1994). Since the pulmonary arterial circulation has low oxygen tension and pressure, low blood velocity, and constricts in response to hypoxia, the lung environment facilitates the polymerization of HbS and is highly vulnerable to ischemic injury (Platt et al., 1994). Therefore, we investigated pulmonary dysfunction at baseline in NY1DD mice.

To determine a baseline pulmonary phenotype, NY1DD mice were compared to C57BL/6 mice with various indices of injury. Quantitative analysis of lung histology revealed marked increases in capillary congestion and alveolar wall thickness in NY1DD mice as compared to C57BL/6 mice (Figure 11A-C). Also, at baseline NY1DD mice had significantly increased vascular permeability (12.4-fold; $P<0.0001$) and decreased arterial oxygen saturation (90 % as compared to 96 % in C57BL/6 mice; $P<0.0001$) (Figure 11D,E). Furthermore, at baseline unrestrained whole body plethysmography revealed that NY1DD mice had an abnormally high rate of respiration and an abnormally low tidal volume, compatible with a restrictive ventilatory defect (Figure 11F,G).

To determine if NY1DD mice had intra-pulmonary leukocytosis we used flow cytometric analysis to define white blood cell (WBC) populations in digested whole lung tissue. Compared to C57BL/6 mice, NY1DD mice had a significantly increased number of pulmonary leukocytes (Table 6). To determine the activation state of lymphocytes from the lung, we analyzed surface expression of CD69 and intracellular expression of IFN-γ, which are both well characterized markers of iNKT cell activation (Sancho et al., 2005). At baseline, expression of CD69 and IFN-γ were significantly increased on all NY1DD pulmonary lymphocytes (Figure 12A-C).

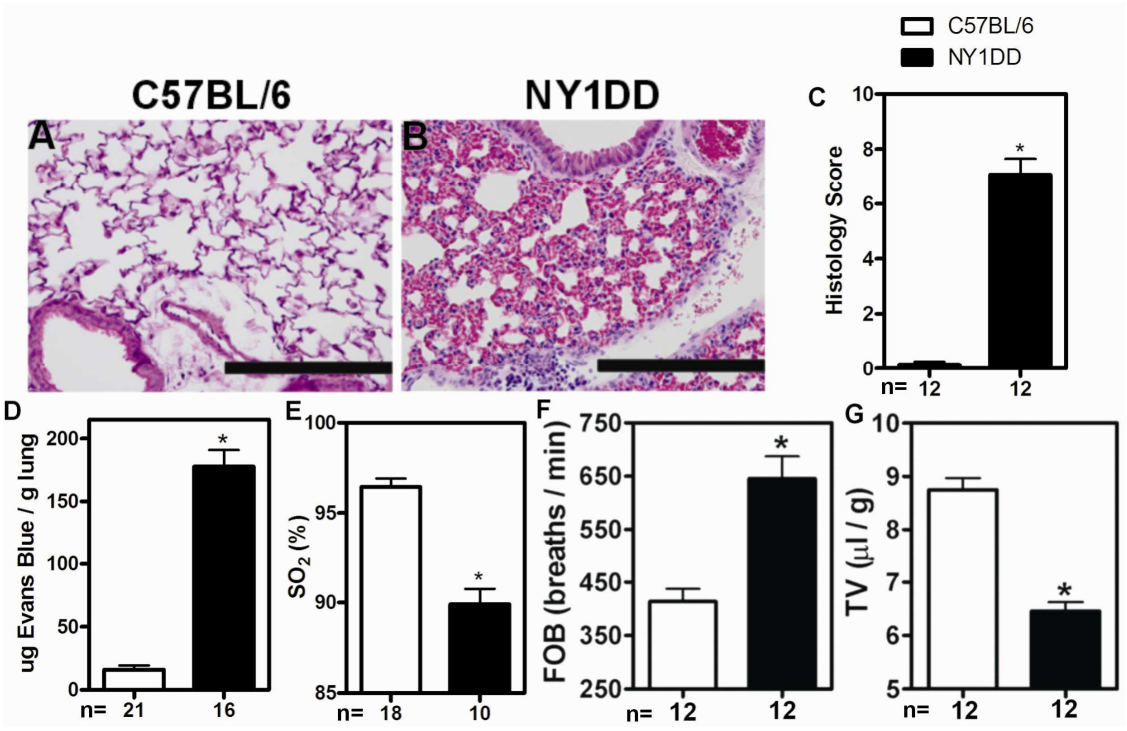

Figure 11. Lungs from NY1DD mice have baseline histological injury and impaired function

(**A-C**) Representative images of H&E stained cells, *bars* represent 200 µm. (**F**) Histopathological scores (0-8, see methods) calculated by analysis of H&E stained mouse lungs. (**D,E**) Vascular permeability is increased and arterial oxygen saturation is reduced in NY1DD mouse lungs at baseline as compared to C57BL/6. (**F,G**) NY1DD mice have significantly impaired breathing (decreased tidal volume and increased frequency of breathing) as compared to C57BL/6 mice. Histological grading (**C**) was analyzed with a nonparametric *t*-test (Mann-Whitney; ***** $P<0.0001$). Data (**D-G**) were analyzed by an unpaired *t*-test. ***** $P<0.0001$. SO_2: arterial oxygen saturation; FOB: frequency of breathing; TV: tidal volume.

Cells (10^5)	C57BL/6 (n=21)	NY1DD (n=17)	*P*-value
PMNs	0.19 (0.04)	1.32 (0.33)	0.0031
CD4	2.10 (0.28)	3.12 (0.37)	0.031
CD8	1.40 (0.15)	2.33 (0.32)	0.0076
NK	2.25 (0.31)	4.45 (0.77)	0.0072
iNKT	0.18 (0.02)	0.43 (0.03)	<0.0001

Table 6. NY1DD mice have baseline pulmonary leukocytosis

Flow cytometric analysis was used to determine pulmonary leukocyte populations and numbers. Data represents mean (standard error of the mean). Data were analyzed by an unpaired *t*-test.

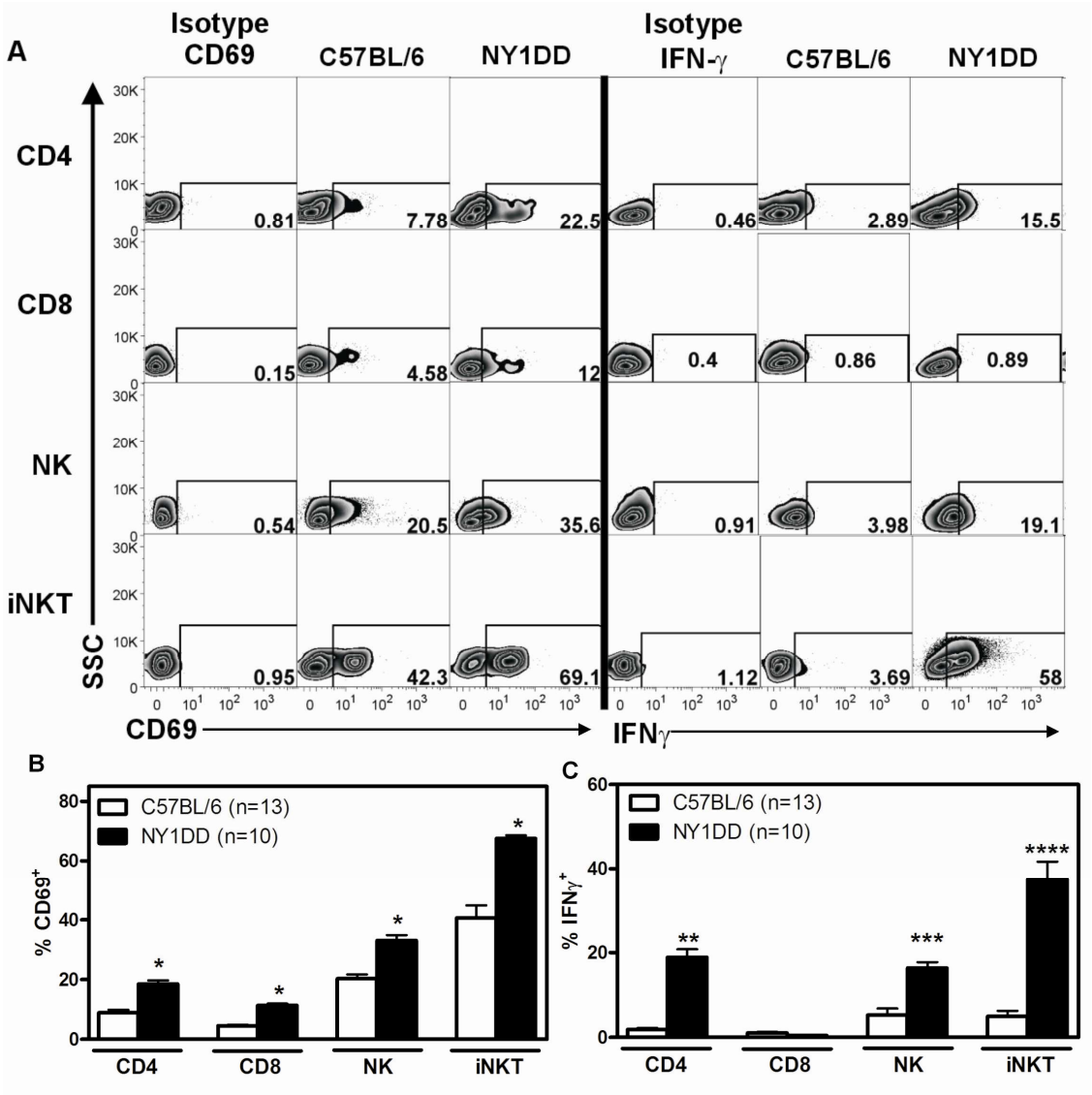

Figure 12. Lung lymphocytes from NY1DD mice express increased markers of activation (CD69 and IFN-γ)

(**A**) Representative flow cytometry plots of lymphocytes derived from C57BL/6 and NY1DD mice. (**B,C**) NY1DD mice have increased surface expression of CD69 and intracellular expression of IFN-γ levels on pulmonary lymphocytes. Data were analyzed by an unpaired *t*-test. * $P<0.0001$; ** $P=0.0001$; *** $P=0.0019$; **** $P=0.0004$.

3.1.4. Conclusions

Our findings confirm that at baseline NY1DD mice display substantial pulmonary inflammation and pathophysiology that is manifested by increased numbers of pulmonary leukocytes, impaired endothelial integrity (increased vascular permeability), and microvascular occlusion. Histological examination of lungs from NY1DD animals revealed striking inflammatory changes. Similar findings have been found in post-mortem specimens from humans with sickle cell disease (Haque et al., 2002). We also found a significant decrease in arterial oxygen saturation (% SO_2) in NY1DD mice. Low oxygen saturation has been associated with increased pulmonary artery pressures in individuals with sickle cell disease and is believed to be a risk factor for the development chronic lung disease (Pashankar et al., 2008; Pashankar et al., 2009).

3.2. iNKT cells mediate pulmonary inflammation and dysfunction via the IFN-γ inducible chemokine CXCR3 axis

3.2.1. NY1DD mice have increased and activated iNKT cells which are further activated during sickle cell crisis

The NY1DD model has been used to elucidate the role of ischemia-reperfusion injury in sickle cell disease. It is believed that NY1DD mice exposed to 3 hours of hypoxia (10 % O_2) followed by reoxygenation (room air) for 4 hours results in acute vaso-occlusion and subsequent sickle cell crisis, as measured by an exaggerated inflammatory response that was not seen in C57BL6 control mice (no red blood cell sickling and thus no ischemia) nor in NY1DD mice exposed to hypoxia alone, suggesting that the pro-inflammatory state in NY1DD animals was due to reperfusion injury (Kaul and Hebbel, 2000). In this study, we first subjected the NY1DD mouse to hypoxia-reoxygenation to induce sickle cell crisis and investigate whether iNKT cells have an exaggerated inflammatory response. Then, we utilized the NY1DD mouse as a model to investigate the role of iNKT cells in baseline pulmonary inflammation and dysfunction associated with moderate sickle cell disease.

We used fluorescently labeled CD1d tetramers to selectively label iNKT cells (defined as tetramer$^+$ CD3$^+$) in the lung, liver, and spleen of C57BL/6 and NY1DD mice, as well as NY1DD mice subjected to 3 hours of hypoxia followed by 4 hours of reoxygenation (Figure 13A). Flow cytometric analysis and counting beads were used to determine the absolute numbers of iNKT cells and the percent of iNKT cells among all lymphocytes (live, CD45$^+$ low side scatter cells) in tissues from all mice. Relative to C57BL/6 mice, NY1DD mice had increased absolute numbers of iNKT cells in all tissues

at baseline (Table 7, Figure 13B). In particular, pulmonary iNKT cells were increased in absolute number from 2.2 ± 0.3 x 10^4 to 3.9 ± 0.4 x 10^4 (P<0.05) and as a percent of all lymphocytes from 1.3 ± 0.09 % to 3.4 ± 0.4 % (P<0.05) (Figure 13A,B). As compared to baseline NY1DD mice, NY1DD mice in acute sickle cell crisis had significantly increased numbers of iNKT cells in all tissues as well as increased percent of all lymphocytes (Table 7, Figure 13A,B). The absolute number of pulmonary iNKT cells was increased to 8.5 ± 2.2 x 10^4 after hypoxia-reoxygenation, a 2.2-fold change (P<0.05).

To determine the activation state of iNKT cells from the lung, liver, and spleen, we analyzed surface expression of CD69 and intracellular IFN-γ, which are both well characterized markers of iNKT cell activation (Sancho et al., 2005). At baseline, iNKT cells from all NY1DD mouse organs displayed significantly increased levels of both markers as compared to C57BL/6 mice (Table 7, Figures 14A,B). In particular, the percent of pulmonary iNKT cells positive for IFN-γ increased from 5 % in C57BL/6 mice to 37 % in NY1DD mice (P<0.05), a difference of 7.4-fold. Organs from NY1DD mice in acute sickle cell crisis displayed an even further increase in the percent activation of iNKT cells, both for CD69 and IFN-γ expression (Table 7, Figures 14A,B).

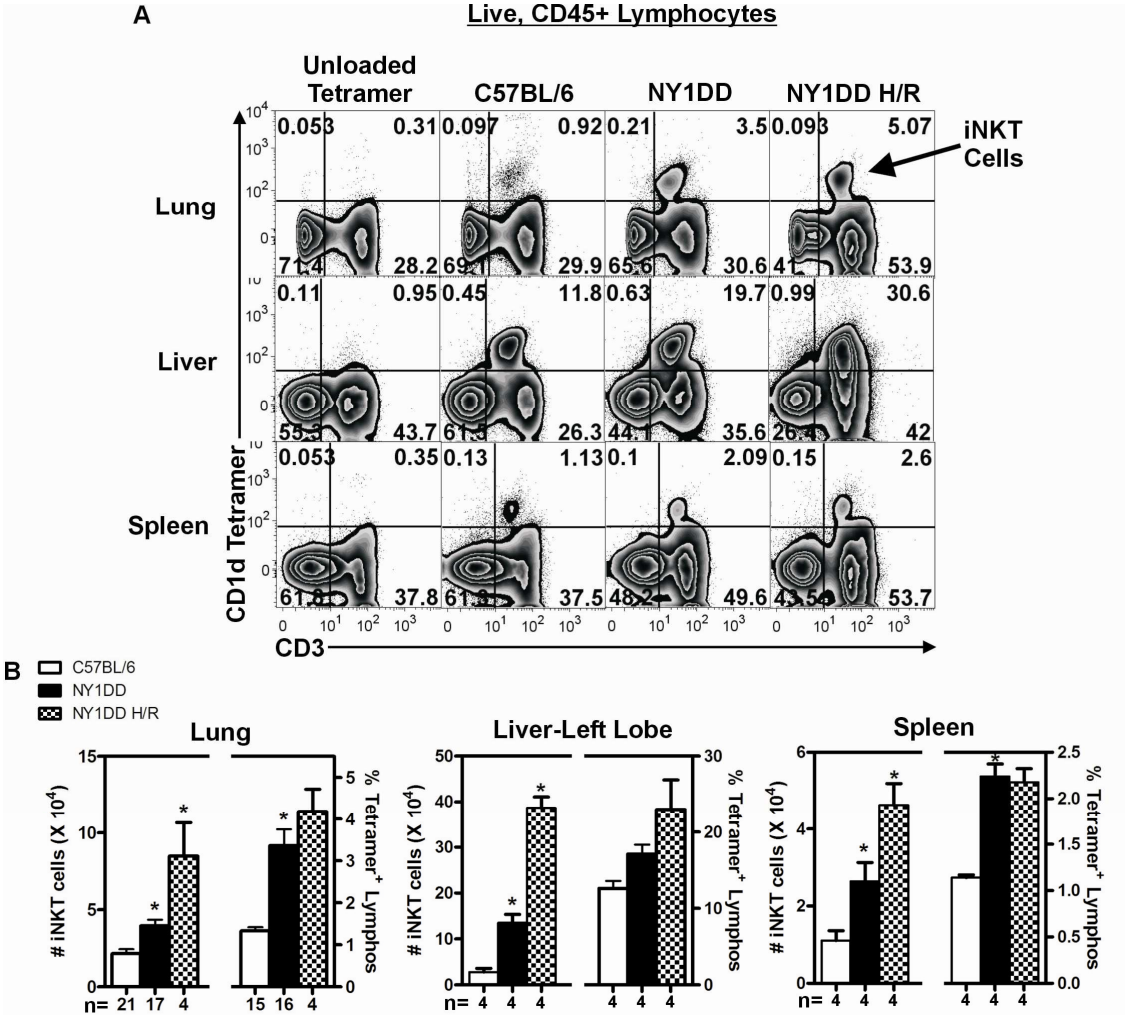

Figure 13. NY1DD mice have increased iNKT cells which are further activated during acute sickle cell crisis

(A) Representative flow cytometry plots of iNKT cells from lung, liver, and spleen. **(B)** iNKT cells were identified from the live, $CD45^+$ lymphocyte gate as CD1d-$tetramer^+$ $CD3^+$ cells. Compared to C57BL/6 mice, NY1DD mouse organs have a higher number of pulmonary iNKT cells. Hypoxia-reoxygenation (3 hrs - 4 hrs) increases both the % and absolute number of tissue iNKT cells. Data were analyzed by one-way ANOVA with Neuman-Keuls post-testing. * *P*-value of <0.05 was considered significant.

Tissue	iNKT cell	C57BL/6	NY1DD	NY1DD H/R
Lung	**# ($x10^4$)**	2.1 (0.3)	4.0 (0.4)*	8.5 (2.1)**
	% of lympho	1.3 (0.1)	3.4 (0.4)*	4.2 (0.5)
	% CD69	40.6 (4.2)	67.5 (1.1)*	76.1 (1.6)
	% IFN-γ	4.9 (0.7)	37.4 (4.4)*	47.5 (3.7)
Liver (Left Lobe)	**# ($x10^4$)**	2.8 (0.8)	13.5 (1.8)*	38.7 (2.4)**
	% of lympho	12.6 (0.9)	17.1 (1.2)	23.0 (3.9)
	% CD69	22.3 (2.7)	48.8 (2.1)*	63.6 (1.3)**
	% IFN-γ	20.7 (1.9)	53.9 (3.8)*	79.9 (6.4)**
Spleen	**# ($x10^4$)**	1.1 (0.3)	2.6 (0.5)*	4.6 (0.6)**
	% of lympho	1.1 (0.03)	2.2 (0.1)*	2.1 (0.2)
	% CD69	10.61 (2.8)	28.6 (0.8)*	32.2 (1.4)
	% IFN-γ	5.4 (0.7)	19.4 (1.2)*	34.4 (2.9)**

Table 7. NY1DD mice have increased and activated iNKT cells which are further activated during acute sickle cell crisis

iNKT cells were identified from the live, $CD45^+$ lymphocyte gate as CD1d-$tetramer^+$ $CD3^+$. Compared to C57BL/6 tissues, NY1DD mouse tissues have a higher number of iNKT cells as well as an increased percent of total lymphocytes. iNKT cells from NY1DD mice are more activated as defined by higher percent of surface CD69 and intracellular IFN-γ. After 3 hours of hypoxia and 4 hours of reoxygenation both the number and percent of iNKT cells in all organs increased. Furthermore, the percent activation of iNKT cells also increased. Data represents the mean (standard error of the mean). Data were analyzed by one-way ANOVA with Neuman-Keuls post-testing. $P<0.05$ was considered significant. * NY1DD vs C57BL/6; ** NY1DD H/R vs NY1DD. H/R: hypoxia-reoxygenation; lymphos: lymphocytes.

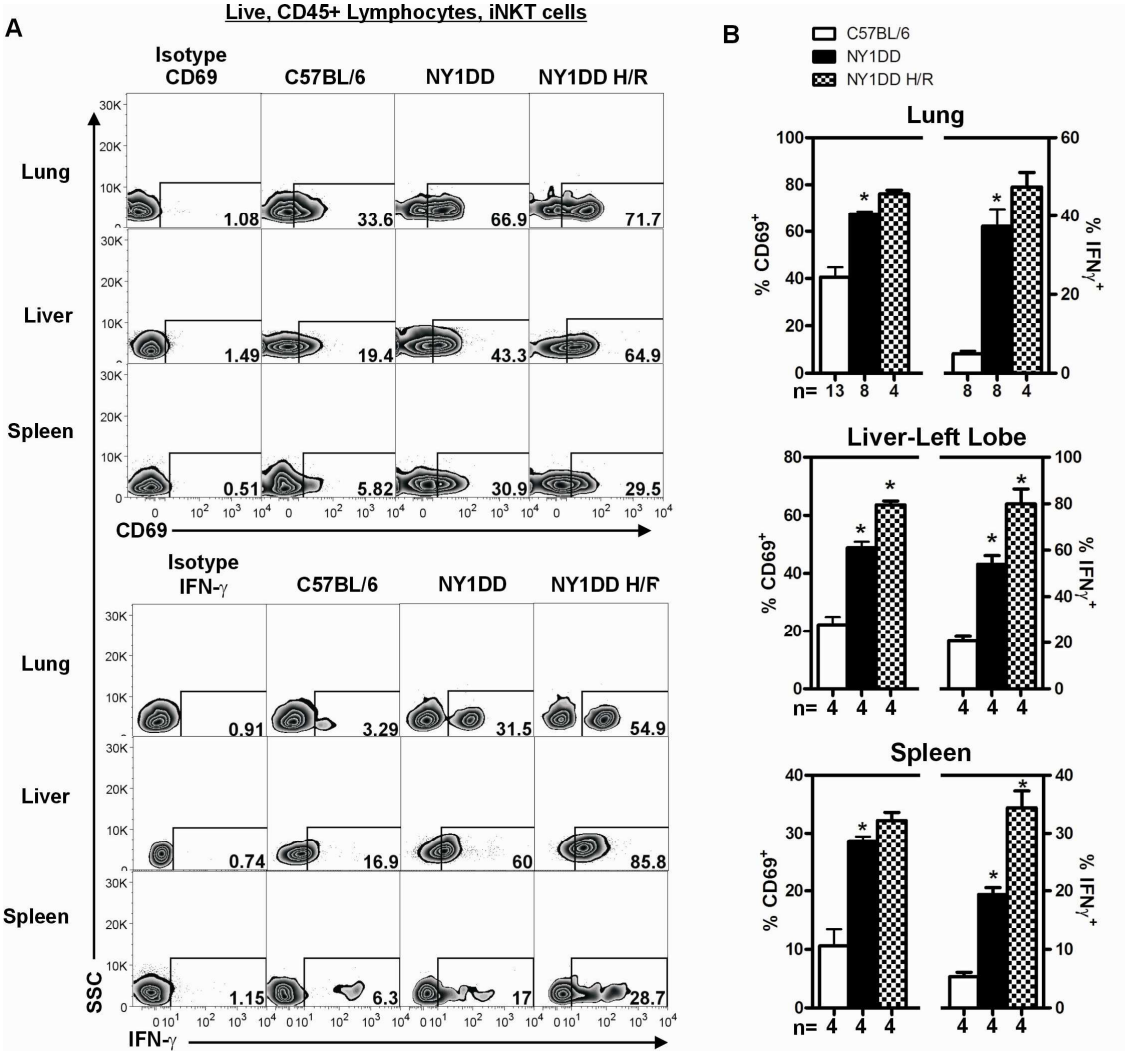

Figure 14. NY1DD mice have activated iNKT cells which are further activated during acute sickle cell crisis

(A) Representative flow cytometry plots of iNKT cell activation (CD69, IFN-γ) from lung, liver, and spleen. **(B)** iNKT cells from NY1DD mice are more activated as defined by higher percent of surface expression of CD69 and intracellular expression of IFN-γ. (**B**) Three hrs of hypoxia followed by 4 hrs of reoxygenation further increases the iNKT cell activation. Data were analyzed by one-way ANOVA with Neuman-Keuls post-testing. * $P<0.05$ was considered significant. H/R: hypoxia-reoxygenation.

3.2.2. Inhibition of iNKT cells transiently improves pulmonary dysfunction in NY1DD mice

In order to determine if iNKT cells were involved in the observed pulmonary injury, NY1DD mice were treated with anti-CD1d (10 μg/g/day, 2 days) to inhibit CD1d-restricted activation of iNKT cells. One treatment group was assessed 1 day after the last anti-CD1d injection and another treatment group was assessed 5 days after the last dose. Treatment of NY1DD mice with anti-CD1d decreased the level of histological pulmonary injury observed after 1 day ($P<0.05$) (Figure 15A-B,D). After 5 days, NY1DD animals reverted to a significantly higher state of increased pulmonary injury as indicated by quantitative analysis of histology ($P<0.05$) (Figure 15C,D). One day after anti-CD1d treatment, NY1DD mice had significantly decreased pulmonary vascular permeability (3-fold) as compared to isotype control treated animals ($P<0.05$) (Figure 15E). NY1DD animals assessed 5 days after anti-CD1d treatment had significantly elevated vascular permeability ($P<0.05$) (Figure 15E). One day after anti-CD1d treatment, NY1DD animals had a significant increase in arterial oxygen saturation (95.4 %) that was decreased at 5 days (92.3 %) ($P<0.05$) (Figure 15F). Anti-CD1d treated NY1DD animals demonstrated normalized breathing parameters 1 day after treatment (decreased respiration rate and increased tidal volume) that was largely reversed at 5 days (Figure 15G).

The pulmonary leukocytosis observed in NY1DD mice decreased to near control levels 1 day after anti-CD1d antibody treatment (Table 8). Five days after anti-CD1d antibody treatment pulmonary leukocyte counts returned to pre-antibody treatment levels (Table 8). One day after anti-CD1d treatment, expression of CD69 and IFN-γ in NY1DD

mice was significantly diminished as compared to isotype control treated NY1DD animals (Figure 16A-C). Expression of CD69 and IFN-γ returned to pre-antibody treatment levels 5 days after anti-CD1d injections (Figure 16A-C).

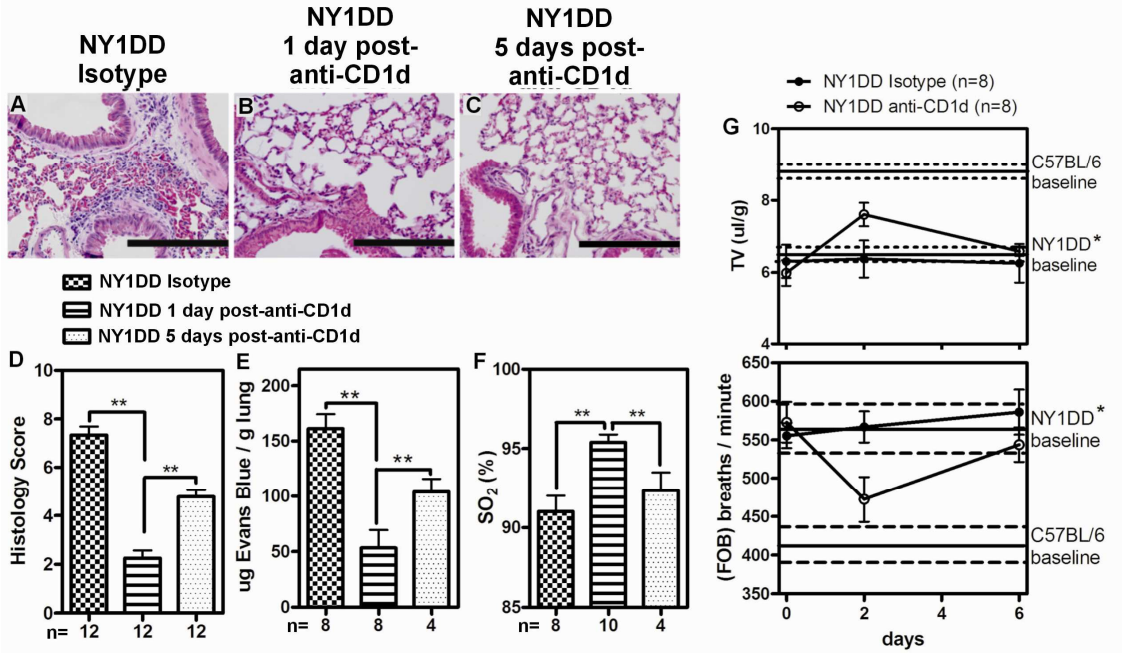

Figure 15. Treatment with anti-CD1d transiently improves pulmonary function in NY1DD mice

(**A-C**) Representative images of H&E stained cells, *bars* represent 200 μm. (**D**) Histopathological scores (0-8, see methods) calculated by analysis of H&E stained mouse lungs. (**D,E**) Vascular permeability is decreased and oxygen saturation is increased 1 day, but not 5 days, after injection of anti-CD1d antibodies. (**G**) In NY1DD mice breathing parameters are improved 1 day, but not 5 days, after injection of anti-CD1d antibodies. The lines represent the means ± the standard error of the mean of baseline breathing parameters. Histological grading (**D**) was analyzed by a nonparametric Kruskal-Wallis test with Dunns post-testing; ** $P<0.05$. Data (**E,F**) were analyzed by one-way ANOVA with Neuman-Keuls post-testing. ** $P<0.05$. Breathing parameters were analyzed by two-way ANOVA with Bonferroni post-testing. ** $P<0.05$. Baseline breathing: * $P<0.0001$. SO_2: arterial oxygen saturation; FOB: frequency of breathing; TV: tidal volume.

Cells (10^5)	(a) NY1DD Isotype (n=10)	(b) NY1DD 1 day post anti-CD1d (n=10)	(c) NY1DD 5 days post anti-CD1d (n=5)
PMNs	1.53 (0.14)	0.84 (0.12)*	1.51 (0.31)**
CD4	2.59 (0.28)	1.04 (0.21)*	3.87 (0.19)**,***
CD8	2.06 (0.44)	0.66 (0.18)*	2.60 (0.27)**
NK	4.64 (0.38)	1.50 (0.22)*	2.36 (0.97)**
iNKT	0.38 (0.04)	0.20 (0.05)	0.65 (0.21)**,***

Table 8. Treatment with anti-CD1d transiently decreases pulmonary leukocytes in NY1DD mice

Anti-CD1d was injected (10 µg/g/day; 2 days) and lungs were harvested either 1 day (a and b) or 5 days later (c). Data represents mean (standard error of the mean). *P*-values were calculated by one-way ANOVA with Neuman-Keuls post-testing. $P<0.05$ was considered significant. * column a vs b; ** column b vs c; *** column a vs c.

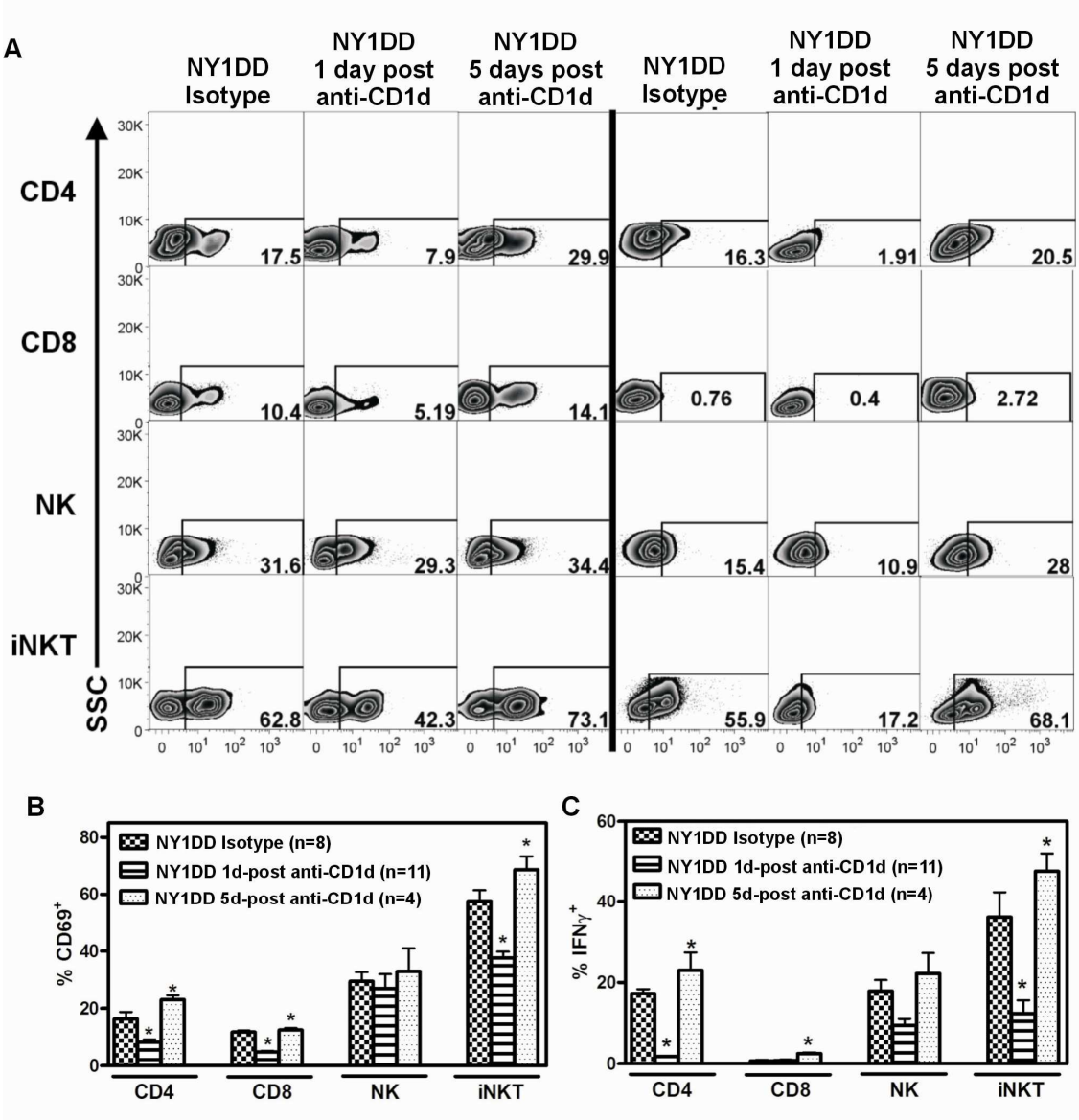

Figure 16. The activation markers CD69 and intracellular IFN-γ are transiently decreased after iNKT cell inhibition with anti-CD1d

(**A**) Representative flow cytometry plots of iNKT cells derived from anti-CD1d-treated NY1DD mice. (**B,C**) CD69 and intracellular IFN-γ levels on pulmonary lymphocytes are decreased 1 day, but not 5 days after treatment with anti-CD1d. Data were analyzed by one-way ANOVA with Neuman-Keuls post testing. * $P<0.05$.

3.2.3. NY1DD-Rag1$^{-/-}$ mice are protected from developing pulmonary injury and the adoptive transfer of wild-type NKT cells reconstitutes injury

The experimental evidence suggesting the involvement of iNKT cells in the pathogenesis of pulmonary injury in the NY1DD mouse led us to hypothesize that NY1DD x Rag1$^{-/-}$ mice (lacking mature T- and B- cells) would be protected from developing pulmonary injury that was noted in NY1DD mice at baseline. The NY1DD x Rag1$^{-/-}$ genotype was confirmed by PCR and the expected phenotype (lacking CD3^{+} cells) was confirmed by flow cytometric analysis (Figure 17A,B). Compared to NY1DD mice, NY1DD x Rag1$^{-/-}$ animals had decreased vascular permeability (2-fold) (Figure 17C). Also, NY1DD x Rag1-/- mice had decreased capillary congestion and alveolar wall thickness (Figure 17D,E). Furthermore, NY1DD x Rag1$^{-/-}$ animals had significantly increased arterial oxygen saturation as compared to NY1DD mice at baseline (Figure 17F). NY1DD x Rag1$^{-/-}$ animals also had near normal breathing parameters (increased tidal volume and decreased frequency of breathing) as compared to NY1DD mice (Figure 17G). Interestingly, NY1DD x Rag1$^{-/-}$ animals have significantly increased pulmonary levels of NK cells, perhaps as a compensatory adaptation for the lack of T- and B-cells (Table 9).

One million NKT cells were adoptively transferred via retro-orbital injection into NY1DD x Rag1$^{-/-}$ animals. Four days after the adoptive transfer pulmonary parameters were analyzed. The adoptive transfer of NKT cells into the NY1DD x Rag1$^{-/-}$ mice resulted in significantly increased pulmonary levels of both NK cells (2-fold) and PMNs (4-fold) (Table 9). Also, the adoptive transfer of NKT cells into NY1DD x Rag1$^{-/-}$ mice caused increased vascular permeability and decreased oxygen saturation (Figure 17C,F).

As control experiments, 20 x 10^6 splenocytes (with NKT cells) and 20 x 10^6 T-cells (NKT depleted) were adoptively transferred into NY1DD x $Rag1^{-/-}$ mice (Figure 17C). Similar to NKT cell induced injury, splenocytes, but not NKT cell depleted T-cells, were able to reconstitute pulmonary injury as indicated by increased vascular permeability, suggesting that although NKT cells constitute a relatively a minor population of pulmonary lymphocytes, they play an important role in the mechanism of pulmonary injury in NY1DD mice. Other subsets of lymphocytes were not adoptively transferred and we cannot rule out the possibility that other cells (B-cells) may be able to induce pulmonary injury in NY1DD x $Rag1^{-/-}$ mice.

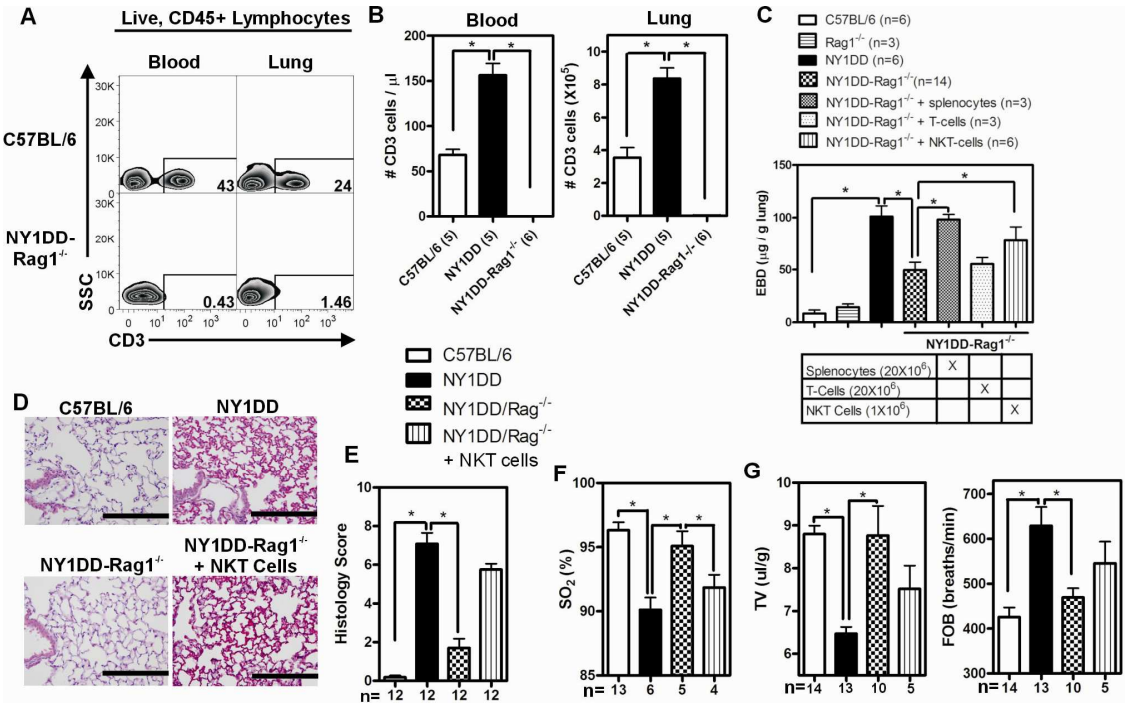

Figure 17. NY1DD x Rag1$^{-/-}$ mice have decreased pulmonary injury that was reversed by the adoptive transfer of wild-type NKT cells

(**A**) Representative flow cytometry plots of CD3^{+} lymphocytes in blood and lungs of C57BL/6 and NY1DD x Rag1$^{-/-}$ animals. (**B**) Number of CD3+ cells in blood and lung from NY1DD x Rag1$^{-/-}$ mice. (**C**) NY1DD x Rag1$^{-/-}$ mice have decreased vascular permeability. The adoptive transfer of 20x10^{6} splenocytes or 10^{6} NKT cells increases vascular permeability. (**D**) Representative images of H&E stained cells in C57BL/6 and NY1DD x Rag1$^{-/-}$ animals, the *bar* represents 200 µm. **(E)** Histopathological scores (0-8, see methods) by analysis of H&E stained mouse lungs. (**F**) NY1DD x Rag1$^{-/-}$ animals have increased arterial oxygen saturation that is reversed by the adoptive transfer of 10^{6} NKT cells. (**G**) NY1DD x Rag1$^{-/-}$ mice have improved breathing (increased tidal volume and decreased frequency of breathing). The adoptive transfer of 10^{6} NKT cells decreased tidal volume and increased frequency of breathing to near baseline levels. Data were

analyzed by one-way ANOVA with Neuman-Keuls post-testing. Histological grading was analyzed with a nonparametric Kruskal-Wallis test with Dunns post-testing; * $P<0.05$. SO_2: arterial oxygen saturation; FOB: frequency of breathing; TV: tidal volume.

Cells (10^5)	(a) NY1DD (n=8)	(b) NY1DD x Rag1$^{-/-}$ (n=8)	(c) NY1DD x Rag1$^{-/-}$ + NKT cells (n=4)
PMNs	2.34 (0.4)	1.63 (0.46)	6.64 (1.9)**,***
NK	4.3 (0.85)	6.71 (1.28)*	12.32 (1.03)**,***

Table 9. The adoptive transfer of 10^6 wild-type NKT cells into NY1DD x Rag1$^{-/-}$ mice increased absolute numbers of pulmonary PMNs and NK cells

At baseline, NY1DD x Rag1$^{-/-}$ have significantly increased pulmonary NK cells. Lungs were harvested 4 days after adoptive transfer of NKT cells harvested from spleen (see methods). Data represents mean (standard error of the mean). Data were analyzed by one-way ANOVA with Neuman-Keuls post-testing. A *P*-value <0.05 was considered significant. * column b vs a; ** column c vs b; *** column c vs a.

3.2.4. NY1DD animals have increased pulmonary IFN-γ inducible CXC chemokines and neutralization of CXCR3 ameliorates pulmonary injury

Our discovery of high levels of IFN-γ in pulmonary iNKT cells from NY1DD mouse lungs led us to hypothesize that the recruitment of pulmonary lymphocytes is through the IFN-γ inducible CXC chemokine-CXCR3 axis. Flow cytometric analysis of pulmonary lymphocytes for CXCR3 revealed that the expression this receptor is significantly higher on CD4 T-cells (6-fold), CD8 T-cells (7-fold), NK cells (4-fold), and iNKT cells (2-fold) from NY1DD animals as compared to C57BL/6 animals (Figure 18A,B). ELISAs of pulmonary tissue homogenate also revealed significantly increased levels of IFN-γ and the IFN-γ inducible CXC chemokines CXCL9 and CXCL10 in NY1DD animals at baseline as compared to C57BL/6 animals (Figure 18C,D).

These data led us to hypothesize that neutralization of CXCR3 would ameliorate pulmonary dysfunction in NY1DD animals by blocking leukocyte trafficking to the sickle cell disease lung. Treatment of NY1DD mice with anti-CXCR3 for 1 week resulted in significantly decreased levels of pulmonary lymphocyte CXCR3 expression on CD4 T-cells, CD8 T-cells, NK cells, and iNKT cells as compared to NY1DD mice treated with goat serum (Figure 18A,B). This treatment also resulted in a significant increase of CXCL9 and CXCL10 in NY1DD mice (Figure 18C). The increase in chemokine concentration in mice with blocked CXCR3 receptors can be attributed to the fact that chemokines are degraded and internalized following binding to chemokines receptors (Pierce et al., 2002; Thelen, 2001). Anti-CXCR3 treatment resulted in a decrease in total pulmonary lymphocyte numbers (Table 10). Quantitative analysis of lung histology in the anti-CXCR3 treated animals revealed decreases in capillary congestion and alveolar wall

thickness as compared to goat serum treated NY1DD mice (Figure 19A,B). Furthermore, anti-CXCR3 treated NY1DD animals had significantly decreased vascular permeability (2-fold) and increased arterial oxygen saturation as compared to NY1DD mice (Figure 19C,D). Anti-CXCR3 treated NY1DD animals also had significantly improved breathing parameters (increased tidal volume and decreased frequency of breathing) as compared to serum treated NY1DD mice (Figure 19E).

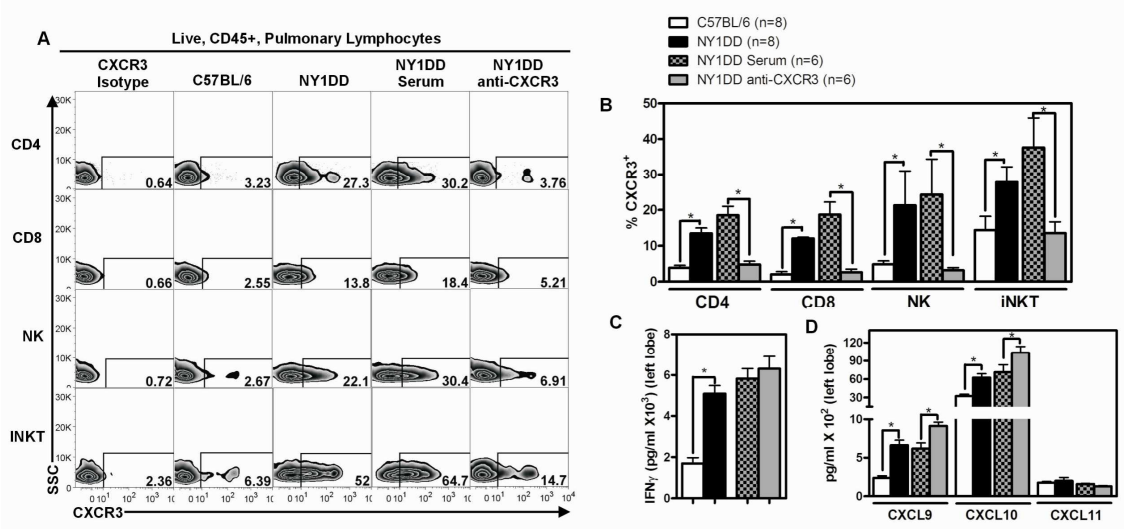

Figure 18. NY1DD mice have increased pulmonary lymphocyte expression of CXCR3 and increased whole lung expression of IFN-γ and IFN-γ inducible chemokines

(**A**) Representative flow cytometry plots of CXCR3 expression on pulmonary lymphocytes from C57BL/6, NY1DD, NY1DD treated with goat serum, and NY1DD treated with goat anti-CXCR3 serum. (**B**) Pulmonary lymphocytes from NY1DD mice express significantly increased levels of CXCR3 as compared to C57BL/6 mice. NY1DD animals treated with anti-CXCR3 display significantly decreased expression of CXCR3 on pulmonary lymphocytes. (**C,D**) Pulmonary homogenates from NY1DD animals have significantly increased levels of IFN-γ and IFN-γ inducible chemokines (CXCL9 and CXCL10). NY1DD animals treated with anti-CXCR3 have significantly elevated levels of IFN-γ inducible chemokines (CXCL9 and CXCL10). Data were analyzed by one-way ANOVA with Neuman-Keuls post-testing, * $P<0.05$.

Cells Right Lung (10^5)	NY1DD Serum (*n=8*)	NY1DD anti-CXCR3 (*n=8*)	*P*-value
PMNs	1.12 (0.35)	0.34 (0.07)	0.037
CD4	1.94 (0.29)	0.54 (0.05)	0.0001
CD8	1.24 (0.15)	0.64 (0.14)	0.01
NK	3.85 (0.45)	1.70 (0.25)	0.0017
NKT	0.37 (0.07)	0.14 (0.03)	0.045

Table 10. Neutralization of CXCR3 in NY1DD mice decreases pulmonary leukocyte infiltration

Mice were injected (1 ml/day; 7 days) subcutaneously with either goat serum or goat anti-CXCR3 (see methods). Total cells in the right lung lobes were counted. Data represents mean (standard error of the mean). *P*-values were calculated by an unpaired *t*-test.

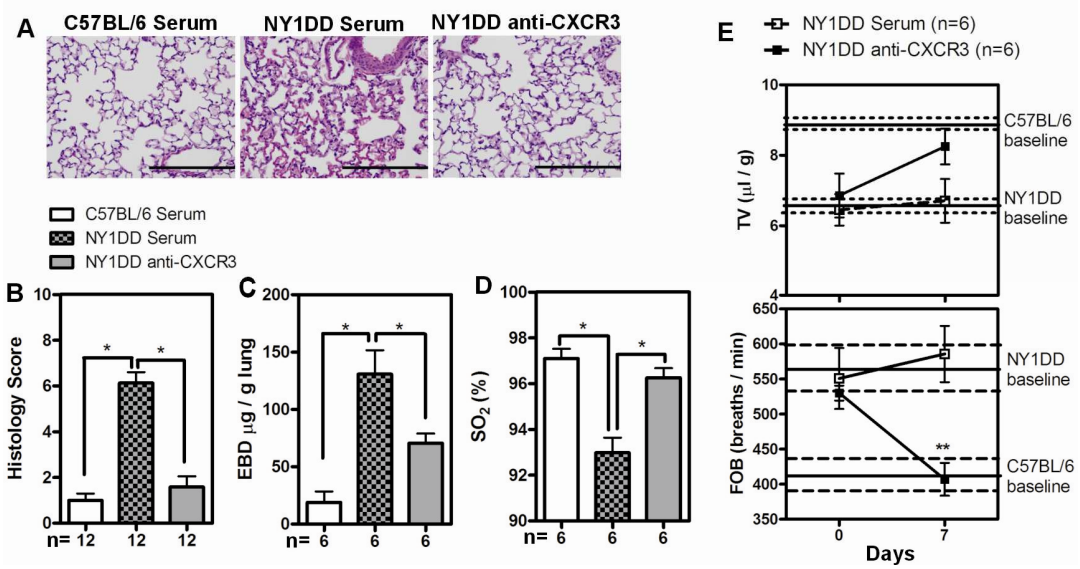

Figure 19. Anti-CXCR3 treatment decreases pulmonary injury in NY1DD mice

(**A**) Representative images of H&E stained lungs from C57BL/6 or NY1DD mice treated with goat serum and NY1DD mice treated with goat anti-CXCR3. The *bar* represents 200 µm. (**B**) Histopathological scores (0-8, see methods) by analysis of H&E stained mouse lungs. (**C,D**) Anti-CXCR3 treated NY1DD animals have decreased vascular permeability and increased arterial oxygen saturation as compared to serum-treated NY1DD mice. (**E**) Anti-CXCR3 treated NY1DD mice have improved breathing (increased tidal volume and decreased frequency of breathing) as compared to serum-treated NY1DD mice. * $P<0.05$. EBD: Evans Blue Dye; SO_2: arterial oxygen saturation; FOB: frequency of breathing; TV: tidal volume.

3.2.5. Anti-CD1d treated NY1DD mice have decreased pulmonary levels of IFN-γ, IFN-γ inducible chemokines, and CXCR3

Since iNKT cells are known to release copious amounts of IFN-γ, we hypothesized that IFN-γ from iNKT cells in NY1DD mice was responsible for the increased levels of IFN-γ inducible chemokines and the recruitment of CXCR3 positive lymphocytes. Blockade of iNKT activation by treatment of NY1DD mice with anti-CD1d for two days resulted in decreased whole lung levels of IFN-γ, CXCL9, CXCL10, and CXCR3 positive lymphocytes (Figure 20A-D). Five days after anti-CD1d treatment all of these parameters returned to NY1DD isotype treated levels (Figure 20A-D).

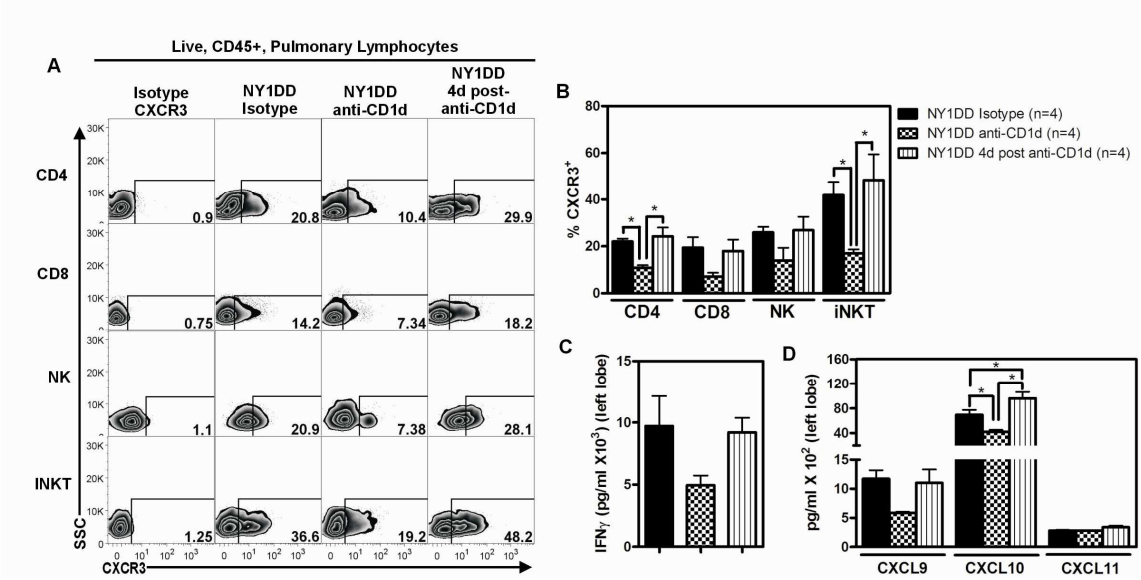

Figure 20. Anti-CD1d treatment decreases the percent of pulmonary lymphocytes expressing CXCR3 and reduces lung homogenate levels of IFN-γ and IFN-γ inducible chemokines

(**A**) Representative flow cytometry plots of CXCR3 expression on pulmonary lymphocytes from NY1DD isotype treated, NY1DD 1 day after anti-CD1d treatment, and NY1DD 5 days after anti-CD1d treatment. (**B**) Pulmonary lymphocytes from NY1DD mice express decreased CXCR3 when harvested 1 day, but not 5 days, after anti-CD1d. (**C,D**) Pulmonary tissues harvested from NY1DD animals have reduced levels of IFN-γ and IFN-γ inducible chemokines when harvested 1 day, but not 5 days, after anti-CD1d. Data were analyzed by one-way ANOVA with Neuman-Keuls post-testing, * $P<0.05$.

3.2.6. Clinical correlate: Individuals with sickle cell disease have increased and activated circulating iNKT cells

We used fluorescently labeled CD1d tetramers to selectively label iNKT cells (defined as tetramer$^+$ CD3$^+$) in the blood of 38 individuals with sickle cell disease and 8 age and race matched controls (Figure 21A). The mean age of participants with sickle cell disease was 32 (range 21 to 65) and 47.5 percent of the cohort were female. In comparison, the mean age of the controls was 41 (range 36 to 49) years and 87.5 percent of the controls were female. Flow cytometric analysis and counting beads were used to determine the absolute numbers of iNKT cells and the percent of iNKT cells among all CD3$^+$ lymphocytes (live, CD45$^+$, CD3$^+$) in the blood samples. Since there was only one control male sample, statistics could not be performed as compared to males with sickle cell disease. However, relative to control females, circulating iNKT cells from females with sickle cell disease were increased in absolute number (P=0.05) and as a percent of all CD3$^+$ cells (P=0.02) (Figures 21A,B). There was no statistical significance between males and females with sickle cell disease (Figure 21B). Also, iNKT cells from females with sickle cell disease at steady-state were found to be highly activated as compared to control females (Figures 21C,D). CD69 and IFN-γ both were found to be increased on iNKT cells from females with sickle cell disease. Furthermore, iNKT cells from females with sickle cell disease were found to express significantly higher levels of CXCR3 as compared to control females (P=0.001). Interestingly, males with sickle cell disease expressed higher levels of the activation markers CD69 and IFN-γ as compared to females with sickle cell disease.

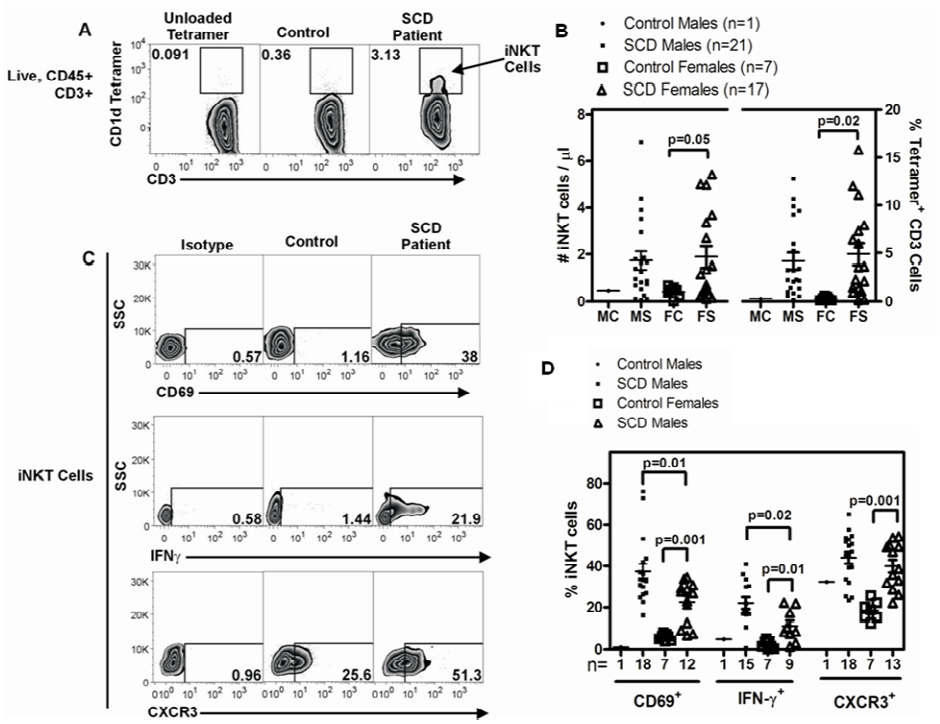

Figure 21. Individuals with sickle cell disease have increased circulating iNKT cells that express activation markers.

Fluorescently labeled CD1d tetramers were used to selectively label iNKT cells (defined as tetramer$^+$ CD3$^+$) in the blood of individuals with sickle cell disease (HbSS) and appropriate age and race matched controls (**A**) Representative flow cytometry plots of circulating human iNKT cells. **(B)** iNKT cells were identified from the live, CD45$^+$ lymphocyte gate as CD1d-tetramer$^+$ CD3$^+$ cells. Compared to controls, males and females with sickle cell disease have a higher number of circulating iNKT cells. **(C,D)** iNKT cells from individuals with sickle cell disease are more activated as defined by higher percent of surface CD69 and CXCR3, and intracellular IFN-γ. Males with sickle cell disease have more activated iNKT cells than females with sickle cell disease. Data were analyzed by an unpaired *t*-test. SSC: side-scatter. MC: male control; MS: male sickle cell disease; FC: female control; FS: female sickle cell disease.

3.2.7. Conclusions

The results of this study provide the basis for a new paradigm to understand the development of pulmonary dysfunction in sickle cell disease. We demonstrate a pivotal role for CD1d-restricted iNKT cells in maintaining chronic pulmonary inflammation and dysfunction in sickle cell disease mice via the IFN-γ inducible CXC chemokine-CXCR3 axis and preliminary data suggesting that this pathway may translate to individuals with sickle cell disease. We found iNKT cells from NY1DD mice to be increased in number and activation state in lung, liver, and spleen as compared to C57BL/6 control mice. Furthermore, acute sickle cell crisis exaggerated this inflammatory response, indicating that iNKT cells may be involved with acute vaso-occlusive injury in NY1DD mice. Although we focused on pulmonary inflammation and dysfunction for our studies, these findings indicate that this mechanism may be occurring in every organ system.

In the lung, compared to C57BL/6 mice, NY1DD mice have moderately increased numbers of iNKT cells (increased from 2.2 to 3.9 x 10^4 cells/lung). A much greater difference is noted in the fraction of iNKT cells that are judged to be activated, based on intracellular IFN-γ production, which increases from 5 % in C57BL/6 mice to 35 % in NY1DD mice. In addition, our data demonstrate that activation of iNKT cells plays an important role in pulmonary dysfunction of sickle cell disease. Pulmonary dysfunction and inflammation in sickle cell disease is largely reversed by inhibition of CD1d-restricted NKT activation and this protection was observed to be transient. Five days after anti-CD1d treatment, NY1DD mice were observed to return to baseline levels of pulmonary inflammation and dysfunction. Also, pulmonary dysfunction and inflammation in NY1DD mice is largely improved by lymphocyte deletion produced by

crossing NY1DD mice to Rag1$^{-/-}$ mice. The beneficial effects on pulmonary function of lymphocyte depletion in NY1DD x Rag1$^{-/-}$ are transiently reversed by adoptive transfer of 1 million NKT cells. Furthermore, 20 million splenocytes, but not 20 million NKT cell depleted T-cells, also can induce pulmonary injury in NY1DD x Rag1$^{-/-}$ mice. These findings indicate that although NKT cells represent only a minor subset of the total lymphocyte population, they play a pivotal role in sustaining the pulmonary pathophysiology in a mouse model of sickle cell disease. However, other subsets of cells were not adoptively transferred and we cannot rule out the possibility that other cells may be able to induce pulmonary injury in NY1DD x Rag1$^{-/-}$ mice. Finally, the fact that individuals with sickle cell disease also have increased numbers of activated circulating iNKT cells, suggests that these cells may be serving a similar role in human disease.

In the current study, we demonstrate a role for CD1d-restricted NKT cells, as treatment of NY1DD mice with anti-CD1d antibodies ameliorates pulmonary pathophysiology. One interpretation of these data is that host lipid antigens for iNKT cells are elevated in sickle cell disease. Another possibility is that lipid antigens remain constant while cytokines that facilitate activation of iNKT cells are enhanced. The most likely possibility is that pulmonary ischemia-reperfusion injury in response to microvascular occlusion with sickled red blood cells leads to increased release or oxidation of self-lipids that are presented via CD1d to activate iNKT cells and also triggers the release of cytokines that facilitate activation of iNKT cells. A resulting inflammatory cascade leads to the release of IFN-γ inducible and hypoxia-inducible chemokines from pulmonary resident epithelial or endothelial cells resulting in the recruitment and activation of CXCR3 positive lymphocytes, which further exacerbate

inflammation and vaso-occlusion (Figure 22). Our data indicate that compared to C57BL/6 lung lymphocytes, the fraction of lung lymphocytes positive for CXCR3 is greatly enhanced in NY1DD mice. This is likely due in part to enhanced production in the lung of CXCL9 and CXCL10 that are chemotactic ligands for CXCR3. In addition, activated iNKT cells release IL-2 which is known to induce expression of CXCR3 on lymphocytes. Consistent with the idea that IL-2 and IFN-γ inducible chemokines stimulate lymphocyte accumulation in the NY1DD lung via CXCR3, we show that blockade of CXCR3 receptors inhibits lung inflammation and injury. Also, our data demonstrates that circulating iNKT cells from individuals with sickle cell disease express increased CXCR3, suggesting that this trafficking mechanism may be pertinent in human disease.

In conclusion, our results suggest a new paradigm for understanding the pathogenesis of pulmonary inflammation and vaso-occlusion in sickle cell disease. Lung iNKT cells are activated in the NY1DD mouse and trigger an inflammatory cascade resulting in increased vascular permeability, decreased arterial oxygen saturation, and abnormal breathing parameters. Furthermore, we show that CD1d-restricted NKT cells are important for recruiting other inflammatory cells to the lung via the IFN-γ inducible chemokines-CXCR3 axis. Also, we demonstrate that circulating iNKT cells from individuals with sickle cell disease are increased in number and highly activated. The results of this study have important translational therapeutic implications. By inhibiting CD1d-restricted NKT cell activation or neutralizing CXCR3 on lymphocytes, it may be possible to reduce vascular occlusion and tissue damage associated with acute and chronic ischemia-reperfusion injury in sickle cell disease.

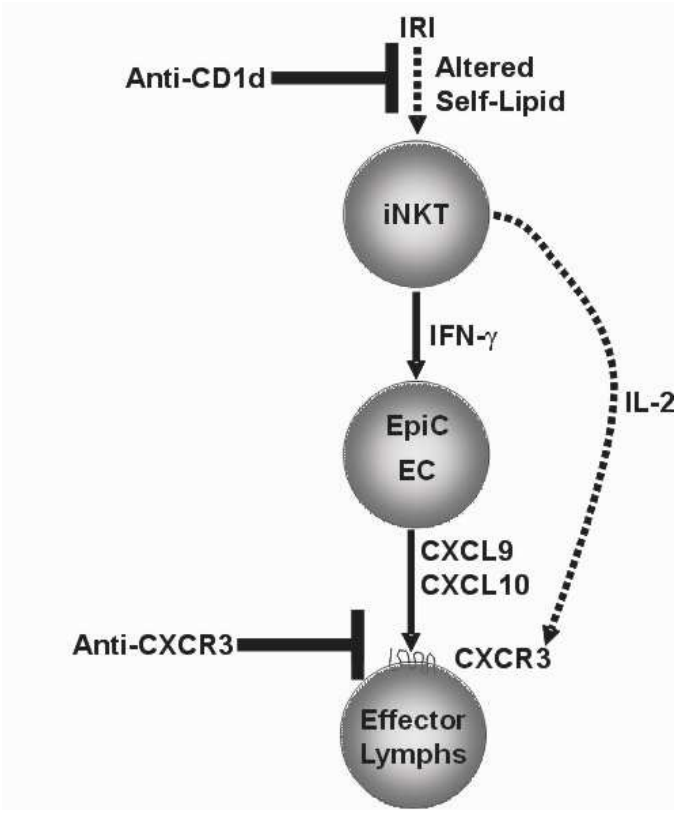

Figure 22. Hypothetical mechanism of iNKT cell mediated vaso-occlusion in sickle cell disease

Chronic ischemia-reperfusion injury in sickle cell disease may create an altered self-lipid that can be presented via CD1d on APCs to iNKT cells. This presentation may activate the iNKT cells to release IFN-γ and IL-2. IFN-γ triggers the release of IFN-γ inducible chemokines (CXCL9 and CXCL10) from resident epithelial (EpiC) or endothelial cell (EC). IL-2 has been previously shown to upregulate CXCR3 expression on lymphocyte effector cells. Taken together, the release of CXCL9/CXCL10 and the upregulation of CXCR3 could potentially enhance the trafficking of lymphocyte effector cells to the lung. IRI: ischemia-reperfusion injury

3.3. Adenosine $A_{2A}R$ agonists ameliorate pulmonary inflammation and dysfunction in murine sickle cell disease

Ischemia-reperfusion injury (IRI) triggers an inflammatory cascade that is initiated by the activation of CD1d-restricted iNKT cells and can be inhibited by activation of adenosine A_{2A} receptors ($A_{2A}R$). In sickle cell disease misshapen erythrocytes evoke repeated transient bouts of microvascular IRI and recent data suggest that iNKT cells are involved with this mechanism. Since ischemia-reperfusion mediated oxidative damage to the blood vessel wall is likely a critical component of the pathogenesis of vaso-occlusion in sickle cell disease and it is known that agonism of adenosine A_{2A} receptors ($A_{2A}R$) reduces ischemia-reperfusion injury, we hypothesized that $A_{2A}R$ agonism would decrease pulmonary inflammation and dysfunction in NY1DD mice (Harada et al., 2000; Jordan et al., 1997; Kaul and Hebbel, 2000; Okusa et al., 2000; Osarogiagbon et al., 2000; Ross et al., 1999; Thiel et al., 2003).

3.3.1. Pulmonary iNKT and NK cells from NY1DD mice contain increased amounts of $A_{2A}R$ mRNA

We used fluorescence activated cell sorting (FACS) to collect live ($DAPI^-$) and $CD45^+$ pulmonary iNKT (CD1d-$tetramer^+$, $CD3^+$), NK ($NKp46^+$, $CD3^-$), and $CD3^+$ T-cells (CD1d-$tetramer^-$, $CD3^+$) (Figure 23A). Quantitative RT-PCR was used to measure the transcript levels of the $A_{2A}R$ in the sorted populations of pulmonary lymphocytes, relative to a housekeeping gene (cyclophilin). Compared to C57BL/6 mice, NY1DD mice displayed increased transcript levels of $A_{2A}R$ in iNKT cells (9.2 ± 1.0 -fold) and NK cells

(6.1 ± 0.5 -fold), whereas $CD3^+$ T-cells had no change in the amount of $A_{2A}R$ mRNA (0.8 ± 0.1 -fold) (Figure 23B).

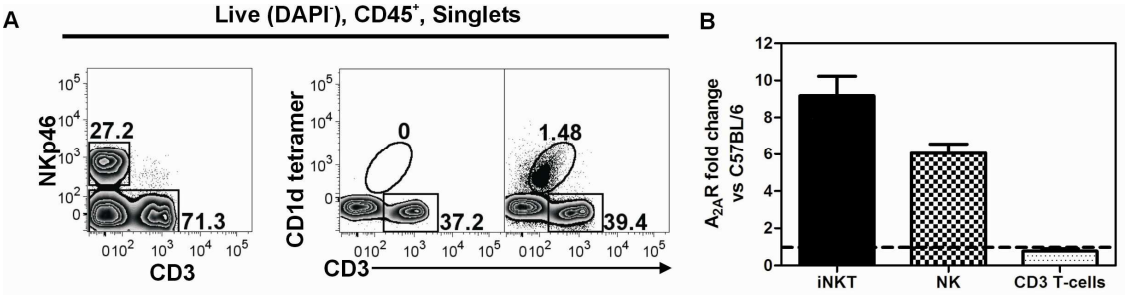

Figure 23. Lung iNKT and NK cells from NY1DD mice have increased amounts of $A_{2A}R$ mRNA

Live ($DAPI^-$) and $CD45^+$ pulmonary cells were sorted based on surface antigen staining: iNKT ($CD1d\text{-}tetramer^+$, $CD3^+$), NK ($NKp46^+$, $CD3^-$), and $CD3^+$ T-cells ($CD1d\text{-}tetramer^-$, $CD3^+$). (**A**) Representative flow cytometry plots of sorted populations. (**B**) Quantitative RT-PCR was used to measure mRNA levels of $A_{2A}R$ in the sorted populations of pulmonary lymphocytes as compared to a housekeeper (cyclophilin). NY1DD mice (n=4) have increased amounts of $A_{2A}R$ mRNA in pulmonary iNKT cells and NK cells, but not in $CD3^+$ T-cells as compared to cells from C57BL/6 mice (n=4).

3.3.2. ATL146e treatment decreases pulmonary dysfunction in NY1DD mice

As demonstrated above, iNKT cells play a central role in the pathogenesis of sickle cell disease. Since iNKT cells from NY1DD mice also have increased $A_{2A}R$ mRNA we hypothesize that agonism of the $A_{2A}R$ may be used as a method to ameliorate pulmonary dysfunction found in these animals.

3.3.2.1. Determination of the optimal dose and time of ATL146e infusion

To determine the optimal dose and time of treatment with the selective $A_{2A}R$ agonist ATL146e, NY1DD mice were infused with ATL146e via osmotic pumps. Previous studies of liver and heart ischemia-reperfusion injury indicated that an infusion rate of ATL146e at 10 ng/kg/min was beneficial in ameliorating post-ischemic increases in alanine aminotransferase (ALT) levels and infarct size respectively (Day et al., 2003; Day et al., 2004; Yang et al., 2006). Vascular permeability, (Evans blue dye accumulation), leukocyte infiltration (flow cytometric analysis of lung leukocyte absolute number), and breathing parameters (tidal volume and frequency of breath) were used as indices of pulmonary inflammation and dysfunction to determine the optimal dose and time of ATL146e treatment. We have previously demonstrated that these markers are reliable measures of pulmonary injury in NY1DD mice. During 3 days of treatment, maximal improvement in pulmonary dysfunction was demonstrated at an infusion rate of 10 ng/kg/min and no further improvement was detected at higher doses (Figure 24). Furthermore, improvements in pulmonary function observed in NY1DD mice treated with ATL146e (10 ng/kg/min) for 3 days remained constant during 7 days of treatment

(Figure 25). These data demonstrate that there is no desensitization of the $A_{2A}R$ during ATL146e treatment for at least 7 days.

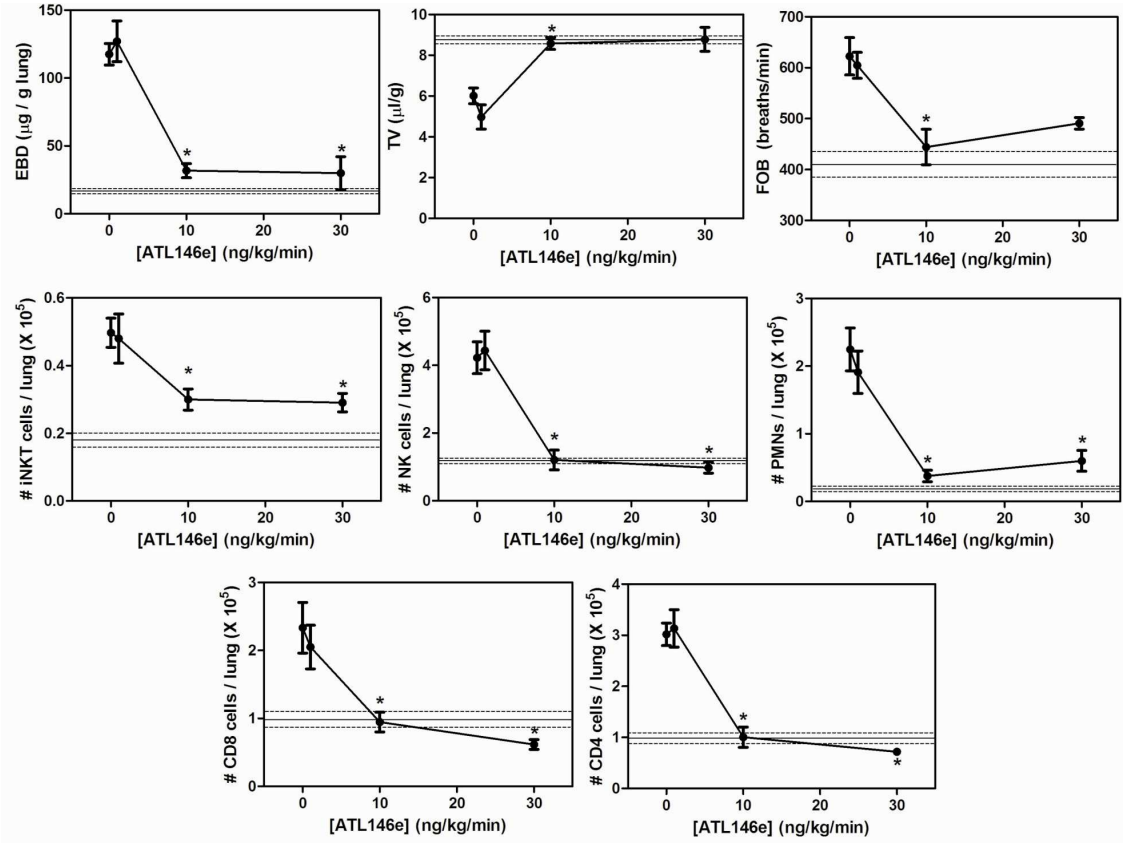

Figure 24. Determination of the optimal dose of ATL146e infusion

NY1DD mice were treated with a constant infusion of ATL146e (1,10,30 ng/kg/min, osmotic pump). After 3 days of treatment, pulmonary parameters were measured in NY1DD treated mice. All parameters measured (vascular permeability [EBD], breathing measurements [TV, FOB], and pulmonary cell infiltrates) were found to be maximally improved at 10 ng/kg/min, as no further improvements were noted at higher doses. The solid and dashed lines represent the mean and standard error of control C57BL/6 mice. Data were analyzed by one-way ANOVA with Neuman-Keuls post-testing. * $P<0.05$. EBD: Evans blue dye; TV: tidal volume; FOB: frequency of breath.

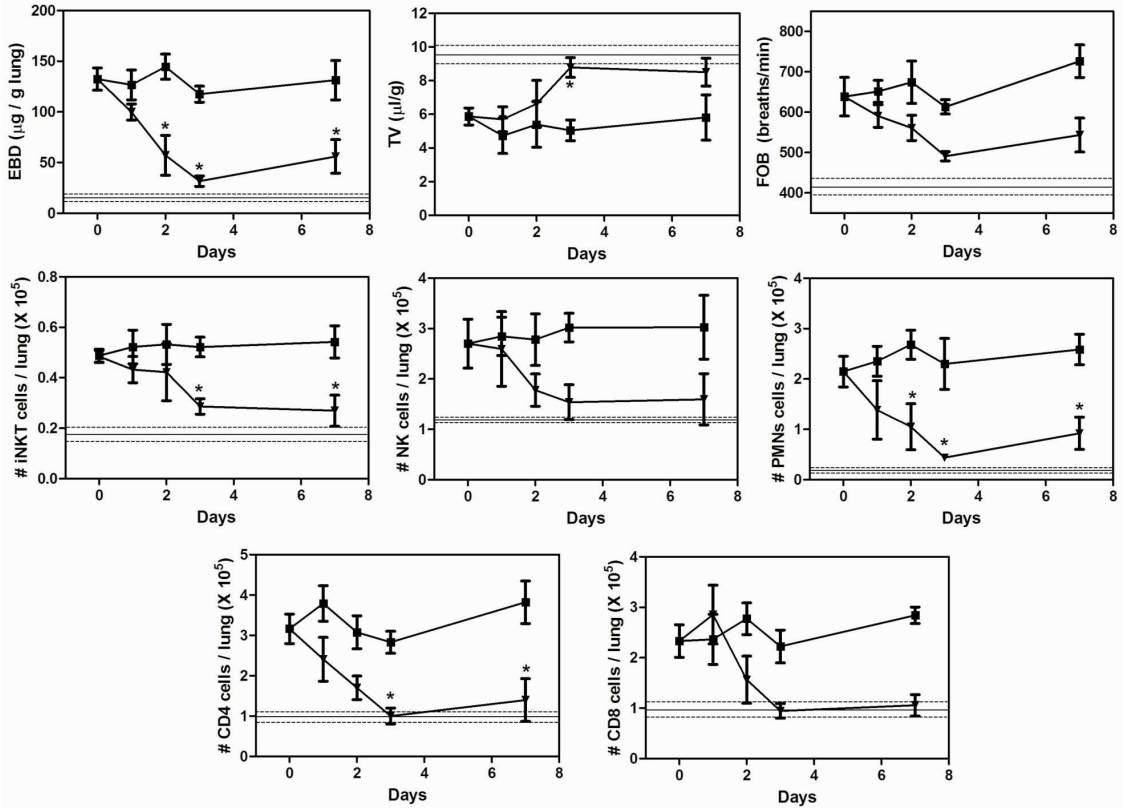

Figure 25. Determination of the optimal time of ATL146e infusion

NY1DD mice were treated with a constant infusion of ATL146e (10 ng/kg/min, osmotic pump). Pulmonary parameters were measured in NY1DD treated mice 1, 2, 3, or 7 days after the start of ATL146e infusion. All parameters measured (vascular permeability [EBD], breathing measurements [TV, FOB], and pulmonary cell infiltrates) were found to be maximally improved by 3 days after the start of ATL146e treatment, as no further improvements were noted at 7 days. The solid and dashed lines represent the mean and standard error of control C57BL/6 mice. Data were analyzed by one-way ANOVA with Neuman-Keuls post-testing. * $P<0.05$. EBD: Evans blue dye; TV: tidal volume; FOB: frequency of breath.

3.3.2.2. ATL146e treatment decreases pulmonary dysfunction and injury by specific agonism of the $A_{2A}R$

Taken together, NY1DD mice treated with ATL146e (10 ng/kg/min, 3 days) demonstrated significant amelioration of pulmonary injury as compared to vehicle treated NY1DD mice. Histologically, the lungs from ATL146e treated NY1DD mice displayed decreased areas of pulmonary capillary congestion as compared to vehicle control NY1DD mice (Figure 26B,E). ATL146e treated NY1DD mice had significantly decreased vascular permeability (3.2-fold decrease compared to vehicle NY1DD mice; $P<0.05$) and increased arterial oxygen saturation (94 % as compared to 90 % in vehicle treated NY1DD mice; $P<0.05$) (Figure 26G,H). Furthermore, unrestrained whole body plethysmography revealed that ATL146e treated NY1DD mice had improved breathing parameters. Tidal volume increased 1.4-fold ($P<0.05$) and respiratory rate decreased from 624 breaths per minute to 444 breaths per minute ($P<0.05$) (Figure 26I,J).

To determine if ATL146e had any effect on intra-pulmonary leukocytosis we used flow cytometric analysis to define WBC populations in digested whole lung tissue. Compared to vehicle treated NY1DD mice, ATL146e treated NY1DD mice had a significantly decreased number of pulmonary leukocytes (iNKT cells, 1.7-fold; NK cells, 3.5-fold; CD4 T-cells, 3-fold; CD8 T-cells, 2.5-fold; PMNs, 5.8-fold) (Table 11). ATL146e did not have any effects on pulmonary measurements of inflammation or dysfunction in C57BL/6 mice, and did not cause any changes based on histological inspection (Figure 26A-J).

To determine if ATL146e ameliorated pulmonary inflammation and dysfunction through the anti-inflammatory $A_{2A}R$, we crossed NY1DD mice with an $A_{2A}R^{-/-}$ mice.

NY1DD x $A_{2A}R^{-/-}$ mice had pulmonary inflammation similar to NY1DD mice (Figure 26C,F; Table 11). However, treatment of NY1DD x $A_{2A}R^{-/-}$ mice with ATL146e (10 ng/kg/min, 3 days) did not confer any protection of pulmonary injury as compared to vehicle treated NY1DD x $A_{2A}R^{-/-}$ animals (Figure 26G-J, Table 11).

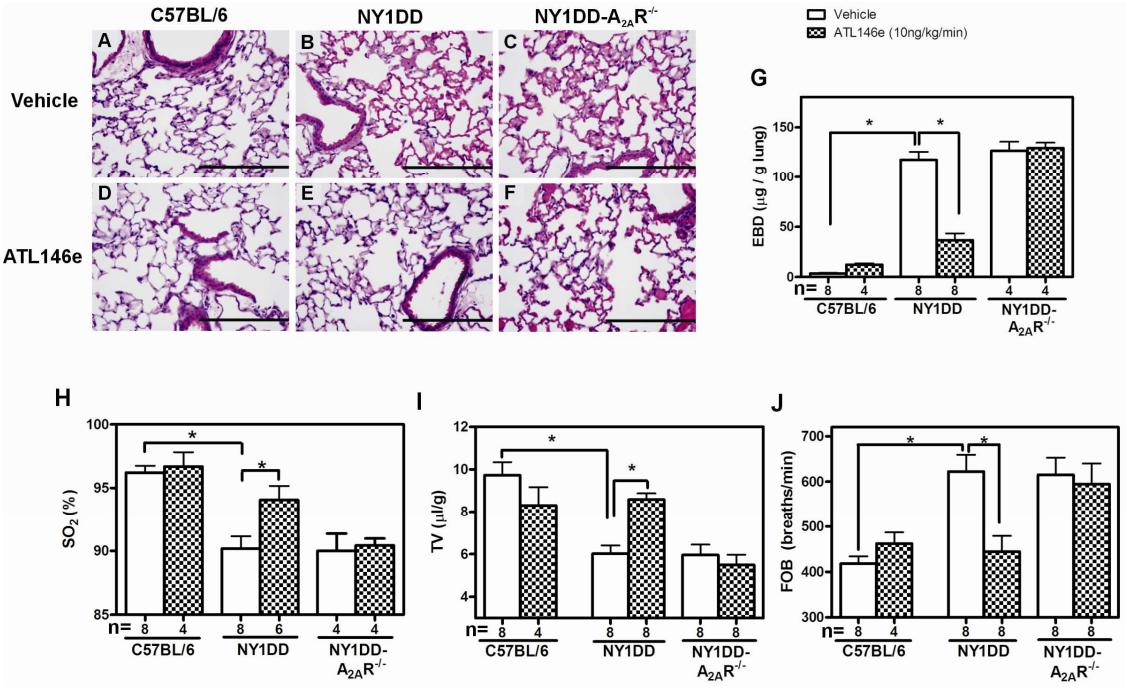

Figure 26. ATL146e treatment decreases pulmonary dysfunction in NY1DD mice by selective agonism of A_{2A}Rs

C57BL/6, NY1DD, or NY1DD x $A_{2A}R^{-/-}$ mice were treated with ATL146e (10 ng/kg/min, 3 days) or vehicle (saline, 0.2% DMSO). (**A-F**) NY1DD mice, but not NY1DD x $A_{2A}R^{-/-}$ mice displayed observable improvements in pulmonary histology after ATL146e treatment. (**G,H**) NY1DD mice, but not NY1DD x $A_{2A}R^{-/-}$ mice, had decreased vascular permeability and increased oxygen saturation after ATL146e treatment. (**I,J**) NY1DD mice, but not NY1DD x $A_{2A}R^{-/-}$ mice, displayed improved breathing parameters after ATL146e treatment. Data were analyzed by one-way ANOVA with Neuman-Keuls post-testing; * $P<0.05$. EBD: Evans blue dye; SO2: arterial oxygen saturation; TV: tidal volume; FOB: frequency of breath.

Cells (10^5)	(a) C57BL/6 Vehicle (n=8)	(b) C67BL/6 ATL146e (n=4)	(c) NY1DD Vehicle (n=8)	(d) NY1DD ATL146e (n=8)	(e) NY1DD-$A_{2A}R^{-/-}$ Vehicle (n=6)	(f) NY1DD-$A_{2A}R^{-/-}$ ATL146e (n=6)
iNKT	0.19 (0.02)	0.13 (0.02)	0.5 (0.04)*	0.29 (0.03)**	0.58 (0.05)	0.55 (0.09)
NK	1.7 (0.2)	1.8 (0.3)	4.2 (0.5)*	1.2 (0.3)**	4.0 (0.5)	4.1 (0.4)
CD4	1.0 (0.09)	1.3 (0.4)	3.0 (0.2)*	1.0 (0.2)**	3.3 (0.8)	3.2 (0.7)
CD8	1.1 (0.1)	1.3 (0.2)	2.3 (0.4)*	0.9 (0.1)**	2.8 (0.4)	2.9 (0.3)
PMNs	0.3 (0.07)	0.3 (0.1)	2.3 (0.3)*	0.4 (0.1)**	2.9 (0.7)	3.1 (0.5)

Table 11. ATL146e treatment decreases pulmonary leukocytosis in NY1DD mice by specific agonism of A_{2A}Rs

NY1DD mice treated with ATL146e (10 ng/kg/min, 3 days) displayed significantly decreased pulmonary leukocytes (column d). C57BL/6 mice were unaffected by ATL146e treatment (column b). NY1DD x $A_{2A}R^{-/-}$ have increased numbers of pulmonary leukocytes (column e), but NY1DD x $A_{2A}R^{-/-}$ mice were unaffected by ATL146e treatment (column f). Data represents mean (standard error of the mean). Data were analyzed by one-way ANOVA with Neuman-Keuls post-testing; * $P<0.05$ (column a vs c), ** $P<0.05$ (column c vs d).

3.3.3. ATL146e treatment ameliorates acute sickle cell crisis induced pulmonary inflammation in NY1DD mice

Even though chronic sub-clinical baseline ischemia-reperfusion occurs during sickle cell disease, individuals present to the emergency room during "crisis," which is defined as a rapidly developing episode of acute pain. Since ATL146e treatment decreased pulmonary dysfunction and inflammation at baseline, we hypothesized that it may reverse the effects of new acute sickle cell crisis. The NY1DD model has been used to elucidate the role of ischemia-reperfusion injury in sickle cell disease. NY1DD mice placed in a hypoxic (10 % O_2) chamber for 3 hours, which induced red blood cell sickling and ischemia, followed by 4 hours of reoxygenation (room air) results in an exaggerated inflammatory response that is believed to mimic human sickle cell crisis, as the response was not seen in C57BL6 control mice (no red blood cell sickling and thus no ischemia) nor in NY1DD mice exposed to hypoxia alone, suggesting that the pro-inflammatory state in NY1DD animals was due to reperfusion injury (Kaul and Hebbel, 2000). In this study, Kaul *et al.* determined that NY1DD mice exposed to 3 hours of hypoxia, to induce ischemia, followed by 4 hours of reoxygenation resulted in maximal levels of inflammatory mediators (i.e. NF-κβ transcription) and 18 hours of reoxygenation resulted in maximal levels of cell infiltration into inflamed tissues. Therefore, we subjected the NY1DD mouse to 3 hours of hypoxia, followed by a period of reoxygenation. Three hours into the reoxygenation period, when inflammatory mediators are known to be increased, we implanted osmotic pumps with ATL146e (10 ng/kg/min). Then 15 hours later, for a total of 18 hours of reoxygenation, we analyzed pulmonary parameters.

Vehicle treated NY1DD mice subjected to hypoxia-reoxygenation were found to have significantly increased vascular permeability as compared to normoxic NY1DD mice (1.6-fold; $P<0.05$). Also, vehicle treated NY1DD mice had increased pulmonary PMNs (4.3-fold; $P<0.05$) and iNKT cells (2.2-fold; $P<0.05$). NY1DD mice that received ATL146e after the start of reoxygenation were found to have significantly decreased levels of pulmonary vascular permeability as compared to NY1DD vehicle treated mice (53.1 ± 12.2 vs 191.9 ± 19.3 µg EBD / g lung; $P<0.05$) (Figure 27A). Furthermore, ATL146e treated NY1DD mice displayed decreased pulmonary cell infiltration as compared to vehicle treated NY1DD mice (Table 12). Specifically, ATL146e treatment decreased pulmonary PMNs (8.9-fold), CD4 T-cells (6.6-fold), CD8 T-cells (6.2-fold), NK cells (1.9-fold), and iNKT cells (4.2-fold) in NY1DD mice. Also, breathing parameters were normalized in ATL146e treated NY1DD mice as compared to vehicle treated NY1DD mice (Figure 27B,C).

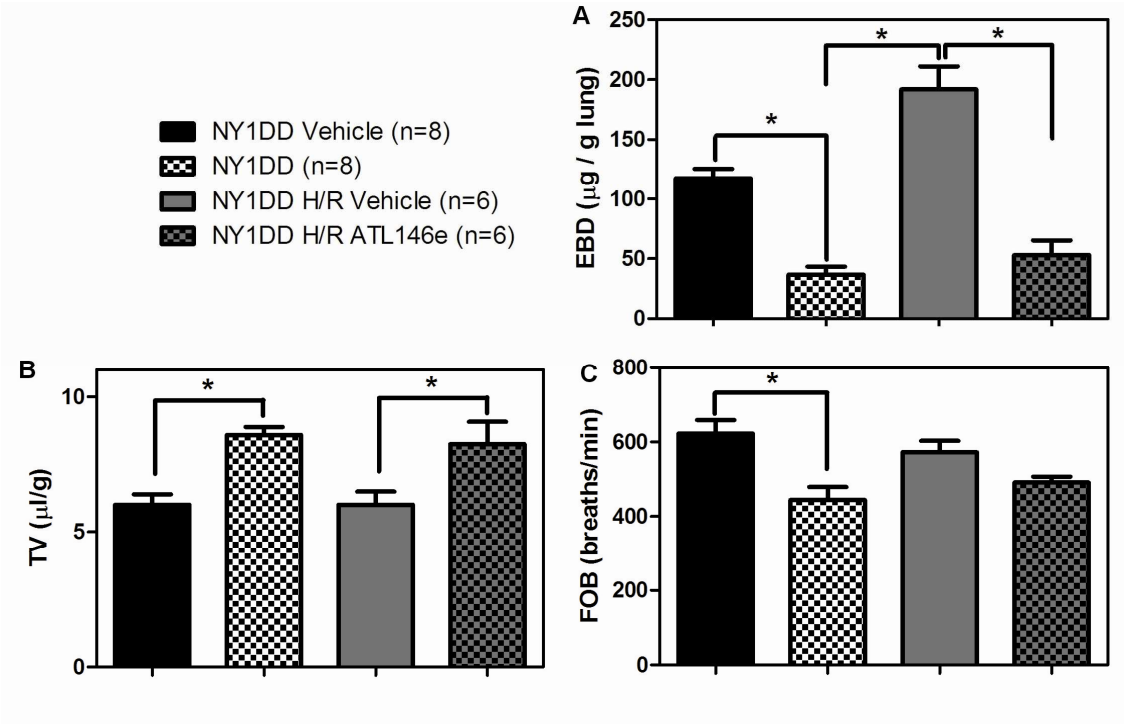

Figure 27. ATL146e treatment ameliorates acute sickle cell crisis induced lung inflammation in NY1DD mice

NY1DD mice were subjected to 3 hours of hypoxia (8 % O_2) followed by 18 hours of reoxygenation (room air). Three hours into reoxygenation NY1DD mice were infused with ATL146e (10 ng/kg/min, osmotic pump) or vehicle (saline, 0.2 % DMSO). NY1DD mice treated with vehicle during reoxygenation displayed increased vascular permeability (**A**), but no changes in breathing parameters (**B,C**) as compared to normoxic NY1DD vehicle treated mice. NY1DD mice treated with ATL146e during reoxygenation displayed significantly decreased vascular permeability (**A**) and moderately improved breathing parameters (**B,C**) as compared to vehicle treated NY1DD mice after hypoxia-reoxygenation. Data were analyzed by one-way ANOVA with Neuman-Keuls post-testing; * $P<0.05$. EBD: Evans blue dye; TV: tidal volume; FOB: frequency of breath.

Cells (10^5)	Normoxia		Hypoxia-Reoxygenation	
	(a) NY1DD Vehicle (n=8)	**(b) NY1DD ATL146e (n=8)**	**(c) NY1DD Vehicle (n=6)**	**(d) NY1DD ATL146e (n=6)**
iNKT	0.5 (0.04)	0.29 (0.03)*	1.1 (0.2)*	0.26 (0.05)**
NK	4.2 (0.5)	1.2 (0.3)*	3.0 (0.6)	1.6 (0.2)
CD4	3.0 (0.2)	1.0 (0.2)*	3.3 (1.0)	0.5 (0.1)**
CD8	2.3 (0.4)	0.9 (0.1)*	3.1 (0.9)	0.5 (0.1)**
PMNs	2.3 (0.3)	0.4 (0.1)*	9.8 (4.1)*	1.1 (0.5)**

Table 12. ATL146e treatment decreases pulmonary cell infiltration during acute sickle cell crisis in NY1DD mice

NY1DD mice were subjected to 3 hours of hypoxia (8 % O_2) followed by 18 hours of reoxygenation (room air). Three hours into reoxygenation NY1DD mice were infused with ATL146e (10 ng/kg/min, osmotic pump) or vehicle (saline, 0.2 % DMSO). NY1DD mice treated with ATL146e during reoxygenation displayed significantly decreased pulmonary leukocytes (column d). NY1DD mice treated with vehicle during reoxygenation displayed significant increases in iNKT cells and PMNs (column c). Data represents mean (standard error of the mean). Data were analyzed by one-way ANOVA with Neuman-Keuls post-testing; * $P<0.05$ (vs column a), ** $P<0.05$ (vs column c).

3.3.4. The protective effects of ATL146e on pulmonary inflammation and dysfunction in NY1DD mice are reversible

To assess the length of protection conferred by ATL146e in NY1DD pulmonary inflammation and dysfunction we treated NY1DD mice with an infusion of ATL146e (10 ng/kg/min) for 3 days and assessed pulmonary injury either 1 day or 4 days after the secession of treatment. One day after secession of ATL146e treatment, pulmonary parameters began to return to baseline NY1DD levels, as indicated by increased vascular permeability, increased pulmonary cell infiltrates, and dysfunctional breathing parameters (Figure 27). By 4 days after secession of treatment, pulmonary parameters had returned to baseline NY1DD levels (Figure 28).

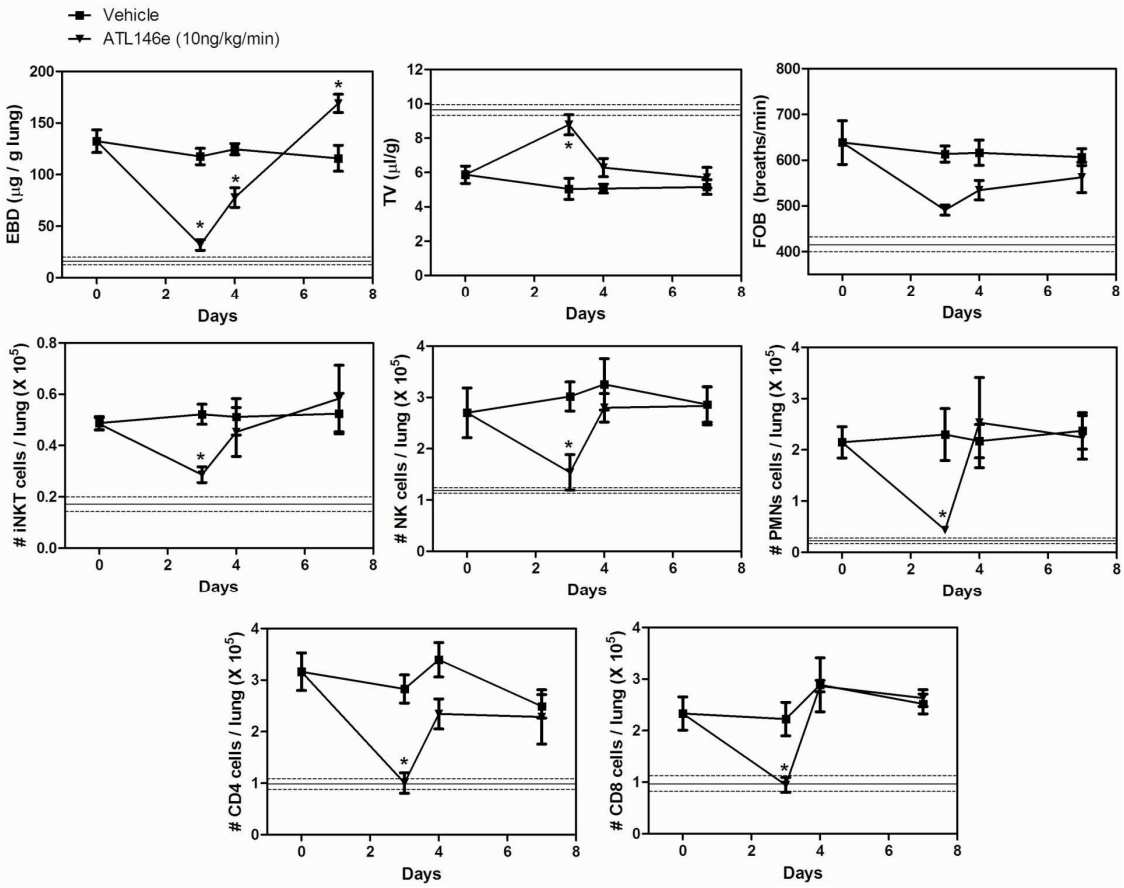

Figure 28. ATL146e treatment transiently ameliorates pulmonary injury in NY1DD mice

NY1DD mice were treated with a constant infusion of ATL146e (10 ng/kg/min, 3 days). Pulmonary parameters were measured 1 day or 4 days after the secession of ATL146e infusion. All parameters measured (vascular permeability [EBD], breathing measurements [TV, FOB], and pulmonary cell infiltrates) began to return to NY1DD baseline levels 1 day after the secession of ATL146e treatment and had returned to baseline levels by 4 days. The solid and dashed lines represent the mean and standard error of control C57BL/6 mice. Data were analyzed by one-way ANOVA with Neuman-Keuls post-testing. * $P<0.05$. EBD: Evans blue dye; TV: tidal volume; FOB: frequency of breath.

3.3.5. ATL146e agonises A_{2A}Rs on iNKT cells to decrease pulmonary injury in NY1DD mice

Since, it has been demonstrated that A_{2A}R agonism exerts its protective effects on controlling ischemia-reperfusion injury by acting on iNKT cells and we have previously demonstrated that iNKT cells play a major role in the perpetuation of pulmonary vaso-occlusive pathophysiology in NY1DD mice, we hypothesized that A_{2A}Rs on iNKT cells might be the primary targets of ATL146e (Lappas et al., 2006; Li et al., 2007).

To test this hypothesis, NY1DD mice were treated with an infusion of ATL146e (10 ng/kg/min, 3 days), anti-CD1d (10 µg/g/days, 2 days), or a combination of both. Treatment of NY1DD mice with either ATL146e or anti-CD1d significantly decreased the level of pulmonary injury observed. However treatment with both ATL146e and anti-CD1d did not confer any additional protection as compared to either treatment alone (Figure 29A-G, Table 13). These data indicate that inhibition of iNKT activation is sufficient to fully account for the pulmonary protection observed by ATL146e.

To further investigate A_{2A}Rs on iNKT cells, we used NY1DD x Rag1$^{-/-}$ mice that lack mature lymphocytes. We have previously demonstrated that this line is protected from developing sickle cell disease induced pulmonary inflammation and dysfunction and that the adoptive transfer of NKT cells recapitulates pulmonary injury. NY1DD x Rag1$^{-/-}$ mice were pre-treated with ATL146e (10 ng/kg/min, 3 days). One day prior to experimentation ATL146e treated NY1DD x Rag1$^{-/-}$ mice were adoptively transferred with 1 x 10^6 iNKT cells pre-treated with either FSPTP (200 µM) or vehicle (saline, 2% DMSO). FSPTP treatment alkylates the A_{2A}R causing it to become unresponsive to agonist (ATL146) treatment. Therefore, only the A_{2A}R on the iNKT cells would be

unresponsive to ATL146e, while host PMNs, NK cells, platelets, epithelial cells, and endothelial cells, all of which had functional A_{2A}Rs, would be able to respond to ATL146e treatment. ATL146e treated NY1DD x $Rag1^{-/-}$ mice adoptively transferred with vehicle treated iNKT cells (functional A_{2A}R) were protected by ATL146e from developing pulmonary inflammation and injury upon adoptive transfer of NKT cells (Figure 30A-C, Table 14). However, NY1DD x $Rag1^{-/-}$ mice adoptively transferred with NKT cells with alkylated A_{2A}Rs displayed pulmonary dysfunction one day after the transfer that was not blocked by ATL146e (Figure 30A-C, Table 14). Also, NY1DD x $Rag1^{-/-}$ mice pre-treated with ATL146e prior to the adoptive transfer of FSPTP treated NKT cells had decreased numbers of pulmonary NK cells, indicating that the A_{2A}R on these cells was responsive to treatment (Table 14).

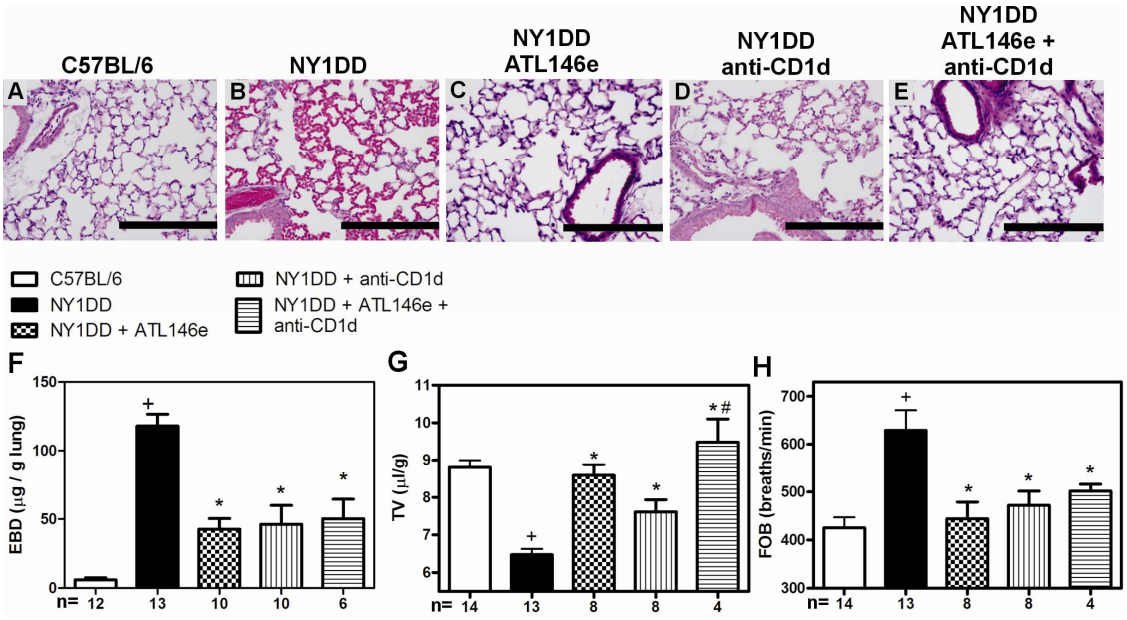

Figure 29. The protective effects of ATL146e and anti-CD1d treatments on decreasing pulmonary inflammation in NY1DD mice are not additive

NY1DD mice were treated with either ATL146e (10 ng/kg/min, 3 days), anti-CD1d (10 µg/g/day, 2 days), or a combination of both. All treatments resulted in significantly improved pulmonary parameters. (**A-E**) Representative H&E staining from lungs of untreated and treated mice. (**B-E**) Treated NY1DD mice appear to have similarly less capillary congestion and decreased alveolar wall thickness as compared to untreated NY1DD mice. (**F-H**) Treated NY1DD mice have similarly decreased vascular permeability and normalized breathing parameters as compared to untreated NY1DD mice. Data were analyzed by one-way ANOVA with Neuman-Keuls post-testing. A *P*-value <0.05 was considered significant. + NY1DD vs C57BL/6; * NY1DD treatment groups vs untreated NY1DD; # NY1DD both treatments vs NY1DD anti-CD1d. EBD: Evans blue dye; TV: tidal volume; FOB: frequency of breath.

Cells (10^5)	(a) NY1DD (n=17)	(b) NY1DD ATL146e (n=8)	(c) NY1DD anti-CD1d (n=10)	(d) NY1DD ATL146e anti-CD1d (n=4)
iNKT	0.43 (0.03)	0.30 (0.03)*	0.20 (0.05)*	0.16 (0.05)*
NK	4.45 (0.77)	1.21 (0.30)*	1.51 (0.22)*	0.90 (0.08)*
CD4	3.12 (0.37)	1.00 (0.20)*	1.04 (0.21)*	1.20 (0.30)*
CD8	2.33 (0.32)	1.00 (0.15)*	0.66 (0.18)*	0.73 (0.23)*
PMNs	2.14 (0.31)	0.38 (0.09)*	0.84 (0.12)*	0.52 (0.13)*

Table 13. The effects of ATL146e and anti-CD1d treatments on pulmonary cell infiltration are not additive

NY1DD mice were treated with either ATL146e (10 ng/kg/min, 3 days), anti-CD1d (10 µg/g/day, 2 days), or a combination of both. All treatments resulted in significantly decreased pulmonary leukocytes. Data represents mean (standard error of the mean). Data were analyzed by one-way ANOVA with Neuman-Keuls post-testing; * $P<0.05$ vs column a.

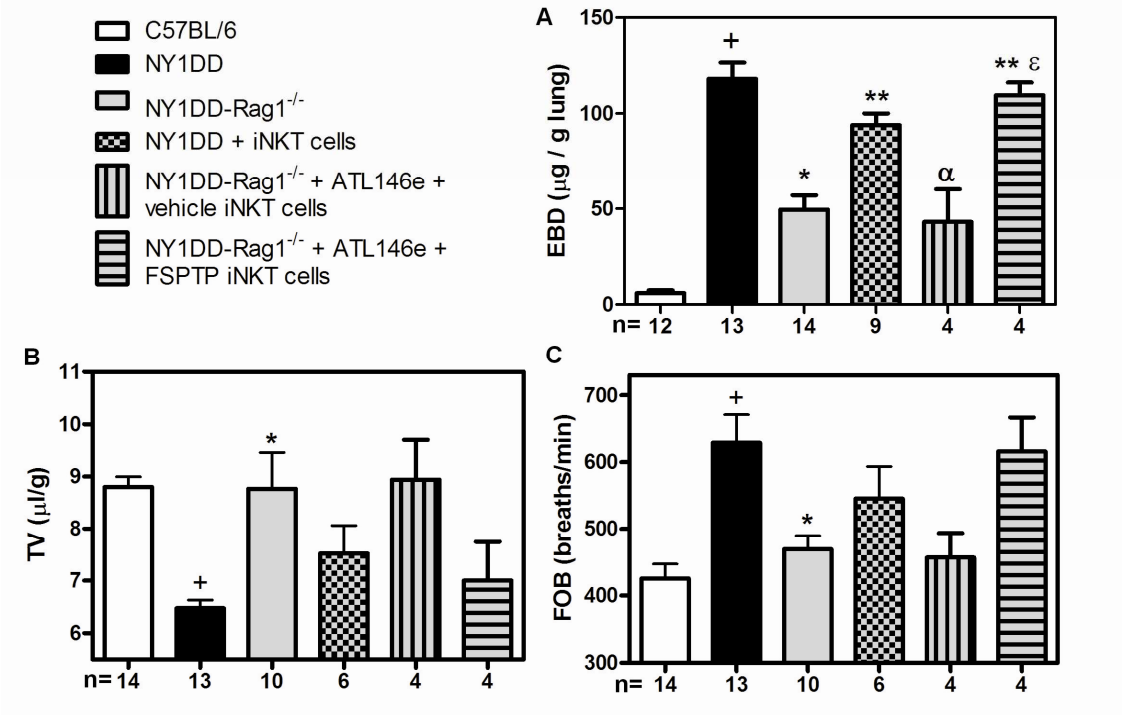

Figure 30. ATL146e acts on A_{2A}Rs on iNKT cells to decrease pulmonary inflammation

NY1DD x Rag1$^{-/-}$ mice were pre-treated with ATL146e (10 ng/kg/min, 3 days). One day prior to experimentation ATL146e treated NY1DD x Rag1$^{-/-}$ mice were adoptively transferred with 1 x 10^6 iNKT cells pre-treated with either FSPTP (an A_{2A}R alkylating agent) or vehicle. (**A**-**C**) NY1DD x Rag1-/- mice pretreated with ATL146e are protected from developing pulmonary injury after the adoptive transfer of NKT cells and FSPTP treatment abrogates this effect. Data were analyzed by one-way ANOVA with Neuman-Keuls post-testing. A *P*-value <0.05 was considered significant. + vs C57BL/6; * vs NY1DD; ** vs NY1DD x Rag1$^{-/-}$; α vs NY1DD x Rag1$^{-/-}$ + NKT cells; ε vs ATL146e pre-treated NY1DD x Rag1$^{-/-}$ + NKT cells. EBD: Evans blue dye; TV: tidal volume; FOB: frequency of breath.

Cells (10^5)	(a) NY1DD (n=8)	(b) NY1DD-Rag1$^{-/-}$ (n=8)	(c) NY1DD-Rag1$^{-/-}$ + NKT cells (n=4)	(d) NY1DD-Rag1$^{-/-}$ + ATL146e + NKT cells (n=4)	(e) NY1DD-Rag1$^{-/-}$ + ATL146e + FSPTP NKT cells (n=4)
NK	4.30 (0.85)	6.71 (1.28)*	12.32 (1.03)*,***	2.80 (1.00)***	2.63 (0.77)***
PMNs	2.34 (0.40)	1.63 (0.46)	6.64 (1.90)*,***	1.23 (0.58)***	6.85 (1.34)*,#
iNKT	0.37 (0.06)	n/a	0.46 (0.12)	0.15 (0.04)	0.63 (0.16)#

Table 14. Pre-treatment with ATL146e protects pulmonary dysfunction in NY1DD-Rag1$^{-/-}$ mice after the adoptive transfer of 1x10^6 NKT cells and this effect is dependent on NKT cell $A_{2A}R$

NY1DD x Rag1$^{-/-}$ mice were pre-treated with ATL146e (10 ng/kg/min, 3 days). One day prior to experimentation ATL146e treated NY1DD x Rag1$^{-/-}$ mice were adoptively transferred with 1 x 10^6 iNKT cells pre-treated with either FSPTP (an $A_{2A}R$ alkylating agent) or vehicle. Data represents mean (standard error of the mean). Data were analyzed by one-way ANOVA with Neuman-Keuls post-testing; * P<0.05 vs column a, ** P<0.05 vs column b, *** P<0.05 vs column c, # P<0.05 vs column d.

3.3.6. Conclusions

Treatment strategies for individuals with sickle cell disease are quite complex, require close monitoring by health care workers, and have limited effectiveness. Briefly, current treatment includes prophylactic and liberal use of antibiotics during infections, transfusion therapy, pain management, and hydroxyurea. Although studies have shown an overall benefit of hydroxyurea in sickle cell disease (via stimulation of HbF production), 10-50 % of individuals do not respond to treatment (Charache et al., 1995). Due to the mechanism of action of hydroxyurea (inhibition of ribonucleotide reductase that inhibits DNA synthesis and repair, which ultimately leads to S-phase cell death), a major concern is that long-term hydroxyurea therapy may be carcinogenic or leukemogenic. This has already been demonstrated in individuals treated with hydroxyurea for polycythemia vera (Dalton et al., 2005). While these therapies have increased the lifespan of individuals with sickle cell disease, morbidity and mortality still remain relatively high with most individuals dying prematurely. Therefore, there is a pressing need for new treatments with minimal side effects. The results of this study provide the basis for new strategies for treatment of sickle cell disease by targeting iNKT cells. We demonstrate a pivotal role for agonism of A_{2A}Rs on iNKT cells to decrease baseline pulmonary inflammation and dysfunction in sickle cell disease mice. Furthermore, acute sickle cell crisis induced pulmonary inflammation was inhibited with A_{2A}R agonism after the start of crisis, suggesting that this treatment may be beneficial in treating sickle cell diseased individuals in the emergent setting.

Compared to lung lymphocytes from C57BL/6 mice, NY1DD mice have increased A_{2A}R mRNA in iNKT and NK cells. This is consistent with recent findings

demonstrating enhanced $A_{2A}R$ promoter activity upon activation of NKT and NK cells in liver IRI (Chen-in press). Pulmonary dysfunction and inflammation in sickle cell disease mice and is largely reversed by treatment with ATL146e (10 ng/kg/min, 3 d) and this protection is mediated by $A_{2A}Rs$, as NY1DD x $A_{2A}R^{-/-}$ mice are unresponsive to ATL146e. The beneficial effects on pulmonary function of ATL146e treatment appear to be due to $A_{2A}R$ agonism on iNKT cells. The co-treatment of NY1DD mice with ATL146e and anti-CD1d were not additive, as together they failed to improve pulmonary injury significantly more than either treatment alone. Also suggesting that iNKT cells are the main cellular targets of ATL146e is the observation that in NY1DD x $Rag1^{-/-}$ mice pre-treated with ATL146e, the adoptive transfer of 1 million iNKT cells with alkylated $A_{2A}Rs$ induced pulmonary injury while the adoptive transfer of 1 million non-alkylated iNKT cells did not induce injury. These findings indicate that although iNKT cells represent only a minor subset of the total lymphocyte population, they play a pivotal role in sustaining the pulmonary pathophysiology in a mouse model of sickle cell disease and inhibition of iNKT cells via agonism of the $A_{2A}R$ may be beneficial in decreasing the symptoms of chronic baseline and acute sickle cell disease.

Several murine models with phenotypes that vary in severity have been developed to model human sickle cell disease. In this study we used the well characterized NY1DD model that expresses 75 % human β^S-globin and 56 % human α-globin (Fabry et al., 1992a). While these mice have been previously described as having a relatively mild hematological pathology (i.e. they have a normal hematocrit), they have been shown to exhibit baseline organ damage to lung, liver, spleen, and kidney (Fabry et al., 1992a). At baseline, individuals with sickle cell disease display various degrees of organ dysfunction

that is often punctuated by periodic exacerbations referred to as sickle “crises.” A disease exacerbation, or crisis, can also be produced in mice exposed to endotoxin or transient hypoxia (Fabry et al., 1992b; Holtzclaw et al., 2004). In the current study we chose to study therapeutic interventions in sickle cell disease at baseline as well as after hypoxia-reoxygenation induced “crisis.” Although acute complications of sickle cell disease are the most common cause of emergency room visits and hospitalizations, baseline intervention is important for several reasons: 1) recent findings suggest that transient microvascular occlusion occurs chronically in a sub-clinical manner in sickle cell disease, and that end-organ damage and short life-span in sickle cell disease are often due to the cumulative effects of repeated bouts of minor ischemic events (Kaul and Hebbel, 2000; Osarogiagbon et al., 2000); 2) relatively little attention has been paid to evaluating the natural progression of chronic organ injury in this model; and 3) the baseline sickle cell disease pulmonary phenotype is more stable and amenable to investigation than are crisis phenotypes.

Our findings confirm that at baseline NY1DD mice display substantial pulmonary inflammation and pathophysiology that is manifested by increased numbers of pulmonary leukocytes, impaired endothelial integrity (increased vascular permeability), and microvascular occlusion and this phenotype is amenable to treatment as ATL146e infusion decreased pulmonary injury after 3 days. Histological examination of lungs from NY1DD animals revealed striking inflammatory changes that were also amenable to ATL146e therapy, which decreased the amount of observable pulmonary capillary congestion in NY1DD mice. Similar baseline findings of pulmonary capillary congestion have been noted on post-mortem autopsies (Haque et al., 2002). We also found that

ATL14e treatment reversed the significant decrease in arterial oxygen saturation (% SO_2) observed in NY1DD mice, which is associated with increased pulmonary artery pressures in individuals with sickle cell disease and is believed to be a risk factor for the development chronic lung disease (Pashankar et al., 2008; Pashankar et al., 2009). Furthermore we demonstrate that in NY1DD mice exposed to hypoxia-reoxygenation to induce acute "crisis," ATL146e treatment given after the start reoxygenation decreases the pulmonary injury observed suggesting that it may be useful in acute complications of sickle cell disease as well.

Recent studies indicate that iNKT cells are activated by ischemia-reperfusion injury and we have demonstrated above that iNKT cells are involved in the pathophysiology of sickle cell disease. In the current study, we demonstrate that co-treatment of NY1DD mice with ATL146e and anti-CD1d ameliorates pulmonary pathophysiology similarly to either treatment alone. Also, we show that in NY1DD x $Rag1^{-/-}$ mice pre-treated with ATL146e, the adoptive transfer of 1 million iNKT cells with alkylated A_{2A}Rs induces pulmonary injury while the adoptive transfer of 1 million non-alkylated iNKT cells does not induce injury. One interpretation of these data is that the main cellular target for ATL146e is iNKT cells.

One limitation of this study is lack of translational human data. It would be beneficial to measure A_{2A}R expression on circulating iNKT cells or to measure the effects of A_{2A}R treatment on iNKT cell activation. Many factors were responsible for the lack of A_{2A}R patient data: one, other than blood, tissue from sickle cell diseased individuals is difficult to obtain (i.e. lung biopsies, post-mortem specimens); two, the experiments have to be completed *in vitro*; and three, the mouse anti-human A_{2A}R

antibody has proven unreliable for use in flow cytometric analysis. Nevertheless, $A_{2A}R$ agonism in sickle cell disease represents a new potential therapy both in chronic and acute settings.

In conclusion, our results suggest new strategies for the treatment of pulmonary inflammation and vaso-occlusion in sickle cell disease. Lung iNKT cells are activated in the NY1DD mouse and trigger an inflammatory cascade resulting in increased vascular permeability, decreased arterial oxygen saturation, and abnormal breathing parameters. Furthermore, iNKT cells have increased expression of the $A_{2A}R$, which when agonized decreases pulmonary injury. The results of this study have important translational therapeutic implications. By inhibiting iNKT cell activation with $A_{2A}R$ agonists, it may be possible to reduce vascular occlusion and tissue damage associated with acute and chronic IRI in sickle cell disease.

4. Future directions

4.1. Activation of iNKT cells in sickle cell disease

4.1.1. Determining the self-lipid antigen that activates iNKT cells in sickle cell disease

iNKT cells are autoreactive in that they react to self-antigens expressed by the host. For example, freshly isolated thymic iNKT cells are activated by a variety of CD1d-positive cells including thymocytes and tumor cells without the addition of exogenous antigens (Bendelac et al., 1995). In particular, iNKT cells react with self-lipid antigens that have been processed through the MHCII compartment (MIIC) (Chui and Dover, 2001; Stanic et al., 2003). The identification of putative endogenous lipid(s) that may be responsible for iNKT activation has been controversial (Figure 31). In 2000 Gumperz *et al.* demonstrated that self-lipids could stimulate iNKT cells, and in 2004 Zhou *et al.* suggested that isoglobotrihexosylceramide (iGb3) was a self-lipid that mediated iNKT activation (Gumperz et al., 2000; Porubsky et al., 2007; Zhou et al., 2004). In summary, their data demonstrated that pathogenic bacteria can activate mouse iNKT cells indirectly through TLR4-, TLR7-, or TLR9-driven maturation of dendritic cells, which then present self-iGb3 in the context of CD1d. However, a recent study demonstrated that iGb3 is not produced in human tissues and other endogenous ligand(s) have yet to be identified (Christiansen et al., 2008). Whether iGb3 is a true endogenous antigen or the sole iNKT cell self-antigen is still a matter of debate. Recently, a number of other cellular lipids including, GD3, phosphatidylinositol (PtdIno), and phosphatidylethanolamine (PtdEtN) have been hypothesized to form endogenous iNKT cell antigens under various physiological conditions (Gumperz et al., 2000; Rauch et al., 2003; Wu et al., 2003).

Until recently, the identification of an iNKT cell antigen expressed by a human pathogen capable of directly activating iNKT cells eluded investigators. In 2006, Kinjo *et al.*, reported that the spirochete *Borrelia burgdorferi*, the etiologic agent of Lyme borreliosis, expresses a diacylglycerol glycolipid that acts as a natural antigen (via CD1d presentation) for murine and human iNKT cells, and to date, is the only known human pathogen containing an antigen capable of directly activating iNKT cells (Kinjo et al., 2006).

Our data suggest a role for CD1d-restricted NKT cells in sickle cell disease, as treatment of NY1DD mice with anti-CD1d antibodies ameliorates pulmonary pathophysiology. An interpretation of these data is that host lipid antigens for iNKT cells are elevated in sickle cell disease. One possibility is that pulmonary ischemia-reperfusion injury in response to microvascular occlusion with sickled red blood cells leads to increased release or oxidation of self-lipids that are presented via CD1d to activate iNKT cells and also triggers the release of cytokines that facilitate activation of iNKT cells and subsequent inflammation. Another possible mechanism of iNKT cell activation is that antigen presenting cells are activated by cytokines released during ischemia-reperfusion causing them to amplify constitutive signaling from self-lipid antigens (iGb3, GD3, PtdIno, PtdEtN) via CD1d. Determining the self-lipid(s) responsible for activating iNKT cells may be an important tool for inhibiting the perpetuation of vaso-occlusion and end-organ damage in sickle cell disease. Furthermore, preventing the presentation of lipids to iNKT cells with glycolipid antagonists may be a beneficial treatment for sickle cell disease.

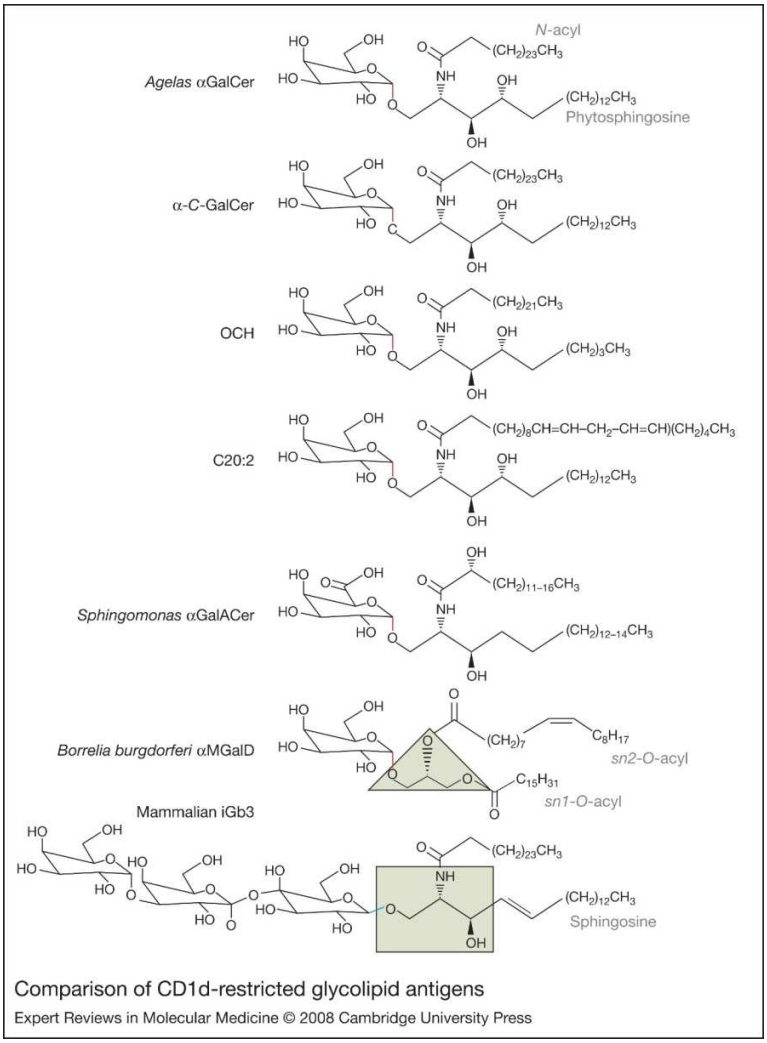

Figure 31. Comparison of CD1d-restricted glycolipid antigens

The α-anomeric glycolipid α-galactosylceramide (α-GalCer), derived from the marine sponge *Agelas*, and its synthetic variants α-*C*-GalCer, OCH and C20:2, have been used widely to probe iNKT cell function. Cell-wall-derived glycolipids from *Sphingomonas* and *Borrelia burgdorferi* have been shown to activate iNKT cells. The triangle and the box indicate differences in the glycerol and sphingosine backbone (Florence et al., 2008).

4.1.2. Determining the CD1d positive antigen presenting cells involved in the activation of iNKT cells in sickle cell disease

iNKT cells are activated by lipid antigen presentation by CD1d (an MHC-I like molecule) found on antigen presenting cells (APCs) (Brigl and Brenner, 2004; Trobonjaca et al., 2001). It is believed that CD1d is present on resting APCs at all times allowing CD1d and iNKT cells to function at early points during host response to infection or other challenges. While resting myeloid lineage cells express low levels of CD1d, circulating and splenic B-cells express very high levels. Furthermore, CD1d is also expressed on epithelial cells, parenchymal cells, and vascular smooth muscle cells, but not on T-cells. It is not clear which of these cells participate in CD1d-restricted activation of iNKT cells in sickle cell disease, and it will be of interest to determine if these various populations have upregualated CD1d in sickle cell disease.

4.1.2.1. B-cells

The highest level of murine peripheral CD1d expression is found on marginal zone B-cells ($CD21^{high}$, $CD23^{low}$, IgM^{high}, IgD^{low}, $CD1d^{high}$) (Roark et al., 1998). This population of B-cells appears at 3 weeks of age and can develop in germ-free mice, $MHCII^{-/-}$ mice, and $TCR\beta^{-/-}$ mice, suggesting that neither antigen nor T-cell help is required for their development (Makowska et al., 1999). Furthermore, these B-cells fail to develop in $CD19^{-/-}$ mice suggesting that they are reliant on BCR signaling (Makowska et al., 1999; Pillai et al., 2005).

It is known that human iNKT cells can upregulate CCR7 and CD62 ligand, both lymphoid tissue homing receptors, allowing them to traffic to the spleen and lymphnodes

where they can interact with B-cells and become activated (Galli et al., 2003). Furthermore, this interaction is CD1d-dependent as B-cells presenting α-GalCer strongly activate iNKT cells and anti-CD1d antibodies abolish this activation (Galli et al., 2003). It will be of interest to determine if circulating or lymphoid B-cells are responsible for CD1d-lipid presentation to iNKT cells, as inhibiting trafficking of iNKT cells into lymphoid tissue or inhibiting vascular iNKT-B-cell interactions may have potential therapeutic benefits.

4.1.2.2. Monocytes and macrophages

Murine and human monocytes and macrophages express CD1d. The ability of these cells to present lipid antigen to iNKT cells is directly dependent on the number of CD1d molecules on the cell surface (Skold et al., 2005). For example, tissue macrophages upregulate CD1d in response to mycobacteria and become highly potent at stimulating iNKT cells (Ryll et al., 2001; Skold et al., 2005). Furthermore, iNKT cells from dendritic cell deficient mice (CD11c promoter-driven diphtheria toxin receptor) were still responsive to α-GalCer stimulation (presented to iNKT cells via CD1d), but depletion of Kupffer cells (liver macrophages) decreased iNKT cell activation (Schmieg et al., 2005). Also, in humans, foam-cells (macrophage-like cells) from atherosclerotic plaques express CD1d and can present lipid antigens to iNKT cells *ex-vivo* (Melian et al., 1999). It will be of interest to determine if there are normal numbers of monocytes/macrophages in sickle cell disease. Also, determining the location of iNKT cell activation, either by circulating monocytes or resident tissue macrophages, may have potential therapeutic benefit.

4.1.2.3. Dendritic cells

Although dendritic cells have low surface expression of CD1d, they are the most effective APC in activating iNKT cells (potent stimulation of iNKT cell proliferation and IFN-γ secretion) (Spada et al., 2000). Furthermore, in a counter-regulatory role, iNKT cells are cytolytic against dendritic cells, but not against other cells, which may be important in downregulating an immune response (Nicol et al., 2000; Yang et al., 2000). It will be of interest to determine if there are normal numbers of dendritic cells in sickle cell disease.

4.1.2.4. Epithelial cells

It is believed that expression of CD1d on epithelial cells plays a role in natural host defense against bacterial colonization and invasion at the mucosal barrier. Germ free $CD1d^{-/-}$ mice display increased intestinal bacterial colonization and $CD1d^{-/-}$ mice infected with *Pseudomonas aeruginosa* display increased colonization of the lung (Colgan et al., 1999; Nieuwenhuis et al., 2002). It will be of interest to determine if there is normal expression of CD1d on gut epithelial cells in sickle cell disease and if this impacts host defense against intestinal infection.

4.1.2.5. CD1d expressing cells in sickle cell disease

Although during inflammation, CD1d expression does not vary as widely as MHCI and MHCII expression, it has an important role in presenting lipid antigen to iNKT cells and it likely is modified during diseases involving activation of iNKT cells.

Many diseases are exacerbated or inhibited by iNKT cells, but which APC is responsible for activating the iNKT cells for these responses remain unanswered. CD1d has been found to have increased expression on APCs from numerous diseases, including gastro-intestinal diseases (inflammatory bowel diease, Chron's disease, ulcerative colitis), hepatic diseases (primary biliary cirrhosis, sarcoidosis, hepatitis C), and auto-immune diseases (psoriasis, experimental autoimmune encephalomyelitis) (Bonish et al., 2000; Busshoff et al., 2001; Canchis et al., 1993; Durante-Mangoni et al., 2004; Page et al., 2000; Tsuneyama et al., 1998). The implication of iNKT cells in the pathogenesis of sickle cell disease suggests that CD1d-expressing APCs are also playing a role in disease progression. Understanding the expression and function of CD1d on particular APCs is critical to understanding the presentation of lipid antigens and the role of self-lipids in immune regulation. Flow cytometric analysis or immunohistochemistry for CD1d positive cells from NY1DD mouse tissue or sickle cell disease patient blood using anti-CD1d antibodies (1B1) may be useful tools in determining which APCs are responsible for self-lipid presentation in sickle cell disease. Inhibition of these cell types or blocking their interactions with iNKT cells may be beneficial in decreasing the perpetuation of vaso-occlusion and inflammation in sickle cell disease.

4.2. Other mediators of vaso-occlusion in sickle cell disease

4.2.1. Cells

4.2.1.1. Type II and Type III NKT cells

Due to the lack of reliable methods to identify other subsets of NKT cells (CD1d-tetramer specific to type I / iNKT cells, NK1.1 downregulates after activation) there is not much known about type II or type III NKT cells (Table 15). Only recently, with the creation of genetically modified mice ($J\alpha18^{-/-}$ mice, lacking type I NKT cells; $CD1d^{-/-}$ mice, lacking both type I and type II NKT cells) and the development of new CD1d-tetramers loaded with sulfatide lipids (specific for type II NKT cells), have researchers been able to further characterize these subsets of NKT cells. Compared to type I / iNKT cells, type II NKT cells express more diverse lipid-binding TCRs and are also CD1d restricted, but are unresponsive to α-GalCer. Type III NKT cells have diverse TCRs that interact with MHCI/MHCII complexes. The majority of type III CD1d-independent NKT cells are believed to be conventional T-cells that express NK cell markers upon activation and are believed to reside mainly in the bone marrow. It will be of interest to determine if type II NKT cells are activated in sickle cell disease.

Recently, there has been an increasing appreciation of type II NKT cells in modulating the innate and adaptive immune system in various diseases. CD1d tetramers that identify all type II NKT cells are not available, although a subset may be identifiable by CD1d-sulfatide tetramers (Jahng et al., 2004). This evidence suggests that type II NKT cells survey a distinct set of glycolipid antigens from those detected by type I NKT cells to complement the function of type I NKT cells for immunological surveillance.

Recently, it has been hypothesized that a new immunoregulatory axis exists between type I / iNKT cells and type II NKT cells (Terabe and Berzofsky, 2008). Activation of type II NKT cells by sulfatide suppresses the proliferative response of type I NKT cells activated by α-GalCer or OCH. NKT cells function as important components of both the innate and the adaptive immune systems, as they are among the earliest immune responders and determine the subsequent adaptive immune responses. Therefore, therapeutic manipulation the hypothesized immunoregulatory axis between type I and type II NKT cells may have profound implications on disease, as immune responses could be shifted towards different outcomes.

Although our data in NY1DD mice focused on the involvement of type I / iNKT cell activation and subsequent end-organ damage, we cannot rule out the fact that type II NKT cells may also be playing a role. We used anti-CD1d treatment, which would inhibit both type I and type II NKT cells, to ameliorate pulmonary pathophysiology in NY1DD and due to lack of reliable techniques to identify type II NKT cells we focused on type I NKT cells. Currently we are in the process of crossing NY1DD mice and $J\alpha18^{-/-}$ mice, which would result in NY1DD mice without type I NKT cells. This will be a useful tool to determine the individual roles of both type I and type II NKT cells in this model of sickle cell disease. If type I, but not type II, NKT cells are found to be pathogenic in sickle cell disease, a useful therapeutic technique may be agonism of type II NKT cells with sulfatides to suppress the exaggerated immune response, and vice versa. Furthermore, treatment of NY1DD mice with $A_{2A}R$ agonists to suppress iNKT cells may function in a similar fashion to the suppression of iNKT cells by type II NKT cells. We

have yet to determine if $A_{2A}R$ activation suppresses activation of type II NKT cells, as is the case with type I NKT cells.

	Type I NKT cells (iNKT / classical)		Type II NKT cells (vNKT / nonclassical)	Type III NKT cells (xNKT / NKT-like cells)
	Mouse	**Human**		
TCR	Va14-Ja18	Va24-Ja18	Diverse	Diverse
Restriction	CD1d		CD1d	MHCI/MHCII
Antigens	**Lipids**: α-GalCer, iGb3, phospholipids		**Lipids**: sulfatide	Diverse **peptides**
Coreceptors	CD4, DN	CD4, CD8α, DN	CD4, DN	CD8α>CD4, DN
NK cell markers	NK1.1	CD56, CD161	NK1.1	DX5 and/or NK1.1
Peripheral phenotype	Effector / memory		Effector / memory	Naïve and effector / memory
Location	Liver, BM, spleen, lung, thymus		Liver, spleen	Liver, BM, spleen
Role in infectious disease	**Protective**: *Spingomonas*, *Ehrlichia*, *Salmonella*, *Pseudomonas*, *Leishmania*, *T. cruzi*, Herpes simplex, EBV **Pathogenic**: schistosomiasis, Chlamydia		**Pathogenic**: viral hepatitis, schistosomiasis, *T.cruzi*	nd
Role in autoimmune disease	**Protective**: type I DM, EAE, MS, collagen-induced arthritis, GVHD **Pathogenic**: asthma		**Protective**: EAE, type I DM, GVHD **Pathogenic**: UC, SLE	nd
Role in cancer	**Protective**		**Pathogenic**: suppress CD8+ T-cell and iNKT cell protection	nd

Table 15. Characteristics of NKT cells

Features of NKT subsets and their proposed role in disease. nd: not defined; BM: bone marrow; EBV: Epstein Barr Virus, DM: diabetes mellitus, EAE: experimental allergic encephalitis; MS: multiple sclerosis; GVHD: graft vs host disease; UC: ulcerative colitis; SLE: systemic lupus erythematosus (Terabe and Berzofsky, 2008; Wingender and Kronenberg, 2008).

4.2.1.2. Platelets

There is evidence that individuals with sickle cell disease have a chronically active coagulation system, which has been reported to increase during vaso-occlusive crisis (Francis and Hebbel, 1994). Since every component of hemostasis is believed to be shifted in the direction of a pro-coagulant phenotype, sickle cell disease is frequently referred to as a "hyper-coagulable" state (Francis, Jr., 1991). The most evident clinical consequence of this activation is ischemic stroke (Hillery and Panepinto, 2004). Clinical evidence has demonstrated that individuals with sickle cell disease have increased thrombin generation and platelet activation (Tomer et al., 2001). Tissue factor has also been found to be abnormally expressed on monocytes and on circulating endothelial cells in individuals with sickle cell disease, and its expression is increased further during pain episodes, supporting the concept of a hypercoaguable state (Solovey et al., 1998). This pro-coagulatory phenotype results in conditions that favor vaso-occlusion.

It is known that individuals with sickle cell disease express numerous plasma factors, including thrombin, interleukin-1 (IL-1), and tumor necrosis factor-α (TNF-α), that could increase tissue factor expression (Ataga and Key, 2007). Also, multiple potential mechanisms for increased tissue factor expression in sickle cell disease have been reported, including ischemia-reperfusion injury (Solovey et al., 2004). NY1DD mice exposed to hypoxia-reoxygenation (8 % O_2; 3hrs-18hrs), to induce vaso-occlusion, displayed increased endothelial tissue factor expression. Although Solovey *et. al.*, discussed potential downstream signaling mechanisms leading to tissue factor expression (i.e. NF-κβ, VEGF), they did not discuss potential proximate stressors. One potential

mechanism may be related to upstream iNKT cell activation during ischemia-reperfusion injury.

Our preliminary data suggest that at baseline, NY1DD mice display increased circulating platelets (Table 5) and platelet-leukocyte heteroaggregates (Figure 32A,B). It is hypothesized that platelets bind to leukocytes and cause leukocyte activation via PSGL-1 and also function to induce leukocyte rolling along the endothelium (Zarbock et al., 2007). Furthermore, depletion of platelets in NY1DD mice acutely, with anti-platelet serum treatment, or chronically, with busulfan treatment, resulted in significantly decreased vascular permeability and decreased absolute numbers of pulmonary leukocytes (Figure 32C-F, Table 16). These data suggest that platelets may play a role in the pathophysiology of sickle cell disease. Further experiments need to be done to explore the mechanisms of iNKT cell and platelet interactions. Importantly, it would be interesting to measure platelet-leukocyte heteroaggregates, tissue factor expression, and other mediators of hemostasis in NY1DD animals treated with anti-CD1d. Ischemia-reperfusion activated iNKT cells in sickle cell disease may cause downstream platelet activation and subsequent leukocyte activation.

Despite the abundant evidence of a pro-coagulatory phenotype observed in sickle cell disease, the results of clinical studies using anticoagulants and antiplatelet agents have been controversial and no convincing benefit in the prevention or treatment of vaso-occlusive complications have been demonstrated (Ataga and Key, 2007). Although these studies have been small and/or poorly controlled, these data suggest that platelets are not the main contributors to vaso-occlusion and may be a result rather than a cause of vaso-

occlusive crisis. Nevertheless, platelet activation potentially driven by upstream iNKT cell activation remains an important area to be further explored.

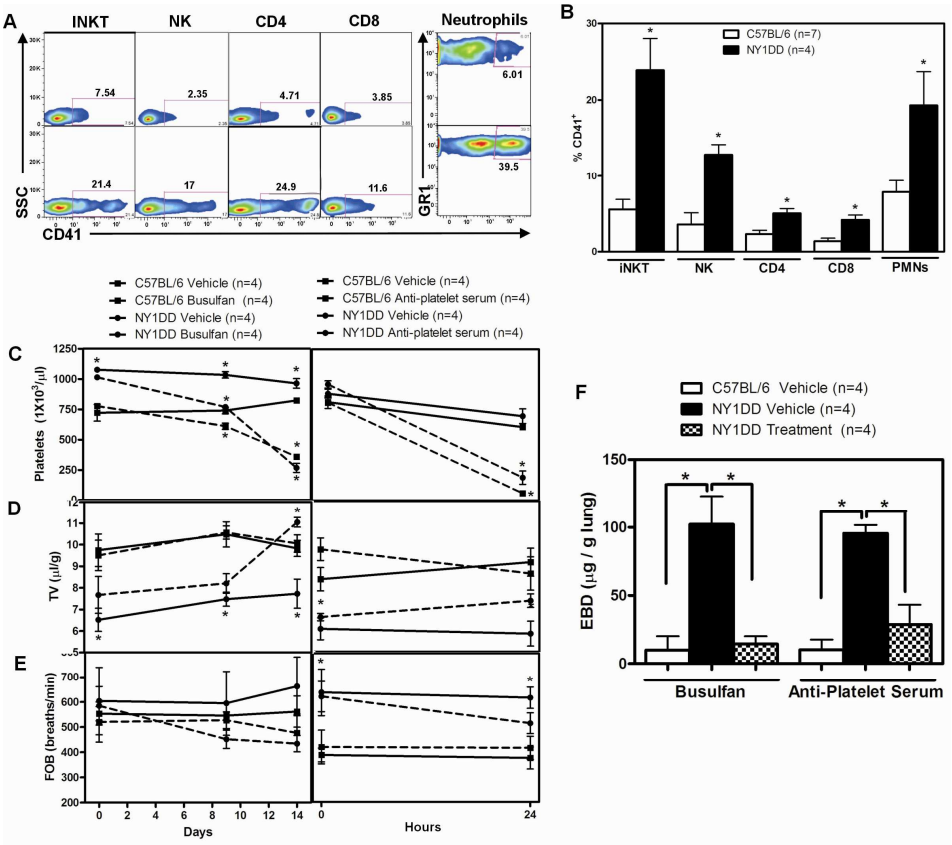

Figure 32. NY1DD mice have increased platelet-leukocyte heteroaggregates and platelet depletion decreases pulmonary injury

(**A**) Representative flow cytometry plots depicting platelet (CD41) positive pulmonary leukocytes in C57BL/6 and NY1DD mice. (**B**) NY1DD mice have increased pulmonary platelet-leukocyte heteroaggregates as compared to C57BL/6 mice. (**C**) Circulating platelets are depleted after chronic (busulfan; 14 days) or acute (anti-platelet serum; 24 hours) therapies. (**D,E**) Breathing parameters from platelet depleted C57BL/6 and NY1DD mice. (**F**) Vascular permeability is decreased after chronic (busulfan; 14 days) or acute (anti-platelet serum; 24 hours) therapies. Data analyzed by (B) unpaired *t*-test, * $p<0.0001$; (C-E) two-way ANOVA with Bonferoni post-testing, * $p<0.05$; or (F) one-way ANOVA with Neuman-Keuls post-testing, * $p<0.05$. TV: tidal volume; FOB: frequency of breath; EBD: Evans blue dye.

Cells (10^5)	NY1DD Vehicle (n=4)	NY1DD Busulfan (n=4)	NY1DD Vehicle (n=4)	NY1DD Anti-platelet serum (n=4)
iNKT	0.50 (0.02)	0.48 (0.02)	0.59 (0.07)	0.49 (0.05)
NK	4.01 (0.35)	1.74 (0.25)*	4.08 (0.32)	0.40 (0.04)*
CD4	2.08 (0.39)	0.87 (0.12)	1.81 (0.32)	1.34 (0.07)
CD8	1.96 (0.33)	1.06 (0.14)*	1.57 (0.20)	0.95 (0.11)
PMNs	2.18 (0.32)	0.08 (0.01)*	1.71 (0.18)	0.32 (0.11)*

Table 16. Platelet depletion decreases pulmonary leukocytes in NY1DD mice

NY1DD mice have decreased pulmonary leukocytes after chronic (14 days; busulfan) or acute (24 hours; anti-platelet serum) platelet depletion.

4.2.1.3. Fibrocytes: chronic pulmonary hypertension in sickle cell disease

Pulmonary disease is the leading cause of death in sickle cell disease (Platt et al., 1994). Since the pulmonary arterial circulation has low oxygen tension and pressure, low blood velocity, and constricts in response to hypoxia, the lung environment facilitates the polymerization of HbS and is highly vulnerable to ischemic injury (Platt et al., 1994). Chronic pulmonary complications are associated with a poor prognosis and can include interstitial fibrosis, restrictive lung disease, obstructive lung disease, and pulmonary hypertension (Aquino et al., 1994; Platt et al., 1994). Chronic complications are more common in individuals with sickle cell disease with a history of multiple episodes of acute chest syndrome (Powars et al., 1988).

Chronic hypoxic exposure, as is hypothesized to occur in sickle cell disease, is characterized by the development of striking fibroproliferative changes in the adventitia of both large and small pulmonary arteries (Stenmark et al., 2002). Historically, it was thought that resident pulmonary artery adventitial fibroblasts were manifesting these changes by increased proliferation and extracellular matrix protein production. Recently, this concept has been challenged by the observations that mononuclear cells with fibroblast-like properties (fibrocytes) in the systemic circulation are recruited to sites of tissue injury and participate in the repair process (Quan et al., 2004; Schmidt et al., 2003; Yang et al., 2002). Furthermore, it has recently been shown that circulating mononuclear fibrocytes originate in the bone marrow and are the major contributors to lung fibrosis after bleomycin-induced injury (Hashimoto et al., 2004; Phillips et al., 2004). Also, hypoxia has been shown to significantly upregulate expression of CXCL12/SDF-1, a chemokine released from resident fibroblasts and endothelial cells that is responsible for

the recruitment of fibrocytes expressing CXCR4 (also upregulated during hypoxia) (Ceradini et al., 2004; Schioppa et al., 2003).

A similar mechanism of fibrocyte recruitment to the sickle cell lung and resulting pulmonary fibrosis may occur in sickle cell disease. Preliminary data collected in collaboration with the Robert Strieter laboratory suggests that NY1DD mice at baseline have increased pulmonary fibrosis, which correlates to human pathology, as total soluble collagen levels are significantly increased (Figure 33A). Total collagen levels were found to be similar to those found after bleomycin, a potent inducer of pulmonary fibrosis, treatment (Figure 33A). Furthermore, NY1DD mice have increased pulmonary and circulating fibrocytes ($CD45^+$, $collagen1^+$) and increased pulmonary levels of CXCL12/SDF-1 (Figure 33B,C). These data suggest that fibrocyte recruitment via the CXCL12/SDF-1-CXCR4 axis may be responsible for the fibroproliferative changes seen in individuals with sickle cell disease, eventually resulting in pulmonary hypertension. Furthermore, inhibition of this axis with anti-SDF-1 therapy may result in decreased pulmonary fibrosis and hypertension, and may be a potential therapy for sickle cell disease. Also, the exact mechanisms driving CXCL12/SDF-1 release are currently unknown. An interesting experiment would be to treat NY1DD mice with anti-CD1d and measure pulmonary CXCL12/SDF-1 levels to determine if iNKT cell activation is involved with the recruitment of circulating fibrocytes to the sickle cell lung.

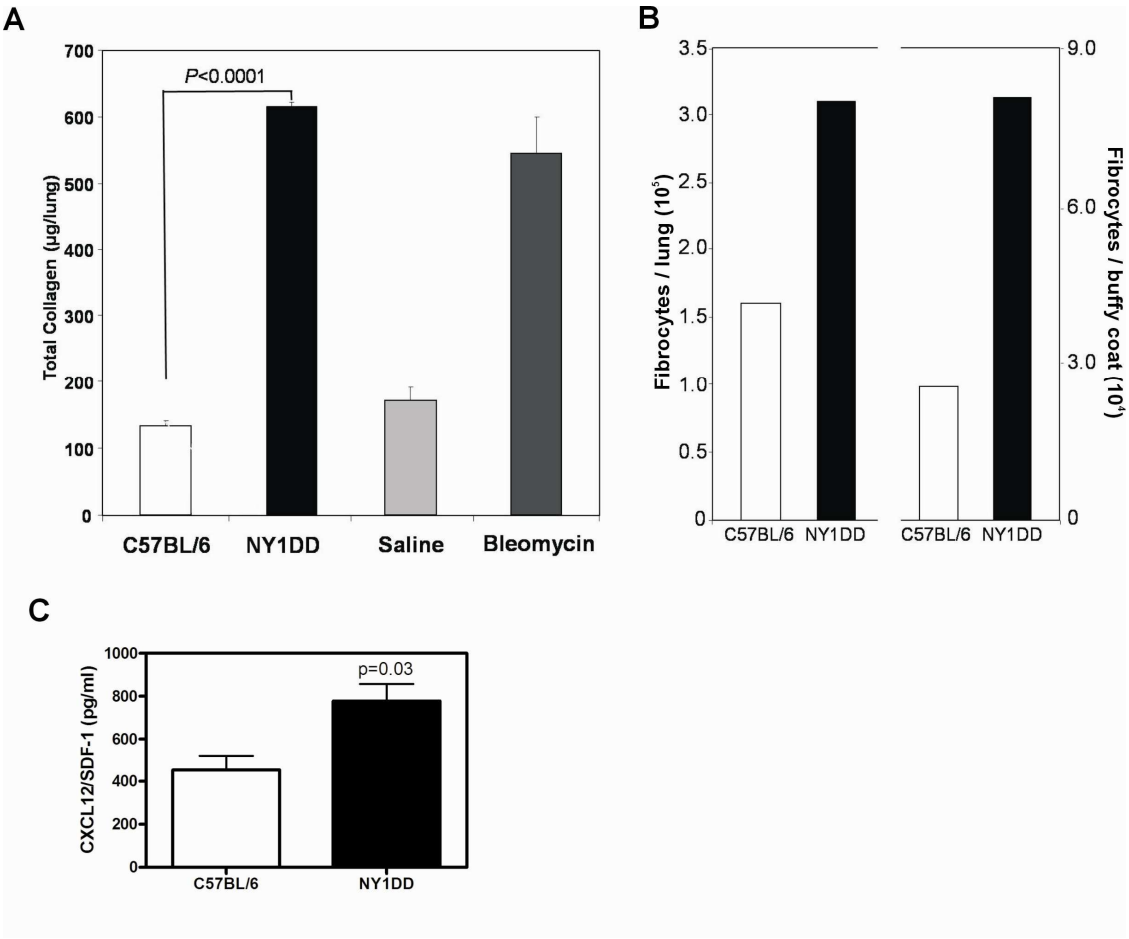

Figure 33. NY1DD mice have increased pulmonary fibrosis

(**A**) Lungs from NY1DD mice have increased total soluble collagen (Sircol) as compared to C57BL/6 mice. The total collagen is comparable to bleomycin (potent pulmonary fibrosing agent) treated animals at 16 days post-treatment. (**B**) NY1DD mice have increased pulmonary and circulating fibrocytes ($CD45^+$, $Collagen1^+$) as compared to C57BL/6 mice. (**C**) NY1DD mice have increased pulmonary CXCL12 (SDF-1), the chemokine responsible for fibrocyte recruitment, as compared to C57BL/6 mice.

4.2.2. Measurement of reactive oxygen species

While our results suggest a novel mechanism for vaso-occlusion and subsequent inflammation, we cannot exclude the fact that other well established pro-inflammatory mechanisms may be simultaneously activated. Over the past decade considerable data have been collected pertaining to the dysregulation of nitric oxide metabolism in sickle cell disease. It is hypothesized that the hemolysis of sickled red blood cells contributes to a state of nitric oxide resistance and limited bioavailability of l-arginine, the substrate for nitric oxide synthesis. Hemolysis contributes to reduced nitric oxide bioavailability and endothelial dysfunction via release of erythrocyte arginase which limits arginine bioavailability, and release of erythrocyte hemoglobin which scavenges nitric oxide (Morris et al., 2005). Abnormal nitric oxide-dependent regulation of vascular tone, adhesion, platelet activation, and inflammation is believed to contribute to the pathophysiology of vaso-occlusion (Weiner et al., 2003). Furthermore, treatment of individuals with sickle cell disease with inhaled nitric oxide gas has been shown, via its vasodilatory effects, to improve pulmonary ventilation-perfusion mismatch and hemodynamics thereby increasing arterial oxygen tension and decreasing inflammation (Atz and Wessel, 1997; Sullivan et al., 1999). This mechanism may co-exist or work in concert with the immune dysregulation effects caused by iNKT cells on the pulmonary vasculature described in this study. It will be of interest to determine if $A_{2A}R$ agonists or anti-CD1d treatment increases nitric oxide production in sickle cell disease.

4.3. Exploring the role of iNKT cells and ATL146e treatment in sickle cell vaso-occlusion in other NY1DD mouse organ systems

Renal and hepatic involvements are common manifestations of sickle cell disease. The medullary environment has low oxygen tension and high osmolality, both of which contribute to osmotic dehydration of the RBCs causing polymerization of HbS, sickling, and vaso-occlusion (Pham et al., 2000). There are many well-described nephropathies that affect individuals with sickle cell disease (Molitierno, Jr. and Carson, III, 2003). Gross hematuria, papillary necrosis, nephrotic syndrome, hyposthenuria (inability to concentrate urine), pyelonephritis, and renal medullary carcinoma are all believed to be the result of repeated ischemia-reperfusion episodes to the microvasculature in the kidney.

Multiple causes of hepatic dysfunction exist in individuals with sickle cell disease. Chronic hemolytic anemia contributes to the formation of pigmented gallstones, which are eventually found in approximately 70 % of individuals (Rennels et al., 1984). Acute hepatic crisis is associated with liver ischemia and presents with fever, right upper quadrant pain, leukocytosis, and abnormal liver function tests and may progress to liver failure, which is associated with a poor prognosis (Rosenblate et al., 1970b; Sheehy et al., 1980). Chronic liver disease is thought to be caused by intrahepatic trapping of sickled RBCs leading to hepatomegaly, liver dysfunction, necrosis, and cirrhosis (Rosenblate et al., 1970b).

Preliminary data suggests that end-organ damage is occurring in other tissues outside the lung in NY1DD mice and that iNKT cells may be involved (Figures 9, 13, 34; Table 7). Therefore, it would be interesting to see if the same mechanism of iNKT cell

activation and downstream recruitment of effector cells causing pathophysiology is occurring in these tissues. The chronic nature of kidney and liver dysfunction observed suggests that NY1DD mice would have measureable liver dysfunction (i.e. increased liver function enzymes) and kidney dysfunction (i.e. urine concentration deficits). Furthermore, chronic pulmonary complications are associated with a poor prognosis and can include interstitial fibrosis, restrictive lung disease, obstructive lung disease, and pulmonary hypertension (Aquino et al., 1994; Platt et al., 1994).

Although we demonstrated significant improvements in pulmonary function in NY1DD mice treated acutely with ATL146e (10 ng/kg/min, 3d) and anti-CD1d (10 µg/g/d, 2d) it would be interesting to see if the same results would occur in the liver and kidney. The liver has an amazing capacity for regeneration and measureable differences may be able to be detected within 2 – 3 days of treatment. However, the severe gross necrosis observed in these organs and the fact that these acute treatments cannot reverse all pulmonary physiological parameters to control levels (i.e. vascular permeability is still elevated as compared to control animals) suggest that end-organ damage may only be preventable by starting treatment before NY1DD mice reach an age of substantial irreversible organ injury, which we have observed around 8 weeks of age.

Chronic treatment is often a difficult task to undertake, as it requires daily injections, which can result in abdominal perforations and infections, or osmotic pump placement, which can cause skin necrosis and infections over time. An interesting experiment would be to place NY1DD mice on $A_{2A}R$ agonist drug-infused chow as soon as they are weened. Therefore the mice would receive chronic therapy, although similar to bolus injections in that soon after feeding NY1DD mice would have peak values of

$A_{2A}R$ that would diminish quickly. Nevertheless, there is a pressing need for long-term therapies to reduce end-organ damage in sickle cell disease.

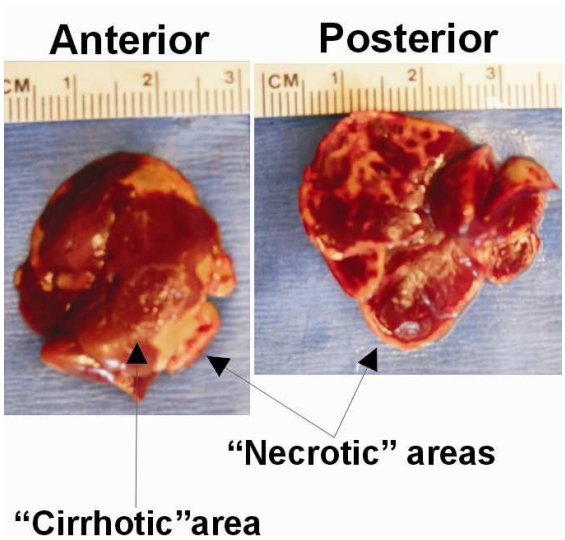

Figure 34. NY1DD mice have observable end-organ damage

Representative picture of a liver from a 13 week old NY1DD mouse showing areas of necrosis (white-yellow areas) and cirrhosis (micro-nodular appearing).

4.4. Human sickle cell disease

4.4.1. Exploring the correlations between iNKT cells and sickle cell disease severity

For years, the “holy grail” of sickle cell disease research has been attempting to identify a biomarker that can accurately predict pain, crisis, and disease outcome so that clinicians can better tailor treatment strategies to each patient. Many biomarkers have been potentially identified only to be shown unreliable in subsequent studies (circulating endothelial cells, C-reactive protein [CRP], platelet counts, white blood cell counts, soluble adhesion molecules [sVCAM-1, sICAM-1], chemokine/cytokine levels, etc) (Etienne-Julan et al., 2004; Kato et al., 2005; Makis et al., 2006; Strijbos et al., 2009). The previous data suggest that iNKT cells be a potential biomarker for sickle cell disease severity, as their inhibition improves disease in a mouse model of sickle cell disease and individuals with sickle cell disease have increased circulating iNKT cells. Currently, studies are underway to correlate iNKT cell numbers and/or activation with many variables of sickle cell disease severity (Table 17). Although the number of individuals analyzed is still relatively small, when individuals with sickle cell disease are divided into tertiles preliminary data suggests that the number of iNKT cells and iNKT cell activation in individuals with sickle cell disease correlates with the number of hospitalized pain crisis reported over 4 years (i.e. the individuals with sickle cell disease with the most number of iNKT cells [upper 33 %] and highest activation [upper 33 %] have the most hospitalization for pain). Additional data needs to be collected over time from the same patient to see if acute increases in iNKT cell number and/or activation can predict acute crisis. If so, clinicians may be able to prevent the occurrence of acute sickle cell crisis by starting treatments before the patient has signs and/or symptoms. It is also possible that

reduction of iNKT cell activation during therapy may be a useful marker of the efficacy of various treatments.

Variables of sickle cell disease severity		
Baseline demographics	Age, gender, transfusion history, hydroxyurea therapy	n=138
Laboratory variables	WBC #, [hemoglobin], platelet #, LDH, serum creatinine, ALT	
Morbidity data	# Pain episodes over 4 yrs, # acute chest syndrome episodes over 4 yrs	
Pulmonary function	Spirometry (FEV1, FVC, FEV1/FVC), bronchodilator response, O_2 saturation	n=75
Pulmonary hypertension	Echocardiogram	n=60
Asthma	History, medications, smoking history	

Table 17. Variables associated with sickle cell disease severity

4.4.2. Treatment strategies for sickle cell disease

Treatment strategies for individuals with sickle cell disease are quite complex and require close monitoring by health care workers. Briefly, current treatment includes prophylactic and liberal use of antibiotics during infections, transfusion therapy, pain management, and hydroxyurea (Hebbel, 2005). Liberal use of antibiotics has been shown to significantly reduce the risk of infection and death. However, since the early 1990s, antibiotic-resistant strains of various bacteria have emerged (Adamkiewicz et al., 2003). Repeated transfusion complications include iron overload and viral transmission, and transfusion therapy has been shown to have limited value (Hebbel, 2005). The mainstays for pain treatment include NSAIDs and opiods, however it has been well documented that continual use of narcotics can lead to addiction by individuals with sickle cell disease and undertreatment by healthcare providers (Kirsh et al., 2002).

Although studies have shown an overall benefit of hydroxyurea in individuals with sickle cell disease (via stimulation of HbF production), 10-50 % of individuals do not respond to treatment (Charache et al., 1995). Due to the mechanism of action of hydroxyurea (inhibition of ribonucleotide reductase that inhibits DNA synthesis and repair, which ultimately leads to S-phase cell death), a major concern is that long-term hydroxyurea therapy may be carcinogenic or leukemogenic, which has already been documented in individuals treated with hydroxyurea for polycythemia vera (Dalton et al., 2005). While these therapies have increased the lifespan of individuals with sickle cell disease, morbidity and mortality still remain relatively high with most individuals with sickle cell disease dying prematurely. It will be of interest to determine if hydroxyurea therapy has any effect on the production or activation of iNKT cells.

The only known cures for sickle cell disease are bone marrow transplants, which removes the genetically altered sickled red blood cell and all of the downstream damaging effects associated with it and replaces it with a normal red blood cell with adult hemoglobin, or stem cell transplantation, which would eliminate sickle red blood cells and progenitors and replace them with normal stem cells that would produce normal red blood cells. With bone marrow transplant it is often difficult to find an exact matching donor and there are difficulties with rates of engraftment, graft rejection, and graft-versus-host-disease (GVHD). Also, the process is very expensive and requires years of follow-up. Stem cell transplantation also has associated unfavorable outcomes, especially the lack of sustained donor engraftment. Therefore, there is a pressing need for new treatments with minimal side effects.

Our data suggest that inhibition of iNKT cells either with antibodies that indirectly inhibit activation (anti-CD1d) or $A_{2A}R$ agonists that directly inhibit activation (ATL146e) would be beneficial treatment strategies for sickle cell disease. Both of these treatments have the benefit of acting on mechanistically upstream iNKT cells, which are potentially involved with the recruitment of further effector cells and perpetuation of ischemia-reperfusion injury induced end-organ damage.

In individuals with sickle cell disease, baseline disease with various degrees of organ dysfunction is often punctuated by periodic exacerbations referred to as acute sickle “crises.” A disease exacerbation, or crisis, can also be produced in mice exposed to endotoxin or transient hypoxia (Fabry et al., 1992b; Holtzclaw et al., 2004). The major cause of emergency room visits and hospitalizations for individuals with sickle cell disease are due to acute pain crisis and/or acute chest syndrome. Previously described

data suggest that treatment of acute sickle pain crisis with $A_{2A}R$ agonists may be a suitable strategy. Sickle cell mice exposed to hypoxia-reoxygenation, which induces ischemia-reperfusion injury that is believed to mimic sickle pain crisis, treated with an $A_{2A}R$ agonist (ATL146e) after the start of reoxygenation demonstrated significant improvements in pulmonary function as compared to vehicle treated sickle cell mice. Further clinical trials need to be done to ensure proper dosing and timing of therapy. Also, many treatments that have been attempted in previous clinical trials (i.e. corticosteroids) have resulted in significant improvements during hospitalizations, but resulted in significant rebound crisis after individuals returned home, with the new pain crisis appearing worse than the former (Bernini et al., 1998). Therefore, it is important to evaluate the efficacy of $A_{2A}R$ agonists for acute treatment of sickle cell crisis in the emergency room setting.

Many individuals with sickle cell disease will never display acute pain crisis or acute chest syndrome yet still have severe end-organ damage and associated increased morbidity and mortality. Recent findings suggest that transient microvascular occlusion occurs chronically in a sub-clinical manner in individuals with sickle cell disease, and that end-organ damage and short life-span in sickle cell disease are often due to the cumulative effects of repeated bouts of minor ischemic events. Furthermore, relatively little attention has been paid to evaluating and treating the natural progression of chronic organ injury in sickle cell disease. One reason for the lack of long-term / chronic treatments may be unknown adverse side effects. Little is known about the long-term side effects of $A_{2A}R$ agonists or chronic inhibition of iNKT cells. Inflammation is a necessary and natural response to pathogenic infections and suppressing the immune system in

sickle cell disease may leave these individuals more prone to developing infections. Further experiments need to be done to determine the proper dosing of these therapies so that the fine balance of inflammation versus anti-inflammation is not swayed too far in one direction. Although much more research needs to be done, inhibition of iNKT cells and $A_{2A}R$ agonism represent potential long-term therapies.

5. References

Adamkiewicz,T.V., Sarnaik,S., Buchanan,G.R., Iyer,R.V., Miller,S.T., Pegelow,C.H., Rogers,Z.R., Vichinsky,E., Elliott,J., Facklam,R.R., O'Brien,K.L., Schwartz,B., Van Beneden,C.A., Cannon,M.J., Eckman,J.R., Keyserling,H., Sullivan,K., Wong,W.Y., and Wang,W.C. (2003). Invasive pneumococcal infections in children with sickle cell disease in the era of penicillin prophylaxis, antibiotic resistance, and 23-valent pneumococcal polysaccharide vaccination. J Pediatr. *143*, 438-444.

Agace,W.W., Roberts,A.I., Wu,L., Greineder,C., Ebert,E.C., and Parker,C.M. (2000). Human intestinal lamina propria and intraepithelial lymphocytes express receptors specific for chemokines induced by inflammation. Eur. J Immunol. *30*, 819-826.

Al-Mehdi,A.B., Zhao,G., Dodia,C., Tozawa,K., Costa,K., Muzykantov,V., Ross,C., Blecha,F., Dinauer,M., and Fisher,A.B. (1998). Endothelial NADPH oxidase as the source of oxidants in lungs exposed to ischemia or high K+. Circ. Res. *83*, 730-737.

Anderson,C.M., Xiong,W., Young,J.D., Cass,C.E., and Parkinson,F.E. (1996). Demonstration of the existence of mRNAs encoding N1/cif and N2/cit sodium/nucleoside cotransporters in rat brain. Brain Res. Mol. Brain Res. *42*, 358-361.

Aquino,S.L., Gamsu,G., Fahy,J.V., Claster,S., Embury,S.H., Mentzer,W.C., and Vichinsky,E.P. (1994). Chronic pulmonary disorders in sickle cell disease: findings at thin-section CT. Radiology *193*, 807-811.

Arch,J.R. and Newsholme,E.A. (1978). Activities and some properties of 5'-nucleotidase, adenosine kinase and adenosine deaminase in tissues from vertebrates and invertebrates in relation to the control of the concentration and the physiological role of adenosine. Biochem. J *174*, 965-977.

Aslan,M., Ryan,T.M., Adler,B., Townes,T.M., Parks,D.A., Thompson,J.A., Tousson,A., Gladwin,M.T., Patel,R.P., Tarpey,M.M., Batinic-Haberle,I., White,C.R., and Freeman,B.A. (2001). Oxygen radical inhibition of nitric oxide-dependent vascular function in sickle cell disease. Proc. Natl. Acad. Sci. U. S. A *98*, 15215-15220.

Ataga,K.I. and Key,N.S. (2007). Hypercoagulability in sickle cell disease: new approaches to an old problem. Hematology. Am. Soc. Hematol. Educ. Program. *2007*, 91-96.

Atz,A.M. and Wessel,D.L. (1997). Inhaled nitric oxide in sickle cell disease with acute chest syndrome. Anesthesiology *87*, 988-990.

Badwey,J.A. and Karnovsky,M.L. (1980). Active oxygen species and the functions of phagocytic leukocytes. Annu. Rev. Biochem. *49*, 695-726.

Bainbridge,R., Higgs,D.R., Maude,G.H., and Serjeant,G.R. (1985). Clinical presentation of homozygous sickle cell disease. J. Pediatr. *106*, 881-885.

Balkaran,B., Char,G., Morris,J.S., Thomas,P.W., Serjeant,B.E., and Serjeant,G.R. (1992). Stroke in a cohort of patients with homozygous sickle cell disease. J. Pediatr. *120*, 360-366.

Belcher,J.D., Bryant,C.J., Nguyen,J., Bowlin,P.R., Kielbik,M.C., Bischof,J.C., Hebbel,R.P., and Vercellotti,G.M. (2003). Transgenic sickle mice have vascular inflammation. Blood *101*, 3953-3959.

Belperio,J.A., Keane,M.P., Burdick,M.D., Londhe,V., Xue,Y.Y., Li,K., Phillips,R.J., and Strieter,R.M. (2002a). Critical role for CXCR2 and CXCR2 ligands during the pathogenesis of ventilator-induced lung injury. J Clin Invest *110*, 1703-1716.

Belperio,J.A., Keane,M.P., Burdick,M.D., Lynch,J.P., III, Xue,Y.Y., Li,K., Ross,D.J., and Strieter,R.M. (2002b). Critical role for CXCR3 chemokine biology in the pathogenesis of bronchiolitis obliterans syndrome. J Immunol. *169*, 1037-1049.

Bendelac,A., Lantz,O., Quimby,M.E., Yewdell,J.W., Bennink,J.R., and Brutkiewicz,R.R. (1995). CD1 recognition by mouse NK1+ T lymphocytes. Science *268*, 863-865.

Bendelac,A., Savage,P.B., and Teyton,L. (2007). The biology of NKT cells. Annu. Rev. Immunol. *25*, 297-336.

Bernini,J.C., Rogers,Z.R., Sandler,E.S., Reisch,J.S., Quinn,C.T., and Buchanan,G.R. (1998). Beneficial effect of intravenous dexamethasone in children with mild to moderately severe acute chest syndrome complicating sickle cell disease. Blood *92*, 3082-3089.

Bonish,B., Jullien,D., Dutronc,Y., Huang,B.B., Modlin,R., Spada,F.M., Porcelli,S.A., and Nickoloff,B.J. (2000). Overexpression of CD1d by keratinocytes in psoriasis and CD1d-dependent IFN-gamma production by NK-T cells. J. Immunol. *165*, 4076-4085.

Bonneau,O., Wyss,D., Ferretti,S., Blaydon,C., Stevenson,C.S., and Trifilieff,A. (2006). Effect of adenosine A2A receptor activation in murine models of respiratory disorders. Am. J. Physiol Lung Cell Mol. Physiol *290*, L1036-L1043.

Boyton,R. (2008). The role of natural killer T cells in lung inflammation. J Pathol *214*, 276-282.

Brigl,M. and Brenner,M.B. (2004). CD1: antigen presentation and T cell function. Annu. Rev. Immunol. *22*, 817-890.

Buchanan,G.R. and Glader,B.E. (1978). Leukocyte counts in children with sickle cell disease. Comparative values in the steady state, vaso-occlusive crisis, and bacterial infection. Am. J. Dis. Child *132*, 396-398.

Bunn,H.F. (1997). Pathogenesis and treatment of sickle cell disease. N. Engl. J. Med. *337*, 762-769.

Burne,M.J., Daniels,F., El,G.A., Mauiyyedi,S., Colvin,R.B., O'Donnell,M.P., and Rabb,H. (2001). Identification of the CD4(+) T cell as a major pathogenic factor in ischemic acute renal failure. J Clin Invest *108*, 1283-1290.

Busshoff,U., Hein,A., Iglesias,A., Dorries,R., and Regnier-Vigouroux,A. (2001). CD1 expression is differentially regulated by microglia, macrophages and T cells in the central nervous system upon inflammation and demyelination. J. Neuroimmunol. *113*, 220-230.

Caldwell-Kenkel,J.C., Currin,R.T., Tanaka,Y., Thurman,R.G., and Lemasters,J.J. (1991). Kupffer cell activation and endothelial cell damage after storage of rat livers: effects of reperfusion. Hepatology *13*, 83-95.

Canchis,P.W., Bhan,A.K., Landau,S.B., Yang,L., Balk,S.P., and Blumberg,R.S. (1993). Tissue distribution of the non-polymorphic major histocompatibility complex class I-like molecule, CD1d. Immunology *80*, 561-565.

Castro,O., Brambilla,D.J., Thorington,B., Reindorf,C.A., Scott,R.B., Gillette,P., Vera,J.C., and Levy,P.S. (1994). The acute chest syndrome in sickle cell disease: incidence and risk factors. The Cooperative Study of Sickle Cell Disease. Blood *84*, 643-649.

Ceradini,D.J., Kulkarni,A.R., Callaghan,M.J., Tepper,O.M., Bastidas,N., Kleinman,M.E., Capla,J.M., Galiano,R.D., Levine,J.P., and Gurtner,G.C. (2004). Progenitor cell trafficking is regulated by hypoxic gradients through HIF-1 induction of SDF-1. Nat. Med. *10*, 858-864.

Cerra,F.B., Lajos,T.Z., Montes,M., and Siegel,J.H. (1975). Hemorrhagic infarction: A reperfusion injury following prolonged myocardial ischemic anoxia. Surgery *78*, 95-104.

Charache,S., Terrin,M.L., Moore,R.D., Dover,G.J., Barton,F.B., Eckert,S.V., McMahon,R.P., and Bonds,D.R. (1995). Effect of hydroxyurea on the frequency of painful crises in sickle cell anemia. Investigators of the Multicenter Study of Hydroxyurea in Sickle Cell Anemia. N. Engl. J. Med. *332*, 1317-1322.

Chen,L.Y., Nichols,W.W., Hendricks,J., and Mehta,J.L. (1995). Myocardial neutrophil infiltration, lipid peroxidation, and antioxidant activity after coronary artery thrombosis and thrombolysis. Am. Heart J. *129*, 211-218.

Chies,J.A. and Nardi,N.B. (2001). Sickle cell disease: a chronic inflammatory condition. Med. Hypotheses *57*, 46-50.

Christiansen,D., Milland,J., Mouhtouris,E., Vaughan,H., Pellicci,D.G., McConville,M.J., Godfrey,D.I., and Sandrin,M.S. (2008). Humans Lack iGb3 Due to the Absence of Functional iGb3-Synthase: Implications for NKT Cell Development and Transplantation. PLoS. Biol. *6*, e172.

Chui,D.H. and Dover,G.J. (2001). Sickle cell disease: no longer a single gene disorder. Curr. Opin. Pediatr. *13*, 22-27.

Cohen,S.B., Gill,S.S., Baer,G.S., Leo,B.M., Scheld,W.M., and Diduch,D.R. (2004). Reducing joint destruction due to septic arthrosis using an adenosine2A receptor agonist. J Orthop. Res. *22*, 427-435.

Colgan,S.P., Hershberg,R.M., Furuta,G.T., and Blumberg,R.S. (1999). Ligation of intestinal epithelial CD1d induces bioactive IL-10: critical role of the cytoplasmic tail in autocrine signaling. Proc. Natl. Acad. Sci. U. S. A *96*, 13938-13943.

Collins,T., Read,M.A., Neish,A.S., Whitley,M.Z., Thanos,D., and Maniatis,T. (1995). Transcriptional regulation of endothelial cell adhesion molecules: NF-kappa B and cytokine-inducible enhancers. FASEB J. *9*, 899-909.

Dalton,R.N., Turner,C., Dick,M., Height,S.E., Awogbade,M., Inusa,B., Okpala,I., O'Driscoll,S., Thein,S.L., and Rees,D.C. (2005). The measurement of urinary hydroxyurea in sickle cell anaemia. Br. J Haematol. *130*, 138-144.

Day,Y.J., Huang,L., McDuffie,M.J., Rosin,D.L., Ye,H., Chen,J.F., Schwarzschild,M.A., Fink,J.S., Linden,J., and Okusa,M.D. (2003). Renal protection from ischemia mediated by A2A adenosine receptors on bone marrow-derived cells. J Clin Invest *112*, 883-891.

Day,Y.J., Marshall,M.A., Huang,L., McDuffie,M.J., Okusa,M.D., and Linden,J. (2004). Protection from ischemic liver injury by activation of A2A adenosine receptors during reperfusion: inhibition of chemokine induction. Am J Physiol Gastrointest. Liver Physiol *286*, G285-G293.

de,P.M., Young,K., Imai,Y., Liu,M., Waddell,T.K., Fischer,S., Zhang,L., and Keshavjee,S. (2003). Recipient T cells mediate reperfusion injury after lung transplantation in the rat. J Immunol. *171*, 4995-5002.

Decking,U.K., Schlieper,G., Kroll,K., and Schrader,J. (1997). Hypoxia-induced inhibition of adenosine kinase potentiates cardiac adenosine release. Circ. Res. *81*, 154-164.

Dias-Da-Motta,P., Arruda,V.R., Muscara,M.N., Saad,S.T., De,N.G., Costa,F.F., and Condino-Neto,A. (1996). The release of nitric oxide and superoxide anion by neutrophils and mononuclear cells from patients with sickle cell anaemia. Br. J. Haematol. *93*, 333-340.

Diggs, LW. Sickle cell crises. Am J Clin Pathol 44. 1965.
Ref Type: Generic

Dunwiddie,T.V., Diao,L., and Proctor,W.R. (1997). Adenine nucleotides undergo rapid, quantitative conversion to adenosine in the extracellular space in rat hippocampus. J Neurosci. *17*, 7673-7682.

Durante-Mangoni,E., Wang,R., Shaulov,A., He,Q., Nasser,I., Afdhal,N., Koziel,M.J., and Exley,M.A. (2004). Hepatic CD1d expression in hepatitis C virus infection and recognition by resident proinflammatory CD1d-reactive T cells. J. Immunol. *173*, 2159-2166.

Eberl,G., Lees,R., Smiley,S.T., Taniguchi,M., Grusby,M.J., and MacDonald,H.R. (1999). Tissue-specific segregation of CD1d-dependent and CD1d-independent NK T cells. J. Immunol. *162*, 6410-6419.

Embury,S.H. (2004). The not-so-simple process of sickle cell vasoocclusion. Microcirculation. *11*, 101-113.

Etienne-Julan,M., Belloy,M.S., Decastel,M., Dougaparsad,S., Ravion,S., and Hardy-Dessources,M.D. (2004). Childhood sickle cell crises: clinical severity, inflammatory markers and the role of interleukin-8. Haematologica *89*, 863-864.

Fabry,M.E., Costantini,F., Pachnis,A., Suzuka,S.M., Bank,N., Aynedjian,H.S., Factor,S.M., and Nagel,R.L. (1992a). High expression of human beta S- and alpha-globins in transgenic mice: erythrocyte abnormalities, organ damage, and the effect of hypoxia. Proc. Natl. Acad. Sci U. S. A *89*, 12155-12159.

Fabry,M.E., Nagel,R.L., Pachnis,A., Suzuka,S.M., and Costantini,F. (1992b). High expression of human beta S- and alpha-globins in transgenic mice: hemoglobin composition and hematological consequences. Proc. Natl. Acad. Sci U. S. A *89*, 12150-12154.

Florence,W.C., Bhat,R.K., and Joyce,S. (2008). CD1d-restricted glycolipid antigens: presentation principles, recognition logic and functional consequences. Expert. Rev. Mol. Med. *10*, e20.

Forestier,C., Molano,A., Im,J.S., Dutronc,Y., Diamond,B., Davidson,A., Illarionov,P.A., Besra,G.S., and Porcelli,S.A. (2005). Expansion and hyperactivity of CD1d-restricted NKT cells during the progression of systemic lupus erythematosus in (New Zealand Black x New Zealand White)F1 mice. J. Immunol. *175*, 763-770.

Fozard,J.R., Ellis,K.M., Villela Dantas,M.F., Tigani,B., and Mazzoni,L. (2002). Effects of CGS 21680, a selective adenosine A2A receptor agonist, on allergic airways inflammation in the rat. Eur. J. Pharmacol. *438*, 183-188.

Francis,R.B., Jr. (1991). Platelets, coagulation, and fibrinolysis in sickle cell disease: their possible role in vascular occlusion. Blood Coagul. Fibrinolysis *2*, 341-353.

Francis, R. B. and Hebbel, R. P. Hemostasis. Embury SH, Hebbel RP Steinberg MH Mohandas N. Sickle Cell Disease: Basic Principles and Clinical Practice , 299-310. 1994. New York, Raven Press.
Ref Type: Generic

Fredholm,B.B., IJzerman,A.P., Jacobson,K.A., Klotz,K.N., and Linden,J. (2001). International Union of Pharmacology. XXV. Nomenclature and classification of adenosine receptors. Pharmacol. Rev. *53*, 527-552.

Frenette,P.S. (2004). Sickle Cell Vasoocclusion: Heterotypic, Multicellular Aggregations Driven by Leukocyte Adhesion. Microcirculation. *11*, 167-177.

Galli,G., Nuti,S., Tavarini,S., Galli-Stampino,L., De,L.C., Casorati,G., Dellabona,P., and Abrignani,S. (2003). CD1d-restricted help to B cells by human invariant natural killer T lymphocytes. J. Exp. Med. *197*, 1051-1057.

Gasperini,S., Marchi,M., Calzetti,F., Laudanna,C., Vicentini,L., Olsen,H., Murphy,M., Liao,F., Farber,J., and Cassatella,M.A. (1999). Gene expression and production of the monokine induced by IFN-gamma (MIG), IFN-inducible T cell alpha chemoattractant (I-TAC), and IFN-gamma-inducible protein-10 (IP-10) chemokines by human neutrophils. J Immunol. *162*, 4928-4937.

Gazoni,L.M., Laubach,V.E., Mulloy,D.P., Bellizzi,A., Unger,E.B., Linden,J., Ellman,P.I., Lisle,T.C., and Kron,I.L. (2008). Additive protection against lung ischemia-reperfusion injury by adenosine A2A receptor activation before procurement and during reperfusion. J. Thorac. Cardiovasc. Surg. *135*, 156-165.

Gerlach,J., Jorres,A., Nohr,R., Zeilinger,K., Spatkowski,G., and Neuhaus,P. (1999). Local liberation of cytokines during liver preservation. Transpl. Int. *12*, 261-265.

Gessi,S., Varani,K., Merighi,S., Ongini,E., and Borea,P.A. (2000). A(2A) adenosine receptors in human peripheral blood cells. Br. J. Pharmacol. *129*, 2-11.

Gombert,J.M., Herbelin,A., Tancrede-Bohin,E., Dy,M., Carnaud,C., and Bach,J.F. (1996). Early quantitative and functional deficiency of NK1+-like thymocytes in the NOD mouse. Eur. J. Immunol. *26*, 2989-2998.

Gumperz,J.E., Roy,C., Makowska,A., Lum,D., Sugita,M., Podrebarac,T., Koezuka,Y., Porcelli,S.A., Cardell,S., Brenner,M.B., and Behar,S.M. (2000). Murine CD1d-restricted T cell recognition of cellular lipids. Immunity. *12*, 211-221.

Hansen,P.R. (1995). Role of neutrophils in myocardial ischemia and reperfusion. Circulation *91*, 1872-1885.

Haque,A.K., Gokhale,S., Rampy,B.A., Adegboyega,P., Duarte,A., and Saldana,M.J. (2002). Pulmonary hypertension in sickle cell hemoglobinopathy: a clinicopathologic study of 20 cases. Hum. Pathol. *33*, 1037-1043.

Harada,N., Okajima,K., Murakami,K., Usune,S., Sato,C., Ohshima,K., and Katsuragi,T. (2000). Adenosine and selective A(2A) receptor agonists reduce ischemia/reperfusion injury of rat liver mainly by inhibiting leukocyte activation. J Pharmacol. Exp. Ther. *294*, 1034-1042.

Hashimoto,N., Jin,H., Liu,T., Chensue,S.W., and Phan,S.H. (2004). Bone marrow-derived progenitor cells in pulmonary fibrosis. J. Clin. Invest *113*, 243-252.

Hasko,G. and Cronstein,B.N. (2004). Adenosine: an endogenous regulator of innate immunity. Trends Immunol. *25*, 33-39.

Hebbel, R. P. Sickle Cell Disease. Hoffman: Hematology: Basic Principles and Practice 4, 591-601. 2005. Elsevier.
Ref Type: Generic

Hebbel,R.P., Eaton,J.W., Balasingam,M., and Steinberg,M.H. (1982). Spontaneous oxygen radical generation by sickle erythrocytes. J. Clin. Invest *70*, 1253-1259.

Herskowitz,A., Choi,S., Ansari,A.A., and Wesselingh,S. (1995). Cytokine mRNA expression in postischemic/reperfused myocardium. Am. J. Pathol. *146*, 419-428.

Hillery,C.A. and Panepinto,J.A. (2004). Pathophysiology of stroke in sickle cell disease. Microcirculation. *11*, 195-208.

Hofstra,T.C., Kalra,V.K., Meiselman,H.J., and Coates,T.D. (1996). Sickle erythrocytes adhere to polymorphonuclear neutrophils and activate the neutrophil respiratory burst. Blood *87*, 4440-4447.

Holtzclaw,J.D., Jack,D., Aguayo,S.M., Eckman,J.R., Roman,J., and Hsu,L.L. (2004). Enhanced pulmonary and systemic response to endotoxin in transgenic sickle mice. Am J Respir. Crit Care Med. *169*, 687-695.

Huang,Q.Q., Yao,S.Y., Ritzel,M.W., Paterson,A.R., Cass,C.E., and Young,J.D. (1994). Cloning and functional expression of a complementary DNA encoding a mammalian nucleoside transport protein. J Biol. Chem. *269*, 17757-17760.

Imanaka,H., Shimaoka,M., Matsuura,N., Nishimura,M., Ohta,N., and Kiyono,H. (2001). Ventilator-induced lung injury is associated with neutrophil infiltration, macrophage activation, and TGF-beta 1 mRNA upregulation in rat lungs. Anesth. Analg. *92*, 428-436.

Jaeschke,H., Bautista,A.P., Spolarics,Z., and Spitzer,J.J. (1992). Superoxide generation by neutrophils and Kupffer cells during in vivo reperfusion after hepatic ischemia in rats. J. Leukoc. Biol. *52*, 377-382.

Jahng,A., Maricic,I., Aguilera,C., Cardell,S., Halder,R.C., and Kumar,V. (2004). Prevention of autoimmunity by targeting a distinct, noninvariant CD1d-reactive T cell population reactive to sulfatide. J. Exp. Med. *199*, 947-957.

Jordan,J.E., Zhao,Z.Q., Sato,H., Taft,S., and Vinten-Johansen,J. (1997). Adenosine A2 receptor activation attenuates reperfusion injury by inhibiting neutrophil accumulation, superoxide generation and coronary endothelial adherence. J Pharmacol. Exp. Ther. *280*, 301-309.

Kato,G.J., Martyr,S., Blackwelder,W.C., Nichols,J.S., Coles,W.A., Hunter,L.A., Brennan,M.L., Hazen,S.L., and Gladwin,M.T. (2005). Levels of soluble endothelium-derived adhesion molecules in patients with sickle cell disease are associated with pulmonary hypertension, organ dysfunction, and mortality. Br. J. Haematol. *130*, 943-953.

Kaul,D.K. and Hebbel,R.P. (2000). Hypoxia/reoxygenation causes inflammatory response in transgenic sickle mice but not in normal mice. J Clin Invest *106*, 411-420.

Kaul,N. and Forman,H.J. (1996). Activation of NF kappa B by the respiratory burst of macrophages. Free Radic. Biol. Med. *21*, 401-405.

Kawakami,K., Yamamoto,N., Kinjo,Y., Miyagi,K., Nakasone,C., Uezu,K., Kinjo,T., Nakayama,T., Taniguchi,M., and Saito,A. (2003). Critical role of Valpha14+ natural killer T cells in the innate phase of host protection against Streptococcus pneumoniae infection. Eur. J. Immunol. *33*, 3322-3330.

Kim,J.D., Baker,C.J., Roberts,R.F., Darbinian,S.H., Marcus,K.A., Quardt,S.M., Starnes,V.A., and Barr,M.L. (2000). Platelet activating factor acetylhydrolase decreases lung reperfusion injury. Ann. Thorac. Surg. *70*, 423-428.

Kinjo,Y., Tupin,E., Wu,D., Fujio,M., Garcia-Navarro,R., Benhnia,M.R., Zajonc,D.M., Ben-Menachem,G., Ainge,G.D., Painter,G.F., Khurana,A., Hoebe,K., Behar,S.M., Beutler,B., Wilson,I.A., Tsuji,M., Sellati,T.J., Wong,C.H., and Kronenberg,M. (2006). Natural killer T cells recognize diacylglycerol antigens from pathogenic bacteria. Nat. Immunol. *7*, 978-986.

Kinjo,Y., Wu,D., Kim,G., Xing,G.W., Poles,M.A., Ho,D.D., Tsuji,M., Kawahara,K., Wong,C.H., and Kronenberg,M. (2005). Recognition of bacterial glycosphingolipids by natural killer T cells. Nature *434*, 520-525.

Kirsh,K.L., Whitcomb,L.A., Donaghy,K., and Passik,S.D. (2002). Abuse and addiction issues in medically ill patients with pain: attempts at clarification of terms and empirical study. Clin J Pain *18*, S52-S60.

Koike,K., Yamamoto,Y., Hori,Y., and Ono,T. (2000). Group IIA phospholipase A2 mediates lung injury in intestinal ischemia-reperfusion. Ann. Surg. *232*, 90-97.

Kronenberg,M. and Gapin,L. (2002). The unconventional lifestyle of NKT cells. Nat. Rev. Immunol. *2*, 557-568.

Kuppusamy,P. and Zweier,J.L. (1989). Characterization of free radical generation by xanthine oxidase. Evidence for hydroxyl radical generation. J. Biol. Chem. *264*, 9880-9884.

Lansman,J.B. (1988). Endothelial mechanosensors. Going with the flow. Nature *331*, 481-482.

Lappas,C.M., Day,Y.J., Marshall,M.A., Engelhard,V.H., and Linden,J. (2006). Adenosine A2A receptor activation reduces hepatic ischemia reperfusion injury by inhibiting CD1d-dependent NKT cell activation. J Exp. Med. *203*, 2639-2648.

Latini,S., Bordoni,F., Corradetti,R., Pepeu,G., and Pedata,F. (1999a). Effect of A2A adenosine receptor stimulation and antagonism on synaptic depression induced by in vitro ischaemia in rat hippocampal slices. Br. J. Pharmacol. *128*, 1035-1044.

Latini,S., Bordoni,F., Pedata,F., and Corradetti,R. (1999b). Extracellular adenosine concentrations during in vitro ischaemia in rat hippocampal slices. Br. J Pharmacol. *127*, 729-739.

Lemay,S., Rabb,H., Postler,G., and Singh,A.K. (2000). Prominent and sustained up-regulation of gp130-signaling cytokines and the chemokine MIP-2 in murine renal ischemia-reperfusion injury. Transplantation *69*, 959-963.

Li,L., Huang,L., Sung,S.S., Lobo,P.I., Brown,M.G., Gregg,R.K., Engelhard,V.H., and Okusa,M.D. (2007). NKT cell activation mediates neutrophil IFN-gamma production and renal ischemia-reperfusion injury. J Immunol. *178*, 5899-5911.

Linden,J. (2005). Adenosine in tissue protection and tissue regeneration. Mol. Pharmacol. *67*, 1385-1387.

Lisbonne,M., Diem,S., de Castro,K.A., Lefort,J., Araujo,L.M., Hachem,P., Fourneau,J.M., Sidobre,S., Kronenberg,M., Taniguchi,M., Van,E.P., Dy,M., Askenase,P., Russo,M., Vargaftig,B.B., Herbelin,A., and Leite-de-Moraes,M.C. (2003). Cutting edge:

invariant V alpha 14 NKT cells are required for allergen-induced airway inflammation and hyperreactivity in an experimental asthma model. J. Immunol. *171*, 1637-1641.

Lloyd,H.G. and Fredholm,B.B. (1995). Involvement of adenosine deaminase and adenosine kinase in regulating extracellular adenosine concentration in rat hippocampal slices. Neurochem. Int. *26*, 387-395.

Lukashev,D., Ohta,A., and Sitkovsky,M. (2004). Targeting hypoxia--A(2A) adenosine receptor-mediated mechanisms of tissue protection. Drug Discov. Today *9*, 403-409.

Ma,X.L., Tsao,P.S., and Lefer,A.M. (1991). Antibody to CD-18 exerts endothelial and cardiac protective effects in myocardial ischemia and reperfusion. J. Clin. Invest *88*, 1237-1243.

Ma,X.L., Weyrich,A.S., Lefer,D.J., Buerke,M., Albertine,K.H., Kishimoto,T.K., and Lefer,A.M. (1993). Monoclonal antibody to L-selectin attenuates neutrophil accumulation and protects ischemic reperfused cat myocardium. Circulation *88*, 649-658.

Makis,A.C., Hatzimichael,E.C., Stebbing,J., and Bourantas,K.L. (2006). C-reactive protein and vascular cell adhesion molecule-1 as markers of severity in sickle cell disease. Arch. Intern. Med. *166*, 366-368.

Makowska,A., Faizunnessa,N.N., Anderson,P., Midtvedt,T., and Cardell,S. (1999). CD1high B cells: a population of mixed origin. Eur. J. Immunol. *29*, 3285-3294.

Matsuda,J.L., Naidenko,O.V., Gapin,L., Nakayama,T., Taniguchi,M., Wang,C.R., Koezuka,Y., and Kronenberg,M. (2000). Tracking the response of natural killer T cells to a glycolipid antigen using CD1d tetramers. J. Exp. Med. *192*, 741-754.

Mattner,J., Debord,K.L., Ismail,N., Goff,R.D., Cantu,C., III, Zhou,D., Saint-Mezard,P., Wang,V., Gao,Y., Yin,N., Hoebe,K., Schneewind,O., Walker,D., Beutler,B., Teyton,L., Savage,P.B., and Bendelac,A. (2005). Exogenous and endogenous glycolipid antigens activate NKT cells during microbial infections. Nature *434*, 525-529.

McCord,J.M. (1985). Oxygen-derived free radicals in postischemic tissue injury. N. Engl. J. Med. *312*, 159-163.

McCurdy,P.R. (1969). 32-DFP and 51-Cr for measurement of red cell life span in abnormal hemoglobin syndromes. Blood *33*, 214-224.

Melian,A., Geng,Y.J., Sukhova,G.K., Libby,P., and Porcelli,S.A. (1999). CD1 expression in human atherosclerosis. A potential mechanism for T cell activation by foam cells. Am. J. Pathol. *155*, 775-786.

Molitierno,J.A., Jr. and Carson,C.C., III (2003). Urologic manifestations of hematologic disease sickle cell, leukemia, and thromboembolic disease. Urol. Clin. North Am. *30*, 49-61.

Morris,C.R., Kuypers,F.A., Kato,G.J., Lavrisha,L., Larkin,S., Singer,T., and Vichinsky,E.P. (2005). Hemolysis-associated pulmonary hypertension in thalassemia. Ann. N. Y. Acad. Sci. *1054*, 481-485.

Nadeem,A., Fan,M., Ansari,H.R., Ledent,C., and Jamal,M.S. (2007). Enhanced airway reactivity and inflammation in A2A adenosine receptor-deficient allergic mice. Am. J. Physiol Lung Cell Mol. Physiol *292*, L1335-L1344.

Nagel,R.L. and Fabry,M.E. (2001). The panoply of animal models for sickle cell anaemia. Br. J. Haematol. *112*, 19-25.

Newby,A.C., Worku,Y., and Holmquist,C.A. (1985). Adenosine formation. Evidence for a direct biochemical link with energy metabolism. Adv. Myocardiol. *6*, 273-284.

Nicol,A., Nieda,M., Koezuka,Y., Porcelli,S., Suzuki,K., Tadokoro,K., Durrant,S., and Juji,T. (2000). Dendritic cells are targets for human invariant Valpha24+ natural killer T-cell cytotoxic activity: an important immune regulatory function. Exp. Hematol. *28*, 276-282.

Nieuwenhuis,E.E., Matsumoto,T., Exley,M., Schleipman,R.A., Glickman,J., Bailey,D.T., Corazza,N., Colgan,S.P., Onderdonk,A.B., and Blumberg,R.S. (2002). CD1d-dependent macrophage-mediated clearance of Pseudomonas aeruginosa from lung. Nat. Med. *8*, 588-593.

Okusa,M.D., Linden,J., Huang,L., Rieger,J.M., Macdonald,T.L., and Huynh,L.P. (2000). A(2A) adenosine receptor-mediated inhibition of renal injury and neutrophil adhesion. Am J Physiol Renal Physiol *279*, F809-F818.

Osarogiagbon,U.R., Choong,S., Belcher,J.D., Vercellotti,G.M., Paller,M.S., and Hebbel,R.P. (2000). Reperfusion injury pathophysiology in sickle transgenic mice. Blood *96*, 314-320.

Oz,M.C., Liao,H., Naka,Y., Seldomridge,A., Becker,D.N., Michler,R.E., Smith,C.R., Rose,E.A., Stern,D.M., and Pinsky,D.J. (1995). Ischemia-induced interleukin-8 release after human heart transplantation. A potential role for endothelial cells. Circulation *92*, II428-II432.

Page,M.J., Poritz,L.S., Tilberg,A.F., Zhang,W.J., Chorney,M.J., and Koltun,W.A. (2000). Cd1d-restricted cellular lysis by peripheral blood lymphocytes: relevance to the inflammatory bowel diseases. J. Surg. Res. *92*, 214-221.

Parks,D.A. and Granger,D.N. (1986). Xanthine oxidase: biochemistry, distribution and physiology. Acta Physiol Scand. Suppl *548*, 87-99.

Parks,D.A., Williams,T.K., and Beckman,J.S. (1988). Conversion of xanthine dehydrogenase to oxidase in ischemic rat intestine: a reevaluation. Am. J. Physiol *254*, G768-G774.

Pashankar,F.D., Carbonella,J., Bazzy-Asaad,A., and Friedman,A. (2008). Prevalence and risk factors of elevated pulmonary artery pressures in children with sickle cell disease. Pediatrics *121*, 777-782.

Pashankar,F.D., Carbonella,J., Bazzy-Asaad,A., and Friedman,A. (2009). Longitudinal follow up of elevated pulmonary artery pressures in children with sickle cell disease. Br. J. Haematol. *144*, 736-741.

Pham,P.T., Pham,P.C., Wilkinson,A.H., and Lew,S.Q. (2000). Renal abnormalities in sickle cell disease. Kidney Int. *57*, 1-8.

Phillips,R.J., Burdick,M.D., Hong,K., Lutz,M.A., Murray,L.A., Xue,Y.Y., Belperio,J.A., Keane,M.P., and Strieter,R.M. (2004). Circulating fibrocytes traffic to the lungs in response to CXCL12 and mediate fibrosis. J. Clin. Invest *114*, 438-446.

Pierce,K.L., Premont,R.T., and Lefkowitz,R.J. (2002). Seven-transmembrane receptors. Nat. Rev. Mol. Cell Biol. *3*, 639-650.

Pillai,S., Cariappa,A., and Moran,S.T. (2005). Marginal zone B cells. Annu. Rev. Immunol. *23*, 161-196.

Platt,O.S. (2000). Sickle cell anemia as an inflammatory disease. J Clin Invest *106*, 337-338.

Platt,O.S., Brambilla,D.J., Rosse,W.F., Milner,P.F., Castro,O., Steinberg,M.H., and Klug,P.P. (1994). Mortality in sickle cell disease. Life expectancy and risk factors for early death. N. Engl. J. Med. *330*, 1639-1644.

Porubsky,S., Speak,A.O., Luckow,B., Cerundolo,V., Platt,F.M., and Grone,H.J. (2007). Normal development and function of invariant natural killer T cells in mice with isoglobotrihexosylceramide (iGb3) deficiency. Proc. Natl. Acad. Sci U. S. A *104*, 5977-5982.

Powars,D., Weidman,J.A., Odom-Maryon,T., Niland,J.C., and Johnson,C. (1988). Sickle cell chronic lung disease: prior morbidity and the risk of pulmonary failure. Medicine (Baltimore) *67*, 66-76.

Quan,T.E., Cowper,S., Wu,S.P., Bockenstedt,L.K., and Bucala,R. (2004). Circulating fibrocytes: collagen-secreting cells of the peripheral blood. Int. J. Biochem. Cell Biol. *36*, 598-606.

Raskovalova,T., Lokshin,A., Huang,X., Jackson,E.K., and Gorelik,E. (2006). Adenosine-mediated inhibition of cytotoxic activity and cytokine production by IL-2/NKp46-activated NK cells: involvement of protein kinase A isozyme I (PKA I). Immunol. Res. *36*, 91-99.

Rauch,J., Gumperz,J., Robinson,C., Skold,M., Roy,C., Young,D.C., Lafleur,M., Moody,D.B., Brenner,M.B., Costello,C.E., and Behar,S.M. (2003). Structural features of the acyl chain determine self-phospholipid antigen recognition by a CD1d-restricted invariant NKT (iNKT) cell. J. Biol. Chem. *278*, 47508-47515.

Reece,T.B., Ellman,P.I., Maxey,T.S., Crosby,I.K., Warren,P.S., Chong,T.W., LeGallo,R.D., Linden,J., Kern,J.A., Tribble,C.G., and Kron,I.L. (2005). Adenosine A2A receptor activation reduces inflammation and preserves pulmonary function in an in vivo model of lung transplantation. J Thorac. Cardiovasc. Surg. *129*, 1137-1143.

Rennels,M.B., Dunne,M.G., Grossman,N.J., and Schwartz,A.D. (1984). Cholelithiasis in patients with major sickle hemoglobinopathies. Am. J. Dis. Child *138*, 66-67.

Reutershan,J., Cagnina,R.E., Chang,D., Linden,J., and Ley,K. (2007). Therapeutic anti-inflammatory effects of myeloid cell adenosine receptor A2a stimulation in lipopolysaccharide-induced lung injury. J. Immunol. *179*, 1254-1263.

Roark,J.H., Park,S.H., Jayawardena,J., Kavita,U., Shannon,M., and Bendelac,A. (1998). CD1.1 expression by mouse antigen-presenting cells and marginal zone B cells. J. Immunol. *160*, 3121-3127.

Rosenblate,H.J., Eisenstein,R., and Holmes,A.W. (1970a). The liver in sickle cell anemia. A clinical-pathologic study. Arch. Pathol *90*, 235-245.

Rosenblate,H.J., Eisenstein,R., and Holmes,A.W. (1970b). The liver in sickle cell anemia. A clinical-pathologic study. Arch. Pathol *90*, 235-245.

Ross,S.D., Tribble,C.G., Linden,J., Gangemi,J.J., Lanpher,B.C., Wang,A.Y., and Kron,I.L. (1999). Selective adenosine-A2A activation reduces lung reperfusion injury following transplantation
8. J Heart Lung Transplant. *18*, 994-1002.

Rudolphi,K.A., Schubert,P., Parkinson,F.E., and Fredholm,B.B. (1992a). Adenosine and brain ischemia. Cerebrovasc. Brain Metab Rev. *4*, 346-369.

Rudolphi,K.A., Schubert,P., Parkinson,F.E., and Fredholm,B.B. (1992b). Neuroprotective role of adenosine in cerebral ischaemia. Trends Pharmacol. Sci. *13*, 439-445.

Ryll,R., Watanabe,K., Fujiwara,N., Takimoto,H., Hasunuma,R., Kumazawa,Y., Okada,M., and Yano,I. (2001). Mycobacterial cord factor, but not sulfolipid, causes depletion of NKT cells and upregulation of CD1d1 on murine macrophages. Microbes. Infect. *3*, 611-619.

Sancho,D., Gomez,M., and Sanchez-Madrid,F. (2005). CD69 is an immunoregulatory molecule induced following activation. Trends Immunol. *26*, 136-140.

Sauty,A., Dziejman,M., Taha,R.A., Iarossi,A.S., Neote,K., Garcia-Zepeda,E.A., Hamid,Q., and Luster,A.D. (1999). The T cell-specific CXC chemokines IP-10, Mig, and I-TAC are expressed by activated human bronchial epithelial cells. J Immunol. *162*, 3549-3558.

Schioppa,T., Uranchimeg,B., Saccani,A., Biswas,S.K., Doni,A., Rapisarda,A., Bernasconi,S., Saccani,S., Nebuloni,M., Vago,L., Mantovani,A., Melillo,G., and Sica,A. (2003). Regulation of the chemokine receptor CXCR4 by hypoxia. J. Exp. Med. *198*, 1391-1402.

Schmidt,M., Sun,G., Stacey,M.A., Mori,L., and Mattoli,S. (2003). Identification of circulating fibrocytes as precursors of bronchial myofibroblasts in asthma. J. Immunol. *171*, 380-389.

Schmieg,J., Yang,G., Franck,R.W., Van,R.N., and Tsuji,M. (2005). Glycolipid presentation to natural killer T cells differs in an organ-dependent fashion. Proc. Natl. Acad. Sci. U. S. A *102*, 1127-1132.

Schnog,J.J., Lard,L.R., Rojer,R.A., van der Dijs,F.P., Muskiet,F.A., and Duits,A.J. (1998). New concepts in assessing sickle cell disease severity. Am. J. Hematol. *58*, 61-66.

Schroeter,M., Jander,S., Witte,O.W., and Stoll,G. (1994). Local immune responses in the rat cerebral cortex after middle cerebral artery occlusion. J. Neuroimmunol. *55*, 195-203.

Serrick,C., Adoumie,R., Giaid,A., and Shennib,H. (1994). The early release of interleukin-2, tumor necrosis factor-alpha and interferon-gamma after ischemia reperfusion injury in the lung allograft. Transplantation *58*, 1158-1162.

Sevigny,C.P., Li,L., Awad,A.S., Huang,L., McDuffie,M., Linden,J., Lobo,P.I., and Okusa,M.D. (2007). Activation of adenosine 2A receptors attenuates allograft rejection and alloantigen recognition. J. Immunol. *178*, 4240-4249.

Sheehy,T.W., Law,D.E., and Wade,B.H. (1980). Exchange transfusion for sickle cell intrahepatic cholestasis. Arch. Intern. Med. *140*, 1364-1366.

Shryock,J.C., Snowdy,S., Baraldi,P.G., Cacciari,B., Spalluto,G., Monopoli,A., Ongini,E., Baker,S.P., and Belardinelli,L. (1998). A2A-adenosine receptor reserve for coronary vasodilation. Circulation *98*, 711-718.

Singh,U.P., Venkataraman,C., Singh,R., and Lillard,J.W., Jr. (2007). CXCR3 axis: role in inflammatory bowel disease and its therapeutic implication. Endocr. Metab Immune. Disord. Drug Targets. *7*, 111-123.

Singhal,A., Doherty,J.F., Raynes,J.G., McAdam,K.P., Thomas,P.W., Serjeant,B.E., and Serjeant,G.R. (1993). Is there an acute-phase response in steady-state sickle cell disease? Lancet *341*, 651-653.

Skold,M., Xiong,X., Illarionov,P.A., Besra,G.S., and Behar,S.M. (2005). Interplay of cytokines and microbial signals in regulation of CD1d expression and NKT cell activation. J. Immunol. *175*, 3584-3593.

Solovey,A., Gui,L., Key,N.S., and Hebbel,R.P. (1998). Tissue factor expression by endothelial cells in sickle cell anemia. J. Clin. Invest *101*, 1899-1904.

Solovey,A., Kollander,R., Shet,A., Milbauer,L.C., Choong,S., Panoskaltsis-Mortari,A., Blazar,B.R., Kelm,R.J., Jr., and Hebbel,R.P. (2004). Endothelial cell expression of tissue factor in sickle mice is augmented by hypoxia/reoxygenation and inhibited by lovastatin. Blood *104*, 840-846.

Spada,F.M., Borriello,F., Sugita,M., Watts,G.F., Koezuka,Y., and Porcelli,S.A. (2000). Low expression level but potent antigen presenting function of CD1d on monocyte lineage cells. Eur. J. Immunol. *30*, 3468-3477.

Stammberger,U., Carboni,G.L., Hillinger,S., Schneiter,D., Weder,W., and Schmid,R.A. (1999). Combined treatment with endothelin- and PAF-antagonists reduces posttransplant lung ischemia/reperfusion injury. J. Heart Lung Transplant. *18*, 862-868.

Stanic,A.K., De Silva,A.D., Park,J.J., Sriram,V., Ichikawa,S., Hirabyashi,Y., Hayakawa,K., Van,K.L., Brutkiewicz,R.R., and Joyce,S. (2003). Defective presentation of the CD1d1-restricted natural Va14Ja18 NKT lymphocyte antigen caused by beta-D-glucosylceramide synthase deficiency. Proc. Natl. Acad. Sci. U. S. A *100*, 1849-1854.

Stenmark,K.R., Gerasimovskaya,E., Nemenoff,R.A., and Das,M. (2002). Hypoxic activation of adventitial fibroblasts: role in vascular remodeling. Chest *122*, 326S-334S.

Strijbos,M.H., Landburg,P.P., Nur,E., Teerlink,T., Leebeek,F.W., Rijneveld,A.W., Biemond,B.J., Sleijfer,S., Gratama,J.W., Duits,A.J., and Schnog,J.J. (2009). Circulating endothelial cells: A potential parameter of organ damage in sickle cell anemia? Blood Cells Mol. Dis.

Stuart,J., Stone,P.C., Akinola,N.O., Gallimore,J.R., and Pepys,M.B. (1994). Monitoring the acute phase response to vaso-occlusive crisis in sickle cell disease. J. Clin. Pathol. *47*, 166-169.

Stuart,M.J. and Nagel,R.L. (2004). Sickle-cell disease. Lancet *364*, 1343-1360.

Sullivan,G.W., Carper,H.T., and Mandell,G.L. (1995). The specific type IV phosphodiesterase inhibitor rolipram combined with adenosine reduces tumor necrosis factor-alpha-primed neutrophil oxidative activity. Int. J. Immunopharmacol. *17*, 793-803.

Sullivan,G.W., Fang,G., Linden,J., and Scheld,W.M. (2004). A2A adenosine receptor activation improves survival in mouse models of endotoxemia and sepsis. J Infect. Dis. *189*, 1897-1904.

Sullivan,G.W., Rieger,J.M., Scheld,W.M., Macdonald,T.L., and Linden,J. (2001). Cyclic AMP-dependent inhibition of human neutrophil oxidative activity by substituted 2-propynylcyclohexyl adenosine A(2A) receptor agonists. Br. J. Pharmacol. *132*, 1017-1026.

Sullivan,K.J., Goodwin,S.R., Evangelist,J., Moore,R.D., and Mehta,P. (1999). Nitric oxide successfully used to treat acute chest syndrome of sickle cell disease in a young adolescent. Crit Care Med. *27*, 2563-2568.

Sultana,C., Shen,Y., Rattan,V., Johnson,C., and Kalra,V.K. (1998). Interaction of sickle erythrocytes with endothelial cells in the presence of endothelial cell conditioned medium induces oxidant stress leading to transendothelial migration of monocytes. Blood *92*, 3924-3935.

Sun,Y. and Oberley,L.W. (1996). Redox regulation of transcriptional activators. Free Radic. Biol. Med. *21*, 335-348.

Suzuki,S. and Toledo-Pereyra,L.H. (1994). Interleukin 1 and tumor necrosis factor production as the initial stimulants of liver ischemia and reperfusion injury. J. Surg. Res. *57*, 253-258.

Swerlick,R.A., Eckman,J.R., Kumar,A., Jeitler,M., and Wick,T.M. (1993). Alpha 4 beta 1-integrin expression on sickle reticulocytes: vascular cell adhesion molecule-1-dependent binding to endothelium. Blood *82*, 1891-1899.

Tahir,S.M., Cheng,O., Shaulov,A., Koezuka,Y., Bubley,G.J., Wilson,S.B., Balk,S.P., and Exley,M.A. (2001). Loss of IFN-gamma production by invariant NK T cells in advanced cancer. J. Immunol. *167*, 4046-4050.

Taniguchi,M., Harada,M., Kojo,S., Nakayama,T., and Wakao,H. (2003). The regulatory role of Valpha14 NKT cells in innate and acquired immune response. Annu. Rev. Immunol. *21*, 483-513.

Taylor,S.C., Shacks,S.J., and Qu,Z. (1999). In vivo production of type 1 cytokines in healthy sickle cell disease patients. J. Natl. Med. Assoc. *91*, 619-624.

Taylor,S.C., Shacks,S.J., Qu,Z., and Wiley,P. (1997). Type 2 cytokine serum levels in healthy sickle cell disease patients. J. Natl. Med. Assoc. *89*, 753-757.

Terabe,M. and Berzofsky,J.A. (2008). The role of NKT cells in tumor immunity. Adv. Cancer Res. *101*, 277-348.

Thelen,M. (2001). Dancing to the tune of chemokines. Nat. Immunol. *2*, 129-134.

Thiel,M., Caldwell,C.C., and Sitkovsky,M.V. (2003). The critical role of adenosine A2A receptors in downregulation of inflammation and immunity in the pathogenesis of infectious diseases. Microbes. Infect. *5*, 515-526.

Thomas,S.Y., Hou,R., Boyson,J.E., Means,T.K., Hess,C., Olson,D.P., Strominger,J.L., Brenner,M.B., Gumperz,J.E., Wilson,S.B., and Luster,A.D. (2003). CD1d-restricted NKT cells express a chemokine receptor profile indicative of Th1-type inflammatory homing cells. J. Immunol. *171*, 2571-2580.

Tomer,A., Harker,L.A., Kasey,S., and Eckman,J.R. (2001). Thrombogenesis in sickle cell disease. J. Lab Clin. Med. *137*, 398-407.

Trobonjaca,Z., Leithauser,F., Moller,P., Schirmbeck,R., and Reimann,J. (2001). Activating immunity in the liver. I. Liver dendritic cells (but not hepatocytes) are potent activators of IFN-gamma release by liver NKT cells. J Immunol. *167*, 1413-1422.

Tsuneyama,K., Yasoshima,M., Harada,K., Hiramatsu,K., Gershwin,M.E., and Nakanuma,Y. (1998). Increased CD1d expression on small bile duct epithelium and epithelioid granuloma in livers in primary biliary cirrhosis. Hepatology *28*, 620-623.

Tupin,E., Nicoletti,A., Elhage,R., Rudling,M., Ljunggren,H.G., Hansson,G.K., and Berne,G.P. (2004). CD1d-dependent activation of NKT cells aggravates atherosclerosis. J. Exp. Med. *199*, 417-422.

Vichinsky,E.P., Styles,L.A., Colangelo,L.H., Wright,E.C., Castro,O., and Nickerson,B. (1997). Acute chest syndrome in sickle cell disease: clinical presentation and course. Cooperative Study of Sickle Cell Disease. Blood *89*, 1787-1792.

Vizi,E., Huszar,E., Csoma,Z., Boszormenyi-Nagy,G., Barat,E., Horvath,I., Herjavecz,I., and Kollai,M. (2002). Plasma adenosine concentration increases during exercise: a possible contributing factor in exercise-induced bronchoconstriction in asthma. J Allergy Clin Immunol. *109*, 446-448.

Wang,E., Ouellet,N., Simard,M., Fillion,I., Bergeron,Y., Beauchamp,D., and Bergeron,M.G. (2001). Pulmonary and systemic host response to Streptococcus

pneumoniae and Klebsiella pneumoniae bacteremia in normal and immunosuppressed mice. Infect. Immun. *69*, 5294-5304.

Watson J, Stahman AW, and Billeo FP. The significance of the paucity of sickle cells in newborn negro infants. Am.J.Med.Sci 215, 419-423. 1948.
Ref Type: Generic

Weiner,D.L., Hibberd,P.L., Betit,P., Cooper,A.B., Botelho,C.A., and Brugnara,C. (2003). Preliminary assessment of inhaled nitric oxide for acute vaso-occlusive crisis in pediatric patients with sickle cell disease. JAMA *289*, 1136-1142.

Weiss,S.J. (1989). Tissue destruction by neutrophils. N. Engl. J. Med. *320*, 365-376.

White,J.G. (1974). Ultrastructural features of erythrocyte and hemoglobin sickling. Arch. Intern. Med. *133*, 545-562.

Williams,T.C. and Jarvis,S.M. (1991). Multiple sodium-dependent nucleoside transport systems in bovine renal brush-border membrane vesicles. Biochem. J *274 (Pt 1)*, 27-33.

Wingender,G. and Kronenberg,M. (2008). Role of NKT cells in the digestive system. IV. The role of canonical natural killer T cells in mucosal immunity and inflammation. Am. J. Physiol Gastrointest. Liver Physiol *294*, G1-G8.

Winn,R.K., Liggitt,D., Vedder,N.B., Paulson,J.C., and Harlan,J.M. (1993). Anti-P-selectin monoclonal antibody attenuates reperfusion injury to the rabbit ear. J. Clin. Invest *92*, 2042-2047.

Wu,D.Y., Segal,N.H., Sidobre,S., Kronenberg,M., and Chapman,P.B. (2003). Cross-presentation of disialoganglioside GD3 to natural killer T cells. J. Exp. Med. *198*, 173-181.

Yang,L., Scott,P.G., Giuffre,J., Shankowsky,H.A., Ghahary,A., and Tredget,E.E. (2002). Peripheral blood fibrocytes from burn patients: identification and quantification of fibrocytes in adherent cells cultured from peripheral blood mononuclear cells. Lab Invest *82*, 1183-1192.

Yang,O.O., Racke,F.K., Nguyen,P.T., Gausling,R., Severino,M.E., Horton,H.F., Byrne,M.C., Strominger,J.L., and Wilson,S.B. (2000). CD1d on myeloid dendritic cells stimulates cytokine secretion from and cytolytic activity of V alpha 24J alpha Q T cells: a feedback mechanism for immune regulation. J. Immunol. *165*, 3756-3762.

Yang,Z., Day,Y.J., Toufektsian,M.C., Xu,Y., Ramos,S.I., Marshall,M.A., French,B.A., and Linden,J. (2006). Myocardial infarct-sparing effect of adenosine A2A receptor activation is due to its action on CD4+ T lymphocytes. Circulation *114*, 2056-2064.

Yilmaz,G., Arumugam,T.V., Stokes,K.Y., and Granger,D.N. (2006). Role of T lymphocytes and interferon-gamma in ischemic stroke. Circulation *113*, 2105-2112.

Zarbock,A., Polanowska-Grabowska,R.K., and Ley,K. (2007). Platelet-neutrophil-interactions: linking hemostasis and inflammation. Blood Rev. *21*, 99-111.

Zhou,D., Mattner,J., Cantu,C., III, Schrantz,N., Yin,N., Gao,Y., Sagiv,Y., Hudspeth,K., Wu,Y.P., Yamashita,T., Teneberg,S., Wang,D., Proia,R.L., Levery,S.B., Savage,P.B., Teyton,L., and Bendelac,A. (2004). Lysosomal glycosphingolipid recognition by NKT cells. Science *306*, 1786-1789.

Zimmermann,H. (2000). Extracellular metabolism of ATP and other nucleotides. Naunyn Schmiedebergs Arch. Pharmacol. *362*, 299-309.

Zwacka,R.M., Zhang,Y., Halldorson,J., Schlossberg,H., Dudus,L., and Engelhardt,J.F. (1997). CD4(+) T-lymphocytes mediate ischemia/reperfusion-induced inflammatory responses in mouse liver. J. Clin. Invest *100*, 279-289.